PROGRAMA DE DOCTORADO EN BIOMEDICINA

UNIVERSIDAD DE GRANADA

Tesis Doctoral

•

Determination of exosomal cancer stem cell biomarkers with cancer diagnostic utility

Memoria presentada por Don. **JOSÉ LUIS PALACIOS FERRER**

para optar a la mención de Doctor Internacional por la Universidad de Granada

Granada, 2021

Editor: Universidad de Granada. Tesis Doctorales
Autor: José Luis Palacios Ferrer
ISBN: 978-84-1306-882-4
URI: http://hdl.handle.net/10481/69104

El progreso, siempre un paso por delante:

andamos y no lo alcanzamos

pero avanzamos, que es lo importante.

Fragmento del tema:
"¿Por qué existe algo en lugar de nada?"
Ozelot

AGRADECIMIENTOS

Transcurridos casi 5 años desde el comienzo de esta tesis, me encuentro redactando finalmente los agradecimientos de la misma. Aunque la empecé en una etapa de mi vida llena de cambios, dudas e incertidumbres, la termino habiendo disfrutado de los que probablemente han sido los mejores años de mi vida, llenos de aprendizaje y mejoría en muchos aspectos.

Entre otras muchas cosas, estos años he aprendido la importancia de no solo perseguir nuestras metas, sino de hacerlo disfrutando del camino. Y a lo largo del que me ha llevado hasta culminar este trabajo y etapa vital, muchas personas han desempeñado un papel clave y me han ayudado a disfrutarlo. A todas ellas, les agradezco y dedico esta tesis doctoral.

Gracias a mis directores de Tesis, Juan Antonio Marchal y Houria Boulaiz, por su guía y apoyo, por toda su orientación y ayuda en todo lo que he necesitado a lo largo de estos años, no solo a nivel científico y docente, sino también a nivel personal. No podría haber tenido mejores tutores y directores que vosotros, por ser grandes investigadores y docentes, pero sobre todo por ser mejores personas.

Gracias a todos los miembros y compañeros del grupo CTS-963 del CIBM, tanto pre- como post-doctorales, Mariang, Esmeralda, Macarena, Eugenia, Elena, Gema, Carmen, Saúl, Cristina, Carlos, Dani, Pablo H, Pablo G, Jesús, Aitor, Julia, Gloria, Yaiza y a más gente que ha pasado por el grupo en estos años, por toda vuestra aportación a mi tesis y a mi vida en general. Aunque no haya estado en el CIBM trabajando día a día, y mi paso por ahí haya sido ocasional, gracias por toda vuestra ayuda, consejos y sobre todo por los buenos ratos compartidos a lo largo de este tiempo. En especial gracias a Belén, por todo lo anterior y por ser la persona que más me enseñó y ayudó cuando llegué, con la que he compartido gran parte de todo este proyecto.

Gracias a todos los miembros del departamento de screening de la Fundación MEDINA, el lugar donde he llevado a cabo la mayor parte de esta tesis doctoral. Gracias a Paqui por hacer posible mi estancia y colaboración con vosotros, y por el trato recibido. A Pepe y Caridad, por acogerme, enseñarme y ayudarme con todo lo que he necesitado desde el primer momento, también habéis sido mis tutores en cierto sentido. A María, por empezar todo este trabajo, del cual cogí el testigo, y por seguir presente a pesar de la distancia. Aunque nuestros caminos se separaron demasiado pronto, está claro el por qué seguimos y seguiremos en contacto. A

Carmen, por todo lo bueno que hemos vivido y compartido, laboral y personalmente, porque esta tesis nos hizo buenos compañeros pero la vida nos ha hecho mejores amigos. A Dani, Ari y Patri, por su aportación clave en todos mis experimentos y análisis, y por vuestra personalidad, que facilita y alegra el día a cualquiera. A Mercedes, Javi, Dani, Ángeles, y a toda la gente de Medina en general, por haberme acogido y haberme hecho sentir siempre uno más. Todos habéis contribuido a que mi experiencia aquí sea no solo fructífera sino también agradable y, lo más importante, divertida.

Gracias a toda la gente que hizo posible y formó parte de mi experiencia en Toronto. Gracias a Thomas Kislinger por darme la oportunidad de hacer una estancia internacional en su grupo del Princess Margaret Cancer Centre. A todos los integrantes de su grupo por acogerme y hacerme partícipe tanto de sus proyectos como de sus planes cotidianos. En especial, gracias a Laura Kuhlmann, por ser la mejor supervisora, mentora, y amiga. Por enseñarme tanto, facilitar mi estancia, y contribuir a que fuese una experiencia fantástica.

Gracias a toda mi gente, a mis "licenciados", a mis "canteros", a los amigos de la "sinpa", a los "monteluceños", a toda esa gente importante de mi vida… Muchos/as forman parte de ella desde que era pequeño, otros/as llegaron en el instituto o en la carrera, y otros/as durante estos años de tesis, algunos/as incluso recientemente. Son amigos/as y compañeros/as de piso, de viajes, de juegos y cenas, de festivales, de laboratorio, de excursiones, de futbol, de fiestas, de crossfit, de sierra, de mil experiencias y planes… Todos y todas forman parte de mi vida por algo, y cada cual sabe por qué, creo que lo hemos hablado unas cuantas veces. Podría escribir muchísimo sobre ellos/as, pero eso da para otra tesis. Por no extenderme demasiado simplemente les doy las gracias por ser como son, por ser uno de los pilares fundamentales en mi vida, por ser responsables de que sea la persona que soy y de lo que he conseguido hasta aquí. Great minds think alike.

Gracias a toda mi familia, porque constituye el otro de los grandes pilares sobre los que se ha cimentado mi vida, y también son grandes responsables de que esté escribiendo todo esto.

Gracias a Miguel, por estar siempre ahí para lo que haga falta, y por los muchos partidos, conversaciones y buenos ratos. Gracias a mis tíos y tías, primos y primas, a Erika y a mis sobrinos Guille, Patri, Miguel, Daniel y Marina. Especial dedicatoria para mis abuelos/as, mi tío Manolo y mi tía Nina. Y como no, también a Pancho y Tango (mi familia peluda), por

acompañarme en todo este camino de forma incondicional, llenando mis días de buenos momentos y felicidad.

Gracias a mi hermano Enrique, por ser un referente y un ejemplo de esfuerzo y constancia, por todos los buenos ratos que hemos compartido y por haber estado siempre ahí para mí cuando lo he necesitado.

Gracias a mi hermana Rocío, por haber sido probablemente la persona más influyente en mi vida. Ha sido no solo una hermana, sino también una segunda madre, pero a la vez una amiga… El impacto que ha tenido en vida es demasiado grande, y no hace falta que lo describa aquí porque ambos lo sabemos. Al margen de lo personal, ha sido toda una referencia y una gran guía en mi carrera académica y profesional, ha tenido mucho que ver en esta tesis y por eso también se la dedico a ella especialmente.

Y por último, gracias a mi padre y a mi madre. Por todo su apoyo y ayuda incondicional a lo largo no solo de estos años de doctorado, sino de toda mi vida, de tantísimas formas y a todos los niveles, académico, profesional y personal. Por haber sido los maravillosos padres que sois y haberme brindado tantas experiencias, oportunidades, facilidades, consejos… Simplemente, gracias por darme todo en esta vida. Vosotros sí que sois la base de lo que soy y de lo que he conseguido en mi vida. Por todo ello, esta tesis es para vosotros.

INDEX

Index

Index

ABSTRACT

Abstract

ABSTRACT

Malignant melanoma (MM) is the most aggressive and life-threatening form of skin cancer and its incidence rapidly continues increasing worldwide. This type of cancer is often curable, but only if detected early. When diagnosed in early stages of disease (I and II), it has an excellent prognosis, but the mortality rate drastically rises in advanced stages (III and IV) after distant spread. Despite the progress made in recent years, diagnosis of MM remains challenging. To date, there are no suitable clinical diagnostic, prognostic or predictive biomarkers for this neoplasia. Several candidate biomarkers have been proposed but few have reached clinical application. Thus, there is still an urgent need for discovering specific useful biomarkers and for developing methods that can sensitively detect this neoplasia at the earlier pre-metastatic stages.

It is known that the extraordinary metastasis capacity and chemotherapy resistance of this type of cancer are mainly due to intratumoral heterogeneity and, specifically, to MM cancer stem cells (CSCs). These cells represent a subpopulation of cancer cells which possess stem-like functional properties such as self-renewal ability and multipotency, and they are responsible for tumor initiation, progression, therapy resistance, relapse and metastasis.

In addition, accumulating evidence supports the idea of the multiple roles that exosomes play in cancer's biology. These small extracellular vesicles are involved in cell-to-cell communication and, by transferring their cargo, cancer cell-derived exosomes are able to induce in target cells diverse signalling pathways involved in tumor initiation, sustenance, progression and metastasis. These tiny messengers are actively released by all cells, including CSCs, to the extracellular matrix and to the bloodstream, making of them an interesting source of circulating biomarkers that can be easily isolated from the different body fluids by liquid biopsies.

Abstract

In this context, several omics technologies and analytical platforms, such as metabolomics and LC-HRMS, represent powerful tools for detecting and analyzing the expression levels of circulating metabolites in liquid biopsies that might serve as potential biomarkers not only for cancer, but also for other diseases.

Taking all these facts into account, the main goal of this study was to identify potential CSC-derived exosomal and serological biomarkers using metabolomics techniques (LC-HRMS) with diagnostic, prognostic or predictive value for malignant melanoma. First, a patient-derived MM cell population enriched in CSCs was appropriately characterized. Next, exosomes derived from those MM-CSCs and serums from patients with MM were also characterized and their metabolomic profile was analyzed by LC-HRMS following an untargeted approach and applying univariate and multivariate statistical analyses. These analyses revealed significant metabolomic differences between exosomes derived from MM-CSCs compared to those from MM differentiated cells, as well as between serum-derived exosomes from patients with MM at several stages of disease and those derived from healthy individuals. Various metabolites showed a clear differential pattern of expression across the different sample groups of comparison and some of them were tentatively identified. Interestingly, we identified similarities in some structural lipids from both CSC-derived exosomes and those derived from patients with MM, such as the glycerophosphocoline PC 16:0/0:0. According to biomarker evaluation models, all those differential metabolites showed an excellent discrimination capacity between the two groups of samples (patients with MM and healthy controls), suggesting that they could be considered as potential exosomal biomarkers for this disease. Taking together, these results proved that metabolomic characterization of CSC-derived exosomes sets an open door to the discovery of clinically useful biomarkers for MM diagnosis.

Along the same line and aiming at the same objective, another similar metabolomic study was also carried out but using a larger sample size. A total of 105 serum samples from both healthy individuals and patients with MM were analysed by LC-HRMS, following a similar nontargeted approach. Here again, significant metabolomic differences were found between patients in stage I of disease and healthy controls, and 10 candidates were consequently selected and identified as different classes of glycerophospolipids such as glycerophosphoethanolamines (PEs), glycerophosphocholines (PCs), cytidine diphosphate diacylglycerol (CDP-DG), or oxidized glycerophospholipids (POB-PS and PKOHA-PG). They all were suggested as potential biomarkers for early diagnosis of MM, since they yielded remarkable diagnostic capacities based on ROC curves analyses and biomarker evaluation models.

All together, the results presented herein provide evidence that metabolomics and LC-HRMS analytical platforms represent powerful tools for the identification and quantification of exosomal and serological metabolites in liquid biopsies, which could serve as potential biomarkers not only for MM, but also for other types of cancer.

Given we are living in the era of effective molecular targeted treatments and immunotherapies, the discovery, validation and implementation into clinic of suitable biomarkers is more necessary than ever. Consequently, more funding and research are needed in order to find suitable biomarkers that could aid or improve early and accurate MM diagnosis. In this regard, untargeted LC-MS-based metabolomics applied to liquid biopsies and circulating compounds could pave the way for those achievements, since studies like this demonstrate its value for biomarker research, as well as its general applicability for translational research and precision medicine in oncology.

Abstract

RESUMEN

Resumen

RESUMEN

El melanoma maligno (MM) es el tipo de cáncer de piel más agresivo y potencialmente mortal que existe, y su incidencia mundial sigue aumentando actualmente a un gran ritmo. Este en particular, es un tipo de cáncer altamente curable, pero solo si se detecta a tiempo. Cuando se diagnostica en un estadio temprano de la enfermedad (I y II), tiene un pronóstico excelente, pero la tasa de mortalidad aumenta notablemente en los estadios avanzados (III y IV) cuando se ha diseminado a otras partes del cuerpo. A pesar de todos los esfuerzos que se han realizado en los últimos años, el diagnóstico del MM sigue presentando dificultades. Por el momento, todavía no existen biomarcadores diagnósticos, pronósticos o predictivos adecuados para esta neoplasia. Aunque varios biomarcadores candidatos han sido propuestos, pocos han demostrado ser eficaces para su aplicación en la práctica clínica. Por tanto, aún existe una urgente necesidad de descubrir biomarcadores útiles específicos y desarrollar métodos sensibles que puedan detectar esta neoplasia en sus etapas tempranas pre-metastásicas.

Se sabe que la extraordinaria capacidad de metástasis y resistencia a la quimioterapia de este tipo de cáncer se debe principalmente a la heterogeneidad intratumoral, y en particular a las células madre cancerígenas (CMCs). Estas células representan una subpoblación de células tumorales que poseen propiedades funcionales similares a las de las células madre, como la capacidad de auto-renovación y diferenciación en distintos tipos celulares, y son responsables del inicio, progresión, resistencia a la terapia, recaída y metástasis de los tumores.

Por otra parte, numerosas investigaciones respaldan las múltiples funciones que desempeñan los exosomas en la biología del cáncer. Estas pequeñas vesículas extracelulares están implicadas en la comunicación intercelular y, al transferir su carga, los exosomas derivados de células cancerígenas pueden inducir en las células diana diversas vías de señalización

implicadas en la formación, el sustento, la progresión y la metástasis del tumor. Estos diminutos mensajeros son liberados activamente por todas las células, incluidas las CMCs, a la matriz extracelular y al torrente sanguíneo, lo que los convierte en una interesante fuente de biomarcadores circulantes fácilmente aislables de los diferentes fluidos corporales mediante biopsias líquidas.

En este contexto, varias tecnologías ómicas y plataformas analíticas, como la metabolómica y la cromatografía líquida acoplada a la espectrometría de masas de alta resolución (LC-HRMS), representan poderosas herramientas para detectar y analizar los niveles de expresión de metabolitos circulantes que podrían servir como potenciales biomarcadores no solo en cáncer, sino también en otras enfermedades.

Por todo ello, el objetivo principal de este estudio fue identificar posibles biomarcadores exosomales y serológicos derivados de CMCs mediante el uso de técnicas metabolómicas (LC-HRMS) con valor diagnóstico para el melanoma maligno. En primer lugar, se caracterizó adecuadamente una población de células de MM enriquecidas en CMCs, en una línea celular primaría derivada de un paciente con MM. A continuación, también se caracterizaron los exosomas derivados de esas CMCs de MM y de sueros de pacientes con MM y se analizó su perfil metabolómico mediante LC-HRMS siguiendo una aproximación no dirigida y aplicando análisis estadísticos univariados y multivariados. Estos análisis revelaron diferencias metabolómicas significativas entre exosomas derivados de CMCs de MM en comparación con los de células diferenciadas de MM, así como entre exosomas derivados de suero de pacientes con MM en distintos estadios de la enfermedad y los derivados de individuos sanos. Varios metabolitos presentaron un patrón claro de expresión diferencial entre los diferentes grupos de muestras comparadas y a algunos de ellos se les pudo asignar una identificación tentativa.

Curiosamente, se detectaron ciertas similitudes en algunos lípidos estructurales de los exosomas derivados de CMCs y los derivados de pacientes con MM, como la glicerofosfocolina PC 16: 0/0:0. En base a los modelos de evaluación de biomarcadores generados, todos los metabolitos diferenciales mostraron una excelente capacidad de discriminación entre los dos grupos de muestras (pacientes con MM y controles sanos), siendo por tanto susceptibles de ser considerados como potenciales biomarcadores exosomales de esta enfermedad. En conjunto, estos resultados demostraron que la caracterización metabolómica de exosomas derivados de CMCs abre una puerta al descubrimiento de biomarcadores clínicamente útiles para el diagnóstico del MM.

En la misma línea y con el mismo objetivo, también se llevó a cabo otro estudio metabolómico similar pero con un tamaño de muestra mayor. Un total de 105 muestras de suero de pacientes con MM y de individuos sanos fueron analizadas por LC-HRMS, siguiendo una aproximación no dirigida similar. De nuevo, se encontraron diferencias metabolómicas significativas entre pacientes en estadio I de la enfermedad y controles sanos, por lo que se seleccionaron 10 candidatos que fueron identificados como distintos tipos de glicerofoslípidos, como glicerofosfoetanolaminas (Fes), glicerofosfocolinas (FCs), citidín difosfato diacilglicerol (CDP-DG) o glicerofosfolípidos oxidados (POB-PS y PKOHA-PG). Todos ellos fueron sugeridos como posibles biomarcadores para el diagnóstico precoz del MM, ya que mostraron notables capacidades diagnósticas basadas en análisis de curvas ROC y los modelos de evaluación de biomarcadores.

En conjunto, los resultados presentados en este trabajo demuestran que la metabolómica y las plataformas analíticas LC-HRMS, representan una poderosa herramienta para la identificación y cuantificación de metabolitos exosomales y serológicos en biopsias líquidas, que

podrían servir como posibles biomarcadores no solo para MM, sino también para otros tipos de cáncer.

Puesto que estamos viviendo una era de múltiples tratamientos moleculares dirigidos e inmunoterapias eficaces, el descubrimiento, la validación y la implementación en la clínica de biomarcadores adecuados son más necesarios que nunca. En consecuencia, todavía se necesita más financiación y más esfuerzos de investigación para encontrar biomarcadores adecuados que puedan ayudar o mejorar el diagnóstico temprano y preciso del MM. En este sentido, la metabolómica no dirigida basada en LC-MS aplicada a biopsias líquidas y compuestos circulantes podría allanar el camino hacia esos logros, ya que estudios como este demuestran su valor para la investigación de biomarcadores, así como su aplicabilidad general a la investigación traslacional y a la medicina de precisión en oncología.

INTRODUCTION

INTRODUCTION

1. CANCER

Cancer can be considered as a heterogenic group of disorders with very different biological properties. The term cancer is used in a general sense for many diseases characterized by a rapid, abnormal and uncontrolled cells proliferation that can grow beyond their normal boundaries, forming distinct masses in a tissue or organ, as well as a great degree of anaplasia (scarce cell differentiation). Malignant tumors also have the property of invading adjacent structures and the ability to spread to other parts of the body through the bloodstream and the lymphatic system by the process known as metastasis [1].

The risk of suffering from many types of cancer can be reduced by keeping healthy lifestyle habits and avoiding certain commonly known risk factors, such as tobacco or alcohol consumption, obesity, or harmful radiation exposure, among others. Furthermore, many cancers have a fairly high cure rate by surgery, radiotherapy or chemotherapy, especially when detected early [2].

1.1. Epidemiology

According to the most updated data compiled by GLOBOCAN, in 2020 there were more than 19.2 million of new cases and almost 10 million of deaths caused by cancer worldwide (**Figure 1**). The incidence and mortality vary depending on the different world areas, developed and developing countries, and sex. At a global level, the most commonly diagnosed types of cancer, for both sexes and all ages are: breast, lung, colorectum, prostate, stomach, liver, cervix uteri, oesophagus, thyroid, bladder, and other cancers (**Figure 1**) [3].

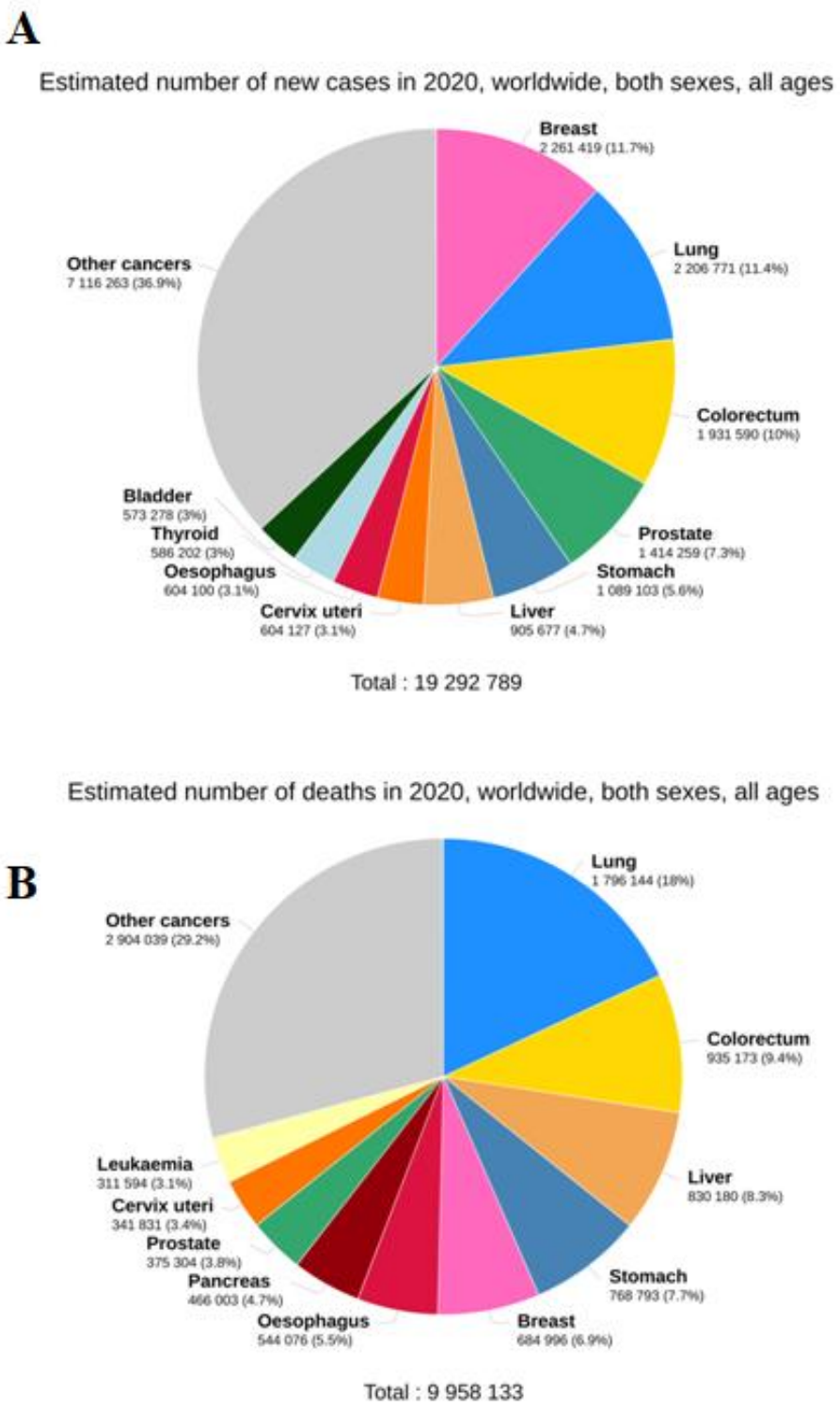

Figure 1. Pie charts representing the distribution of cases (**A**) and deaths (**B**) for the 10 most common cancers in 2020 for both sexes (worldwide). Source: GLOBOCAN 2020.

Noncommunicable diseases (NCDs) currently accounts for most global deaths and cancer, in particular, is expected to become the main cause of death worldwide in near future, being their incidence and mortality rates estimated to continue to rapidly increase (+49.7% and +62.5%, respectively) in the next decades (**Figure 2**), partially due to demographic changes [3].

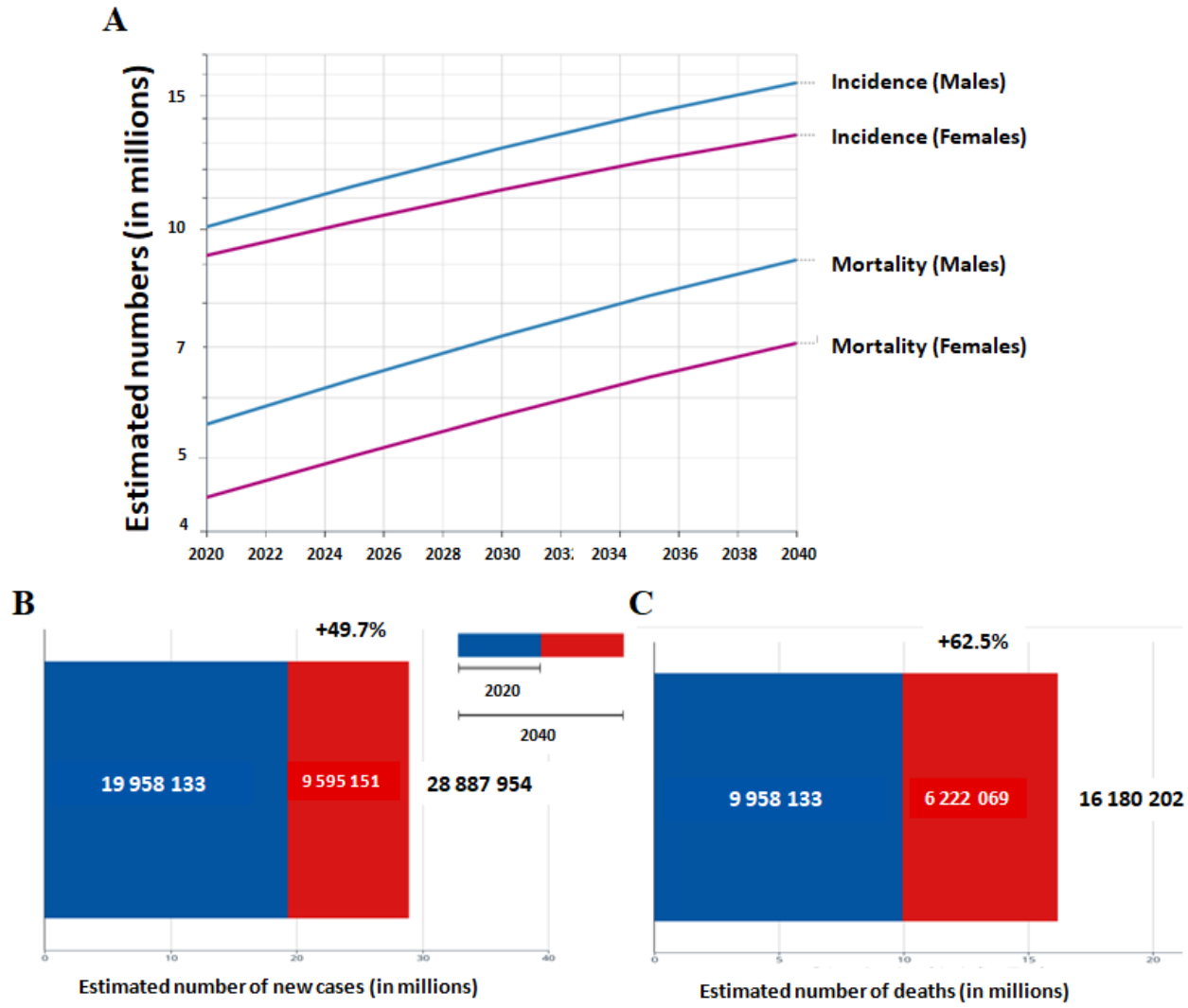

Figure 2. Future trends for incidence and mortality rates in both sexes (**A**) and estimated numbers for new cases (**B**) and deaths (**C**) from 2020 to 2040. Source: GLOBOCAN 2020.

Introduction

In Europe, incidence and mortality rates differ from the global ones, being higher in certain types of cancer such as non-melanoma skin cancer or melanoma of skin, which is relevant to the content of this work [3].

In Spain, malignant tumors still represent one of the most important causes of mortality. In 2020, according to the latest data released by the National Statistics Institute, cardiovascular diseases remained the leading cause of death, representing 23.0% of the total deaths. Historically, malignant tumors were ranked in the second place, but last year they were narrowly overcome by infectious diseases (20.9%), which caused an increase of 1,687.7% compared to the first five months of 2019. It should be noted that 67.5% of deaths in this group corresponded to confirmed cases of COVID-19 and 26.9% to supposed cases. Consequently, in 2020 neoplasms were relegated to the third place (20.4%) in this mortality ranking, even though they were increased by 0.5% compared to the previous year. The most frequently diagnosed types of cancer in Spain (**Figure 3**) are colorectal, which represents 14.3%, of total cases, prostate (12.3%), breast (12.1%), lung (10.3%) and urinary bladder (6.6%) [3].

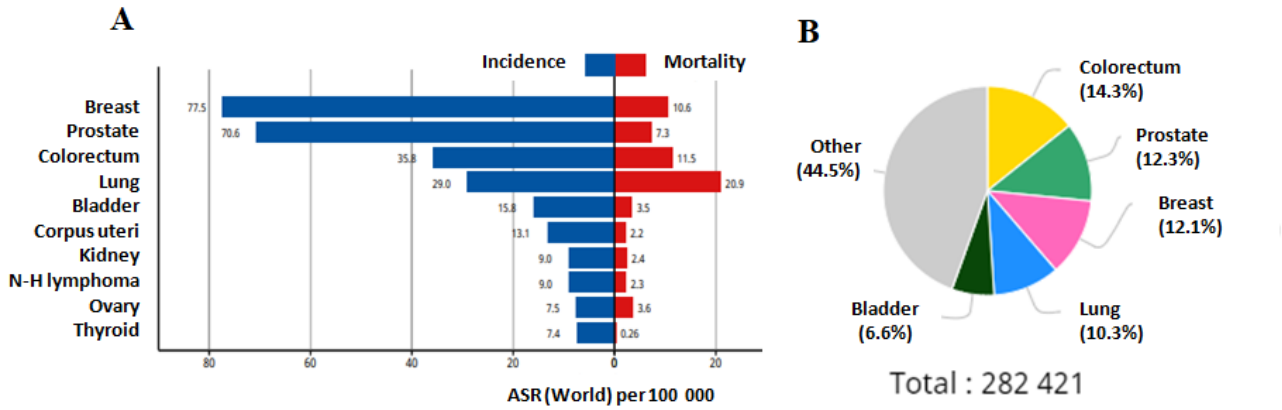

Figure 3. Dual bars representing the age-standardized incidence and mortality rates (**A**) and pie chart representing the number of new cases (**B**) for the most common cancers in Spain. Source: GLOBOCAN 2020.

1.2. Etiology

Malignant tumor cells are originated from normal cells that typically suffer a precancerous lesion and go under a stepwise process by which they suffer several changes. That process is triggered by a combination of both individual's genetic and environmental factors [4].

Among the external agents, carcinogens deserve a special mention, since they are substances, radionuclides and radiation able to enhance the probabilities of cancer development. They can be classified according to their physical, chemical or biological nature [5,6]. Physical carcinogens include several types of ionizing radiation from X-rays or from radioactive materials in industry, or ultraviolet (UV) rays from sunlight, which is the most harmful type of radiation in terms of carcinogenic power. Indeed, it is highly associated to a notorious increase of developing skin cancer [4]. Among chemical carcinogens are included several chemical products effluents from industry and environmental pollutants from automobiles, residences, and factories such as acrylamide, arsenic, formaldehyde, benzene, or tobacco smoke, which contains nitrosamines, polycyclic aromatic hydrocarbons and many other carcinogenic compounds. Indeed, tobacco smoke represents the major source of chemical carcinogens for humans, and it is highly responsible for many cancer cases in developed countries, being lung cancer the most associated one. The last kind of carcinogenic agents are the biological ones, which include several microorganisms or viruses, such as human papillomaviruses, the Epstein-Barr virus, or the hepatitis B and C viruses, which are capable of induce cancer formation [4].

Other external factors are those related to lifestyle. For instance, it has been widely demonstrated that obesity or alcoholism are highly associated with higher risk of certain types of cancers, whereas other healthy lifestyle-related habits such as regularly practicing physical activity or keeping a balanced diet significantly reduce the probabilities of suffering from other

tumors. Furthermore, these healthy habits remarkably improve life's quality of cancer patients, their treatment outcomes and reduce the risk of recurrence [7].

On the other hand, individual's genetic-related factors must be also taken into account, although it is estimated that only about 5-10% of some types of cancers seem to have an hereditary risk component due to certain genetic variations [6]. In this regard, several mutations in specific genes have been proved to be associated with higher risk of some types of cancer [8].

1.3. Carcinogenesis

Carcinogenesis, also called oncogenesis or tumorigenesis, is a stepwise process whereby normal cells are transformed into cancer cells, by going through great changes at the metabolic, genetic, epigenetic and behavioral levels. As a consequence, cell division regulatory mechanisms are disrupted, leading to an uncontrolled and premature cell proliferation. In addition, cancerous cells are able to avoid the defensive mechanisms of immune system and, eventually, migrate to distant organs and cause metastases (**Figure 4**) [1,7].

To date, several biological characteristics are firmly established as hallmarks of cancer (**Figure 5**). In 2011, Hanahan and Weinberg originally highlighted six of them: sustainability of proliferative signaling, evasion of growth suppressing mechanisms, induction of angiogenesis, activation of invasion and metastasis ability, resistance to cell death, and enablement of replicative immortality [9]. However, it has been shown that the promotion of inflammation and the increase in genome instability and mutation rates contribute to the acquisition of deregulation of cellular energy metabolism and the prevention of immune destruction, all of which are facilitating factors of the tumor cells that should be included along with the hallmarks mentioned above (**Figure 5**) [10,11].

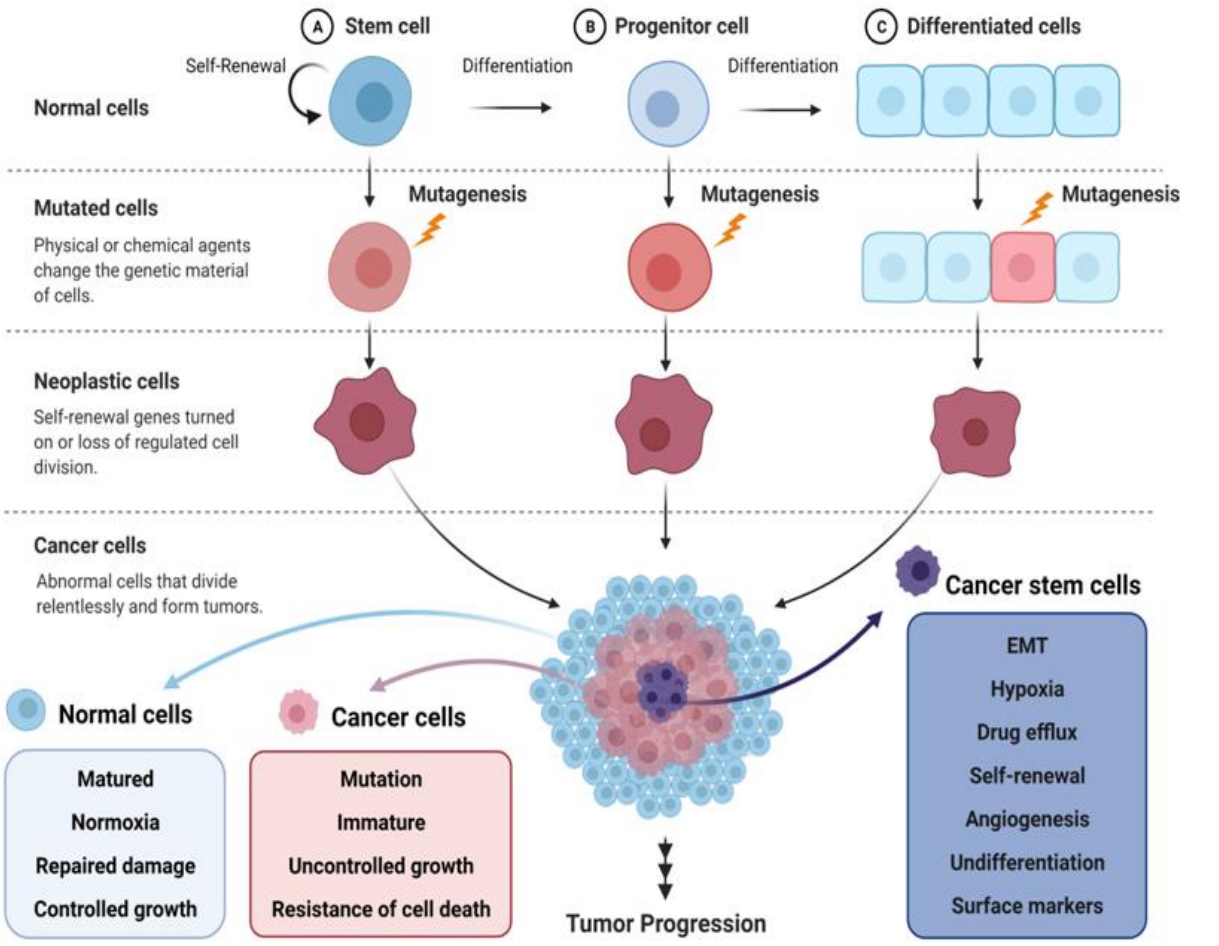

Figure 4. Schematic representation of cancer cell transformation. Normal cells (whether stem, progenitor or differentiated) can undergo several mutagenic events that affect their genetic material, including genes involved in the regulation of self-renewal or normal cell division. As a consequence, they become cancer cells that divide uncontrollably and show specific differential characteristics.

There are different ways for a cancer cell to maintain proliferative signaling, including autocrine mechanisms such as growth factors production and release by the tumor cells themselves [12], or by paracrine interactions with closely located supporting normal cells [13], as well as increasing the expression of the corresponding surface receptors in order to increase their sensitivity to those factors. Also, mutations or expression disruptions in several proto-oncogenes or oncogenes, along with the subsequent altered expression of their corresponding

oncoprotein products, are also involved in this complex process of cell proliferation maintenance [14,15]. On the other hand, cancer cells must also evade growing suppressing mechanisms, by inactivating the expression of certain tumor suppressor genes that are involved in the regulation of normal cell proliferation [15,16].

In order to meet all their metabolic requirements and blood supply, cancer cells stimulate angiogenesis, the process by which new blood vessels are formed. Nevertheless, this tumor-associated neovasculature is structurally and functionally different from the normal one, and it is characterized by its anarchic and heterogenic organization [17].

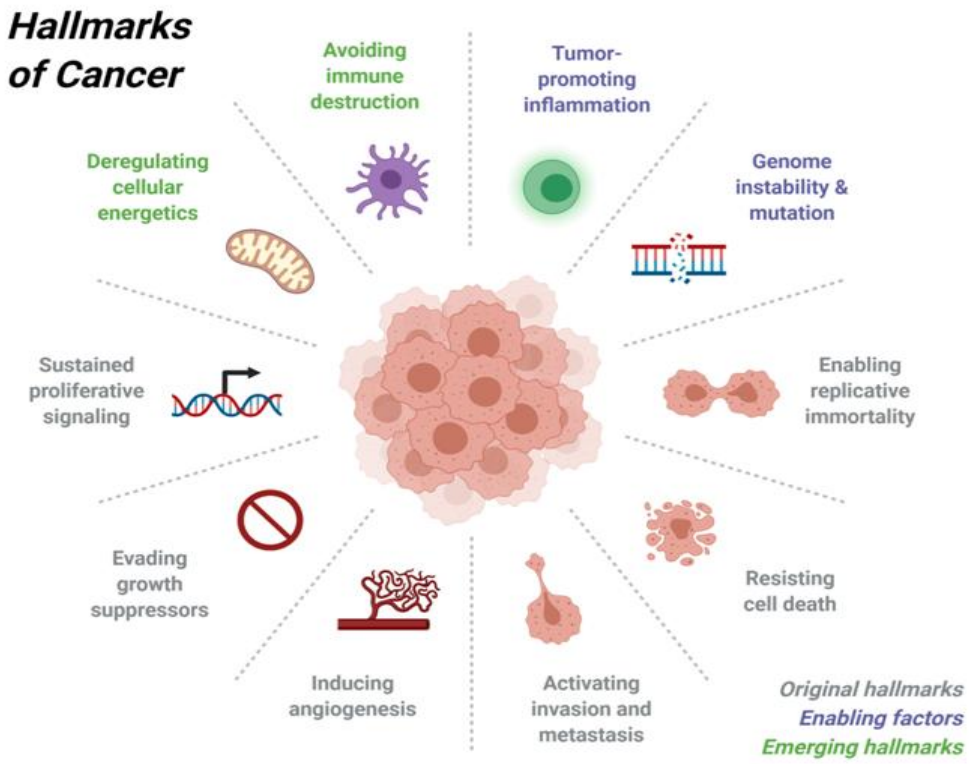

Figure 5. Hallmarks of cancer. The scheme encompasses the ten main biological capabilities acquired during the staggered development of human tumors. These hallmarks traits might be gained at different stages of the carcinogenesis process and are functional within the context of the tumor microenvironment.

From primary tumor formation, tumor cells eventually acquire the capacity to spread and invade distant organs within the body. This process is known as metastasis, and it is a complex staggered process which involves several steps. First, the primary tumor generates new vasculature (neoangiogenesis) and grows until it starts local invasion through the extracellular matrix and cell layers of the surrounding stroma. Eventually, there is an intravasation of tumor cells to the blood and lymphatic vessels, where they survive and circulate until they are arrested in distant organs, and their extravasation to the tissue parenchyma takes place. At this point, these cells start to create a pre-metastatic niche, which leads to micrometastases and ultimately macroscopic tumors formation, being the metastatic colonization process completed (**Figure 6**) [18,19].

Tumor cells are also capably of avoiding apoptosis, which is the programmed type of cell death that plays an essential role in many processes, including maintaining homeostasis and normal development, as well as elimination of infected or transformed cells. The two main branches of this strictly regulated cell death are the intrinsic and extrinsic pathways, in which the signals initiating cell death are originated inside or outside the cell, respectively [20,21]. In addition, cancer cells also acquire an unlimited replication potential in a process known as cell immortalization [9].

Apart from those classically accepted hallmarks of cancer, there are other emerging characteristics and enabling factors that allow tumor cells to achieve those previously described ones. One the one hand, several inflammatory processes take place within the tumor context, and there is certain tumor-promoted inflammation that also contribute to the acquisition of some of the previously described properties of tumor cells [22,23]. On the other hand, it has been also shown that cancer cells present a particular genome instability and a high mutation rate,

attributable to certain damages in DNA maintenance and repair mechanisms as well as to telomeric dysfunction [11,24].

Last but not least, while some cancer cells are successfully destroyed by host immune cells, some others manage to survive throughout several mechanisms, highlighting the two roles that immune system plays in oncogenesis by both cancer promotion and prevention [25].

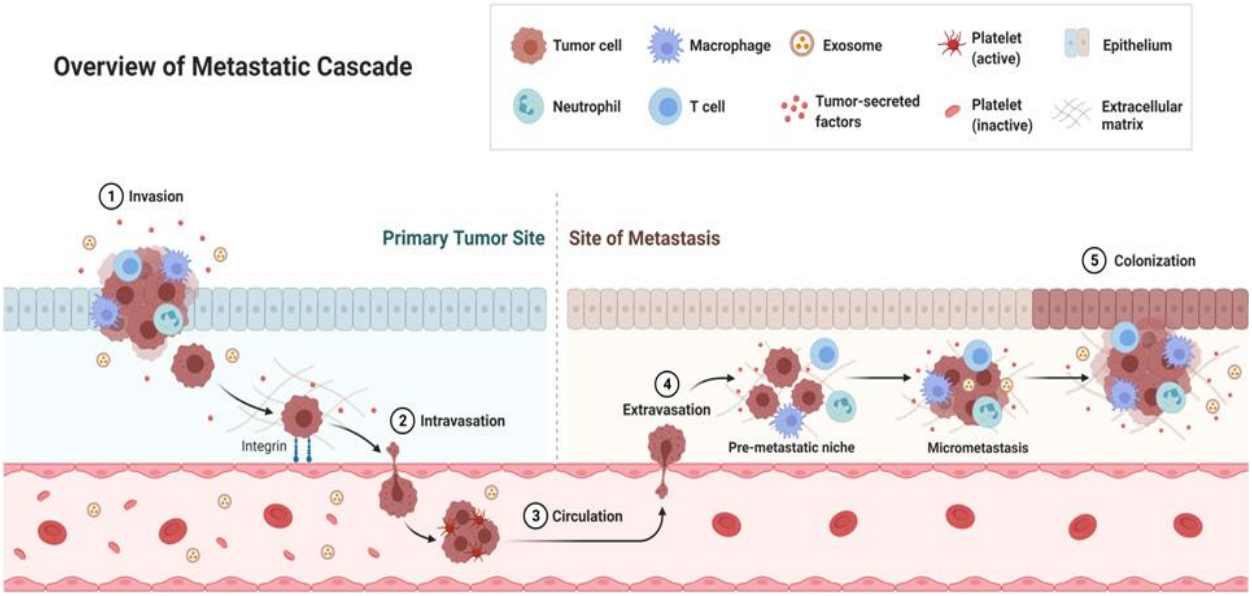

Figure 6. Schematic representation of the invasion-metastasis cascade. Metastasis is a multistep process where: 1) tumor cells migrate into adjacent tissues (local invasion); 2) translocate and enter the systemic circulation (intravasation); 3) survive in the circulation and reach distant parts of the body; 4) attach to endothelial cells, translocate again and enter to a distant tissue or organ (extravasation), where tumor cells adapt to survive and form pre-metastatic niches, micro-metastasis; 5) proliferation and formation of macrometastasis (colonization). This process is also orchestrated by several tumor-secreted factors, such as cytokines or exosomes.

Another relevant concept that must be taken into account is the tumor microenvironment (TME) or also called niche. Apart from the heterogeneous population of cancer cells within the tumor mass, their TME consists of a variety of resident and infiltrating host cells, secreted factors and extracellular matrix proteins. Tumor growth and progression is profoundly influenced by interactions of tumor cells with niche stromal and inflammatory cell populations, that ultimate determine the tumor development, establishment of metastases or dormant micrometastases, and even resistance to treatment. (**Figure 7**) [9,26].

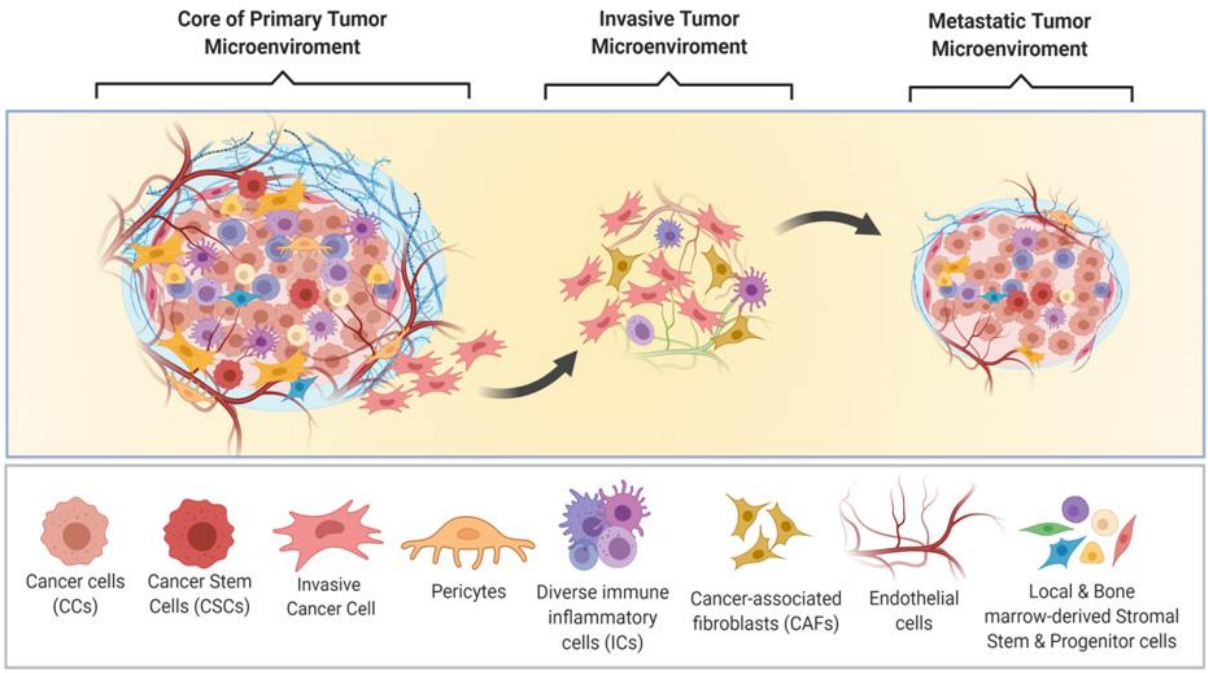

Figure 7. Representation of the distinct cell types that constitute most solid tumors and the distinctive tumor microenvironments (TMEs), which change and evolve as tumors invade normal tissue and thereafter seed and colonize distant tissues. The abundance, histological organization, and phenotypic characteristics of these different cell types, as well as of the extracellular matrix, determine the character of the different TMEs.

2. MALIGNANT MELANOMA

Skin cancer (SC) is a type of cancer originated by the uncontrolled growth of aberrant skin cells due to several oncogenic events that lead them to proliferate beyond their natural limits, causing malignant tumors. The vast majority of skin cancers are commonly classified in two main groups: melanoma and non-melanoma skin cancers [27].

Non-melanoma skin cancers (NMSCs) refers to the most common types of SC that slowly develop in the upper layers of the skin, including basal cell carcinoma (BCC), squamous cell carcinoma (SCC), as well as others much more unusual skin tumors. These cancers are normally originated in body areas exposed to the sun, such as the arms, legs, head or neck, but they might be found elsewhere as well. BCCs, which are the most common ones (~80%), normally show a slow progression and highly unlikely propagation to distant organs unless left untreated. SCCs, which represent the second most form of SC (~20%) show higher chances of invading deeper skin layers and spreading to distant parts of the body [28]. The term NMSCs is meant to distinguish these more common types of skin cancer from the less common one: Melanoma [27].

Melanoma, or also known as malignant melanoma (MM), is a more dangerous form of skin cancer that originates from melanocytes (pigment-producing cells) and presents much higher chances of growing and spreading to distant organs if it is not treated at an early stage. Although it is least common type of SC (~1%), is the most aggressive and lethal one, accounting for the highest number of deaths caused by skin cancers [3,27,29].

2.1. Epidemiology

Historically, melanoma was an unusual type of cancer, but in the last 50 years its incidence has been increased more than almost any other cancer [3,30]. Over the last decade, the annual cases of MM have risen up by nearly 50% to over 287,000 new cases, which translates to over 60,000 MM-related deaths per year [31]. Actually, dermatologists believe that skin cancer should be currently considered, with all due caution, a global epidemic.

According to the latest data from World Health Organization (WHO), it is estimated that there are currently over one million cases of skin cancer each year, including both NMSCs and MMs. However, it should be taken into account that NMSCs is under reported, since several countries do not have official records, so the real incidence is widely acknowledged to be higher. Thus, this type of cancer is one of the most extended around the world [3].

Considering both NMSC and MM number of deaths, it is estimated that one person dies from SC every 4 minutes, which is a tremendously shocking statistic considering that this type of cancer is one of the most preventable and curable, if detected early [32]. Nonetheless, the predictions for the next 20 years are even more disturbing. According to the new online tool created by the Global Cancer Observatory, it is estimated that the number of new MM cases diagnosed worldwide will rise 18% and 62% by 2025 and 2040, respectively, and the number of melanoma-related deaths will suffer an increase of 20% by 2025 and of 74% by 2040 [3].

Regarding melanoma, according to the most updated data reported by GLOBOCAN, in 2020 there were reported 324,635 new cases (1.7% of total cancers) and almost 57,043 deaths (0.6% of total) caused by MM worldwide (**Figure 8**). Its incidence and mortality rates continue to steadily increase every year by 4-6%, and rose between 2008 and 2018 by 44% and 32%,

respectively. However, they considerably vary among different populations depending on several factors, including ethnicity, geography, age, sex, and anatomic distribution [3,29,30,33].

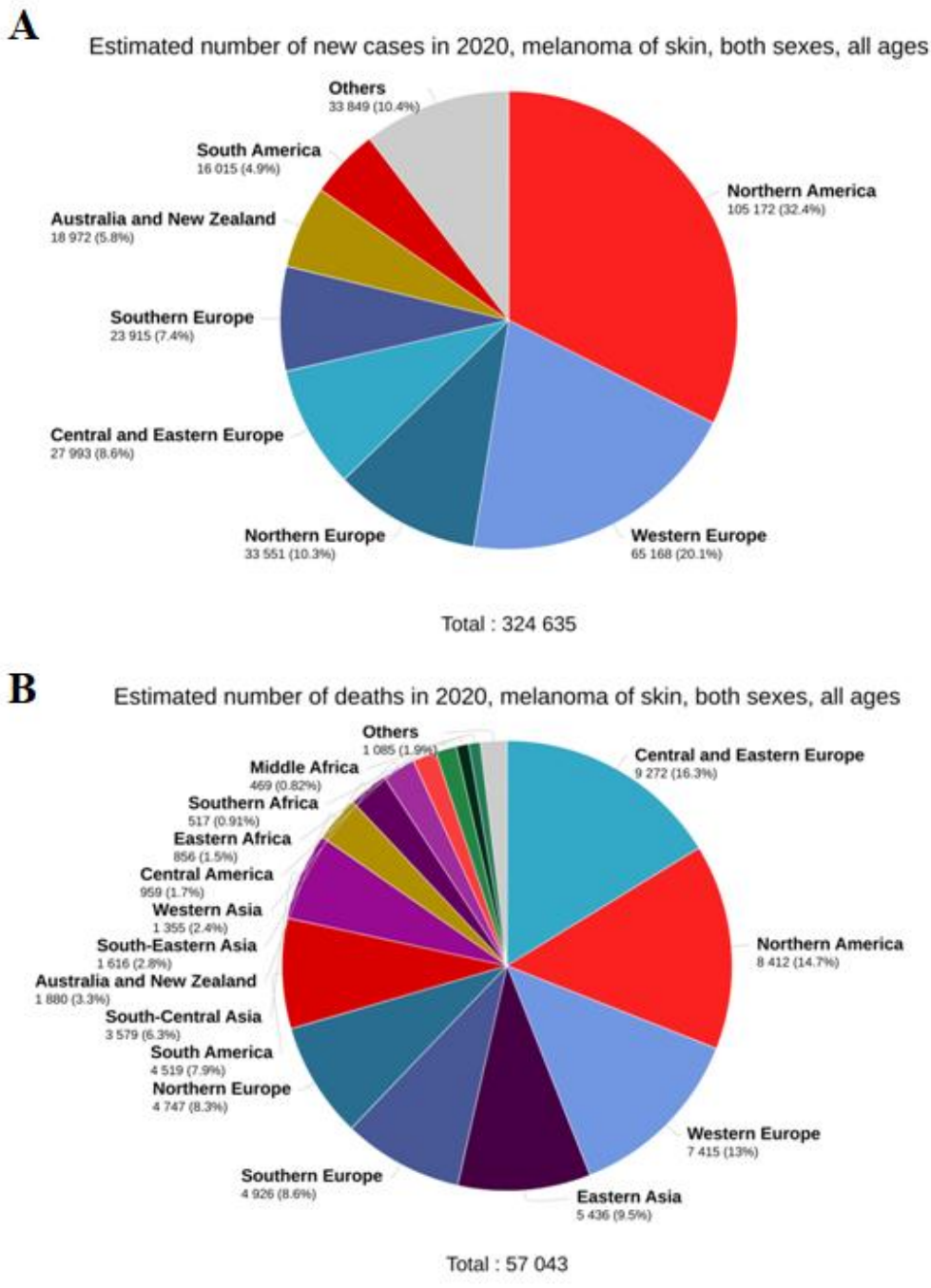

Figure 8. Pie charts representing the distribution of cases (**A**) and deaths (**B**) for malignant melanoma in 2020 for both sexes (worldwide). Source: GLOBOCAN 2020

With regards to its incidence, it is disproportionally diagnosed among fair-skinned Caucasian populations, since they have decreased levels of melanin in the skin, and therefore they are less protected from UV radiation than darker-skinned people [34]. Regardless ethnicity, there are also geographic differences, which can be attributed to differences in several factors. For instance, those related to incident UV radiation, such as atmospheric features, latitude or altitude, which explains a higher MM incidence in regions like Northern Europe, North America, Australia and New Zealand (**Figure 9**). Also, according to the mortality-to-incidence ratio (MIR), MM is one of the most treatable cancers (MIR=21%), but it there is also a marked disparity between the treatment outcomes of different countries. Overall, people in countries with a high human development Index (HDI) score are more likely to be diagnosed with melanoma, but people in countries with a lower HDI score are more likely to die from it [3,29,35].

Worldwide MM incidence is also age- and sex- dependent. For example, it steadily increases with age, reaching the highest peaks at the seventh and eighth decades of life. This trend becomes even more evident among most high-risk populations, such as Australia and New Zealand, and Northern Europe [36,37]. Additionally, despite MM is less common among people under 40 years of age, it is becoming one of the most reported cancers among adolescent and young adults in the United States [38]. Overall, men are 10% more susceptible to develop melanoma (especially after the age of 40) and 4% likely to die, which is the general trend related to sex (**Figure 10**) [29]. However, in the last year a higher rate of MMs is being reported among adolescent and young women under 40 years of age, probably due to their more frequent use of indoor tanning [38].

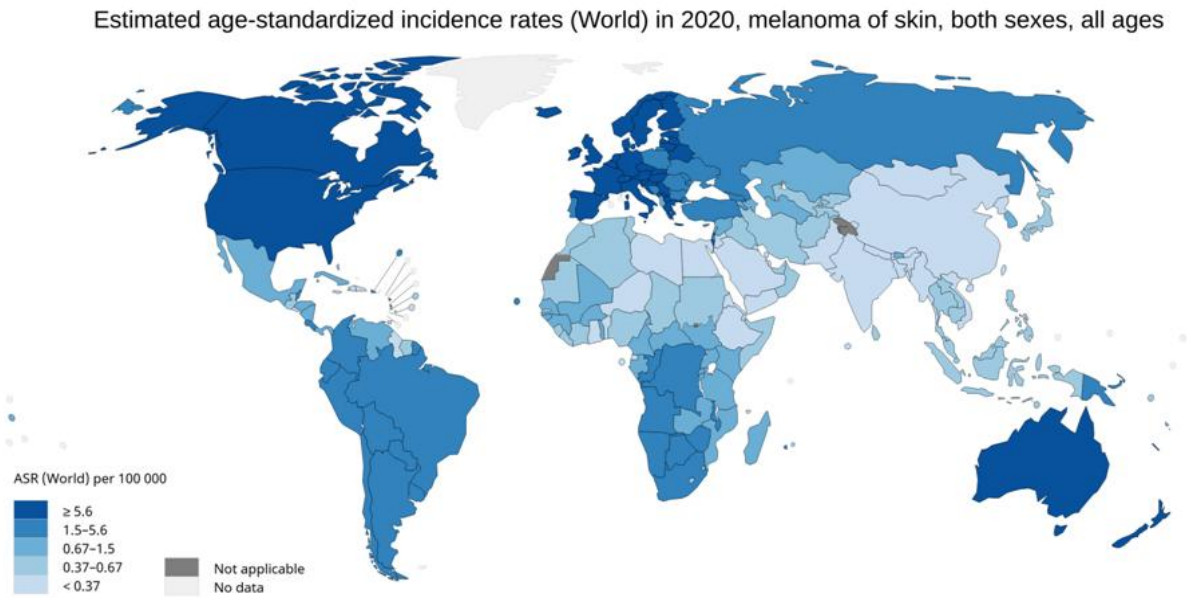

Figure 9. Global map representing worldwide melanoma age-standardized annual incidence rate by geography. Age-standardized rate (ASR) by world is expressed per 100,000 persons. Source: GLOBOCAN 2020.

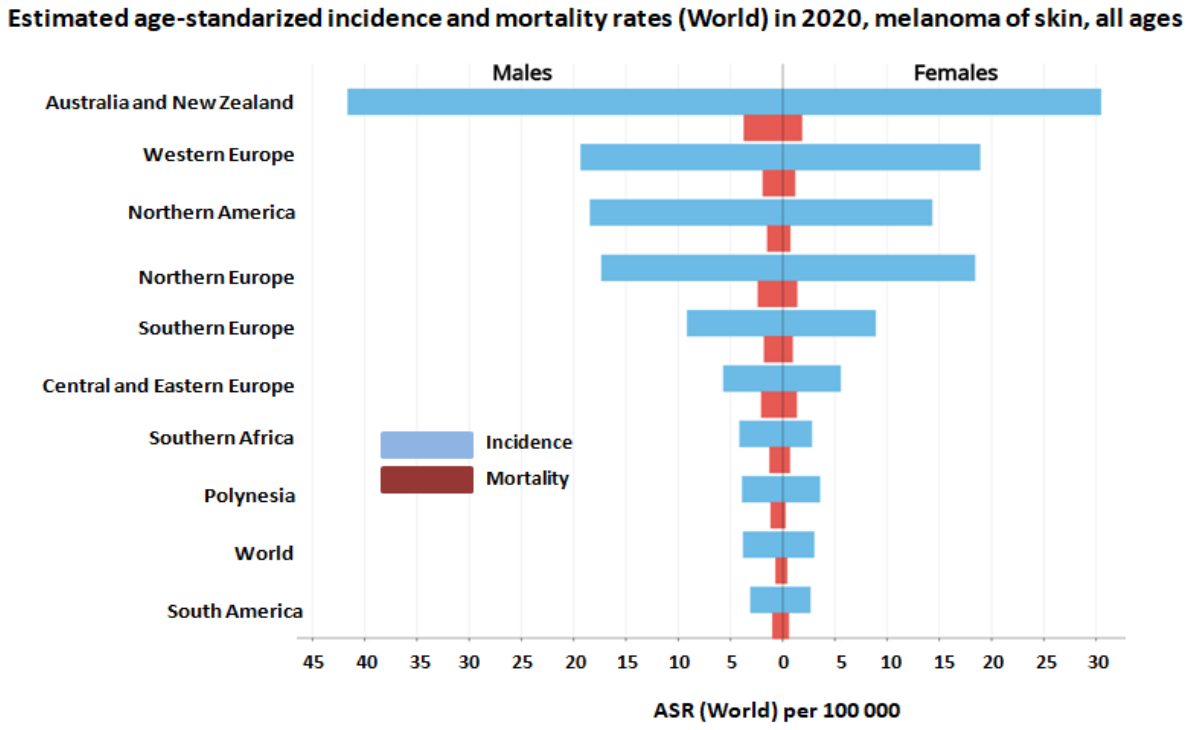

Figure 10. Dual bar graph representing the ~~Age~~age-standardized incidence and mortality rates (**A**) for malignant melanoma by sex, all ages. Source: GLOBOCAN 2020.

Regarding MM anatomic distribution, MMs are generally reported on high sunlight-exposed parts of the body such as the head, neck, arms and limbs. However, some age- sex- or geographic-dependent differences have also been reported [39,40]

2.2. Etiology

There are several risk factors that predispose to the development of not only melanoma, but also any type of skin cancer. The most important ones include UV light exposure, presence of moles, fair skin, freckling and light hair, family or personal history of skin cancer, having a weakened immune system, some other factors associated with ethnicity, sex and age [27,28].

The vast majority of MMs (about 86%) seems to be associated with sun light (UV) exposure to and a history of sunburns [41]. The carcinogenic role of UV is widely known, representing a classical risk factor associated with several types of cancer, including MM [34,42,43]. On average, a person has double chances of developing a MM if they have struggled with more than 5 sunburns throughout their lifetime [44] or just by having suffered one blistering sunburn during their childhood or adolescence [45]. In addition to the recreational outdoors exposure, indoor tanning represents one of the most dangerous practices with regards to SC appearance. Those people who have ever tanned indoors have tremendously higher risk of developing different types of SC, including MM. In fact, the chances of suffering from SC because indoor tanning are greater than developing lung cancer because of smoking [46].

The majority of moles are completely benign, but the presence of many of them increases the probabilities of developing a MM, since 20-30% of them are originated in previously existing moles [47].

Ethnicity, age, and sex-related factors also increase the risk of developing MM. For example, people with fair complexion, blond or red hair, blue eyes and freckles are more susceptible of developing MM. Generally speaking, SC incidence is about 20 times higher in White people than in other ethnicities, and is more likely to occur in older people, being white men over age 55 the most commonly diagnosed cases. Also, it is estimated than men have higher probabilities of MM appearance than women in their life time [28,30]

Another important risk factor is having a family history of MM as well as having already suffered any type of SC, including oneself. About 10% of people diagnosed with this disease have one or more first-degree relatives who have previously had MM. Besides, this type of SC tends to occur at younger age when it runs in families [27,28].

The molecular mechanisms underlying the carcinogenesis of this type of cancer, as well as those responsible for the sporadic transformation of some moles into a MM are still under revision. However, several mutations have been associated to MM development; some of them are acquired during a person's lifetime, while other are inherited. The majority of melanomas arise from somatic acquired mutations, which are by the way highly associated to UV radiation [48]. For instance, some of the most common mutations in MM are found in the MAPK signaling pathway, such as BRAF or other MAPK mutations like V600E. MAPK and BRAF mutations have been reported in ~70% and ~50 of MM, respectively. This signaling pathway, and BRAF in particular, has garnered a lot of interest from a therapeutic point of view, since this oncogene is only active in malignant cells, easy to target and mutated in a high percentage of MM patients [49,50].

Among inherited mutations, which account for 5-12% of MMs, the most common ones are found in CDKN2A and NER pathway, such as XP genes. CDKN2A (also known as P16),

which is a tumor suppressor involved in cell cycle control and p53 stabilization, is present in 40% of hereditary MMs [51]. Mutations in NER genes, which are associated with repair of radiation-induced DNA damage, result in accumulated mutations in the skin caused by UV radiation or chemicals and therefore, an increased risk of SC. That is the reason why people with xeroderma pigmentosum, a diseased caused by inherited mutations in these genes, have higher risk of suffering from MM [28,50,51].

Other mutations commonly driving MM tend to be found in signaling pathways involved in proliferation (NRAS and NF1), growth and metabolism (PTEN and C-KIT), apoptosis resistance (TP53), cell identity (ARID2) or replicative lifespan (TERT). However, their frequencies vary among different tumors. For example, C-KIT is more frequent in MMs that develop in parts of the body rarely exposed to sunlight [28,49,50].

2.3. Subtypes

Malignant melanoma is a heterogeneous type of skin cancer, and different subtypes can be distinguished according to several characteristics such as physical appearance, location, thickness, presence or absence of ulceration, mitotic rate, presence of tumor-infiltrating immune cells, margin status in a biopsy sample or different mutations like those previously described [27].

The most reliable features used by dermatologists in terms of first visual examination are the thickness, ulceration and mitotic rate of primary MM. A mole can be thin (<1 mm), associated with low risk of spreading, intermediate (1-4 mm), or thick (>4 mm), associated with higher chances of spread and recurrence. At the same time, the presence of ulceration and an

elevated mitotic rate are also related with higher risk in this regard. All combined are helpful in terms of determining stage, treatment options, and prognosis.

Overall, the 4 most commonly known subtypes of MM are:

- Superficial spreading melanoma, which is the most usually diagnosed subtype, making up 70% of MM. It usually develops from an existing mole.
- Lentigo maligna melanoma, which tends to occur in older people. It is commonly found on higher sunlight-exposed locations, such as the face, ears or arms.
- Nodular melanoma, which accounts for about 15% of MM. It often develops rapidly as a bump on the skin, and it is usually black (but it may be pinkish or reddish).
- Acral lentiginous melanoma, which usually appears on the palms of the hands, soles of the feet, or under the nail bed. It occurs more frequently on darker-skinned people, and it is not as related to sun exposure as other subtypes.

However, several molecular MM subtypes are also defined by different mutations in some of the genes previously mentioned, such as BRAF (~50% of MMs), NRAS (~20% of MMs), NF1 (~10-15%) or C-KIT (Higher in lentigo maligna melanomas) [27].

2.4. Staging

According to the American Joint Committee on Cancer (AJCC) [52], which is an international institution that regularly revises and updates the TNM (tumor, node, metastasis) staging system of several types of cancer, MM present 4 different stages (**Figure 11**) [27,53]:

- Stage 0: It refers to MM in situ, which means melanoma cells are found only in the outer layer of skin or epidermis. This stage is very unlikely to spread to other parts of the body.

- Stage I: The primary tumor is still very thin (<1 mm), localized but slightly more invasive, reaching deeper layers of skin. This stage is subdivided into 2 subgroups, IA or IB, depending on the thickness (<0.8 or >0.8 mm) and ulceration (presence or absence), respectively.

Stage 0 and I are considered early localized, not spread MMs (**Figure 11**).

- Stage II: The primary tumor is thicker (>1 mm), extended through the epidermis and further into the dermis. Although they might not yet have advanced beyond the primary location, the risk of spreading is higher. In these cases, a sentinel lymph node biopsy is recommended to verify whether melanoma cells have spread to the local lymph nodes. Stage II is divided into 3 subgroups, IIA, IIB, or IIC, also depending on thickness and ulceration, which conditions the risk of spreading and the treatment regimen.

Stage II MMs are considered intermediate or high-risk MMs, still localized but more likely to spread (**Figure 11**).

- Stage III: This stage corresponds to MMs that has spread locally to a skin site located more than 2 cm away from the primary tumor, or through the lymphatic system to one or more nearby lymph nodes (sentinel lymph nodes). This phenomenon is called in-transit metastasis or satellite metastasis. This stage can also be divided into 4 subgroups, (IIIA, IIIB, IIIC, or IIID) depending on the size and number of lymph nodes involved, whether the primary tumor has satellite or in-transit metastasis, and the presence of ulceration. Thickness no longer plays a staging role.
- Stage IV: This stage describes MMs that have spread through the bloodstream to distant body areas, and can be also further classified depending on whether the cancer has spread

only to distant skin or soft tissue (M1a), to other distant organs like the lung (M1b) or to other locations not related or related with the central nervous system (M1c or M1d, respectively).

Stage III and IV are considered advanced MMs, spread beyond the primary tumor to distant parts of the body and therefore associated with poor prognosis and worse treatment outcomes (**Figure 11**).

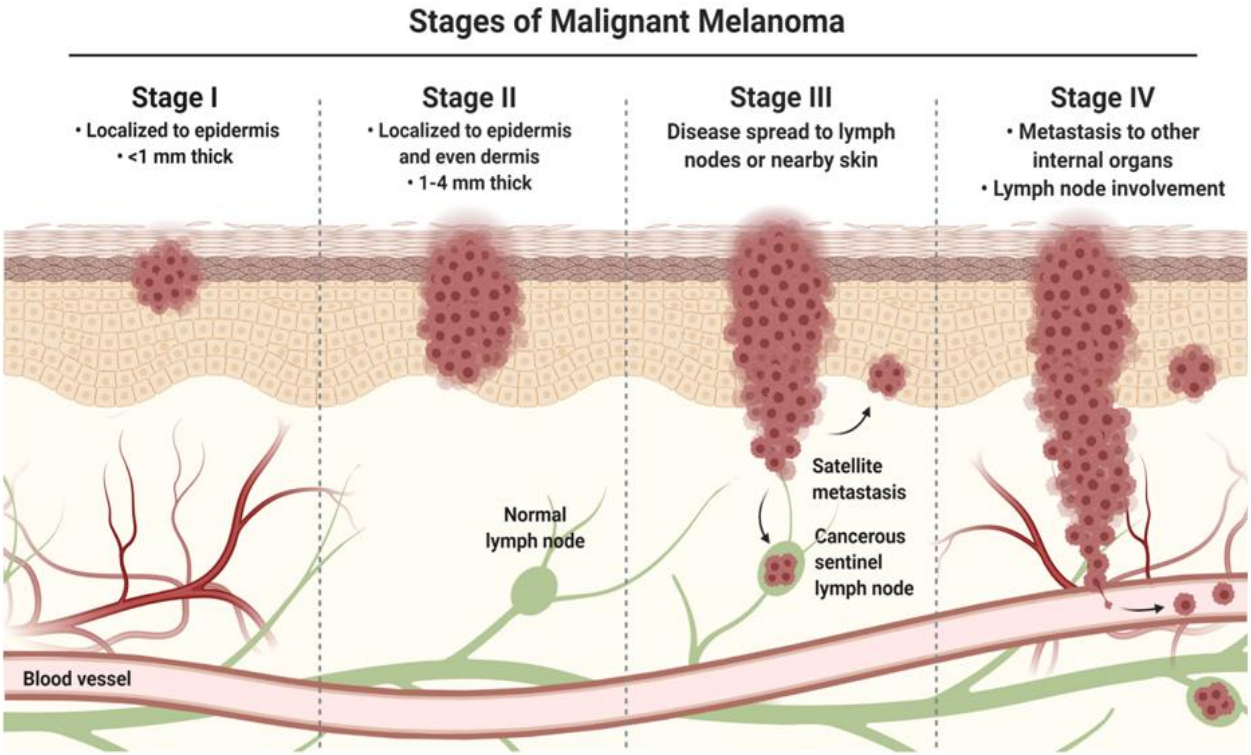

Figure 11: Schematic representation of the malignant melanoma tumor progression at different stages of disease. The discrimination between the different stages defined by the AJCC staging system is based on several characteristics of primary tumor such as thickness, ulceration or location, spread to regional lymph nodes or nearby skin, and distant metastasis.

2.5. Diagnosis

Nowadays, the diagnosis of MM mainly depends on frequent visual self-examinations by the naked eye, as well as an annual complete skin inspection and a dermoscopy. Visual examinations base the MM detection in the so-called ABCDE in reference to the most important hallmarks of this type of malignancy: asymmetry (A), border irregularity (B), color (C), diameter (D) and evolution (E) [54]. Dermoscopy consists on a non-invasive skin surface microscopy-based examination, using a device called dermoscope, which allows the *in vivo* evaluation of colors and microstructures of the epidermis not visible to the naked eye. However, these methods are not sufficiently precise, resulting in a handful of false positives and commonly failing in the accurate identification of many skin malignancies. Therefore, whether a suspicious cutaneous melanocytic lesion is detected, histopathological examinations are also required in order to confirm its malignancy [55]. Nonetheless, despite this method represent the real gold standard for MM diagnosis, it is an invasive technique that requires the surgical excision of the tumor (biopsy) (**Figure 12**) [56].

Hence, MM detection currently remains challenging, and it is still a long-term, resource-consuming and costly process [57]. Basically, it relies on the patients' commitment to their self-exams and medical appointments, dermatologists' availability as well as on the invasive and pricey method of histological examination, on the pathologists' interpretation, which are subjective and neither accurate nor reproducible (especially in the early stages) [58,59].

Nowadays, the necessity of new sophisticated diagnostic tools to support pathologists and compliment visual assessments is clearly evident, since diagnostic errors lead not only to under or overtreatment, but also to a higher economic cost of MM management. Huge efforts have

been made in recent years to develop quantitative and non-invasive novel diagnostic tools, based on the fact that skin is easily accessible. For instance, the state-of-the-art methods that are starting to be increasingly used in this regard include imaging techniques such as confocal microscopy, multispectral imaging, 3D topography, optical coherence tomography, self-mixing interferometry and polarized imaging [60,61].

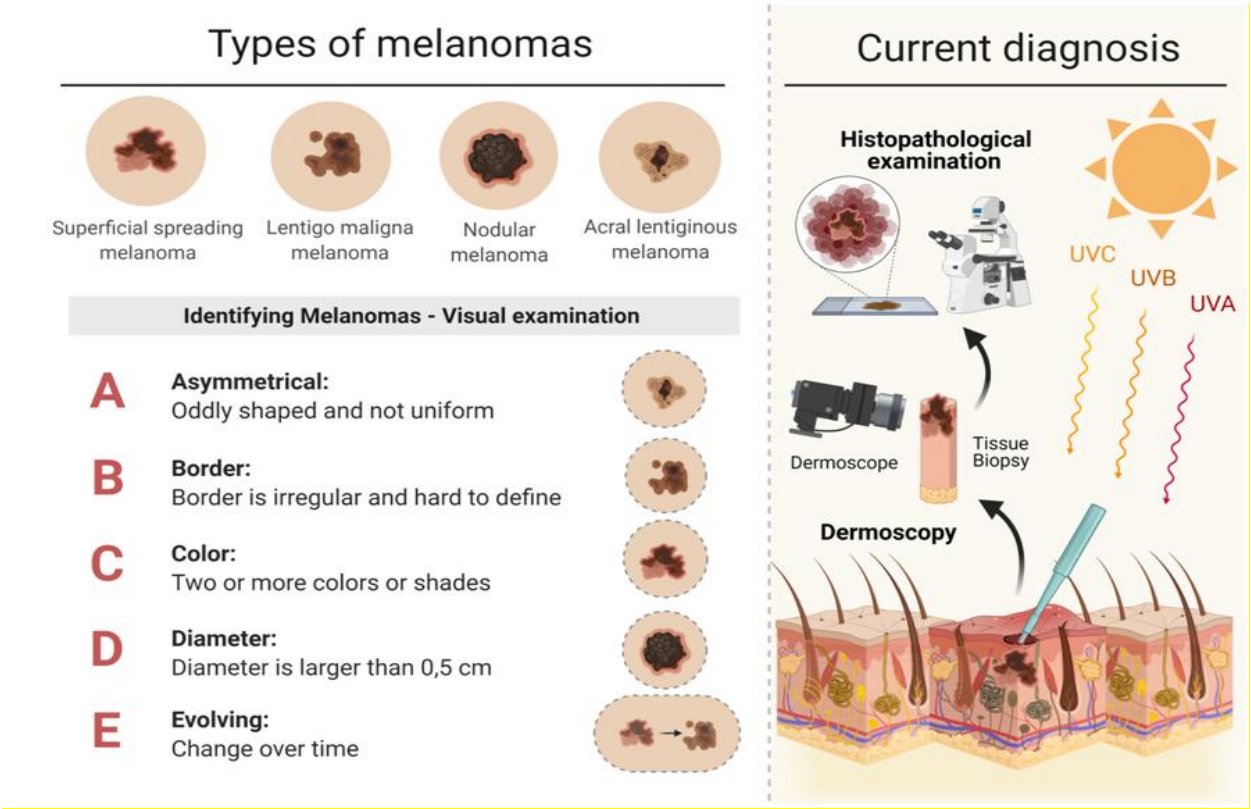

Figure 12. Schematic representation of the different types of malignant melanomas, the main hallmarks considered for identifying melanomas by visual examination (ABCDE), and current state of diagnosis based on tissue biopsy, dermoscopy examination, and histopathological assessment.

Additionally, the other major focus of attention of researchers in this field during the last years, has been the discovery and validation of biomarkers clinically useful for early diagnosis, prognosis and prediction, as well as for patient counsel and appropriate management, and ultimately for a better personalized therapy. This, by the way, has also been the one of this thesis.

3. THEORIES ABOUT TUMORAL HETEROGENEITY

Phenotypic and functional heterogeneity arises from diverse cell types recruited to the tumor, environmental differences, and from genetic, epigenetic and functional changes amongst the tumor cells themselves [62,63]. This diversity within a given tumor is a consequence of several intrinsic and extrinsic cell features. Cell-intrinsic factors are those inherent properties of a cell that contribute to its oncogenic phenotype, whereas cell-extrinsic factors are those ones from its surrounding TME that also make an influence [63]. Furthermore, variability can occur within individual tumors -intratumoral heterogeneity-, in which the tumor cells often belong to different phenotypes with a wide range of functional properties and a diverse expression of markers, and also between tumors arising in the same organ -intertumoral heterogeneity- leading to the classification of discrete tumor subtypes that are typically characterized by their molecular profile, morphology and expression of specific markers [64].

3.1 Intratumoral heterogeneity

The origins of the complex process of intratumoral heterogeneity have been widely debated and different theories have been proposed to account for the diversity within a tumor [65–67].

The first theory is the stochastic or clonal evolution model (**Figure 13**), which suggests that tumors evolve progressively during staggered carcinogenesis in a monoclonal way. This means that neoplasms come from a single malignant cell, whose progeny eventually accumulate heritable genetic and epigenetic changes that provide them certain advantages in terms of survival. Therefore, those heritable mutations are responsible for selection and outgrowth of those fitter clonal subpopulations with a marked intratumoral heterogeneity [63,68,69]. According to this theory, all cancer cells are equivalent in terms of capacity to give rise, boosting

or regenerate a tumor, being their intratumoral heterogeneity due to random or stochastic intrinsic or extrinsic factors [69–71].

A second theory corresponds to the hierarchical or Cancer Stem Cells (CSCs) model (**Figure 13**), which proposes that intratumoral heterogeneity is a consequence of certain states of stemness or differentiation of several cancer cells subpopulations within a given tumor. According to this theory, tumors arise from a subset of malignant cells, the so-called CSCs, which are predisposed to drive the progression, metastasis and therapeutic resistance of the tumor. These cells show stem-like functional properties such as self-renewal capacity and differentiation ability into other subsets of non-CSCs, as well as other specific features that make them susceptible to be specifically isolated [63,70,72].

More recently, several investigations have suggested that CSC phenotype is not as rigid and stable as the hierarchical model assumed, being actually much more plastic and highly regulated by the TME. The ability of cells to switch states *via* different programs such as epithelial-mesenchymal-transition (EMT) has given rise to the dynamic CSCs model (**Figure 13**), according to which cellular plasticity allows bidirectional switching between CSCs and non-CSCs that plays a key role in tumor biology [63,73–78].

This third theory also take into account the importance of TME stromal cells and their interactions with tumor cells in cancer development, progression, dissemination and resistance to treatment. These niche stromal cells, including inflammatory cells, fibroblasts and mesenchymal stem cells, produce different cytokines, growth factors and extracellular matrix (ECM) components which have been reported to promote several CSC properties such as self-renewal, invasion capacity or chemoresistance [79–82].

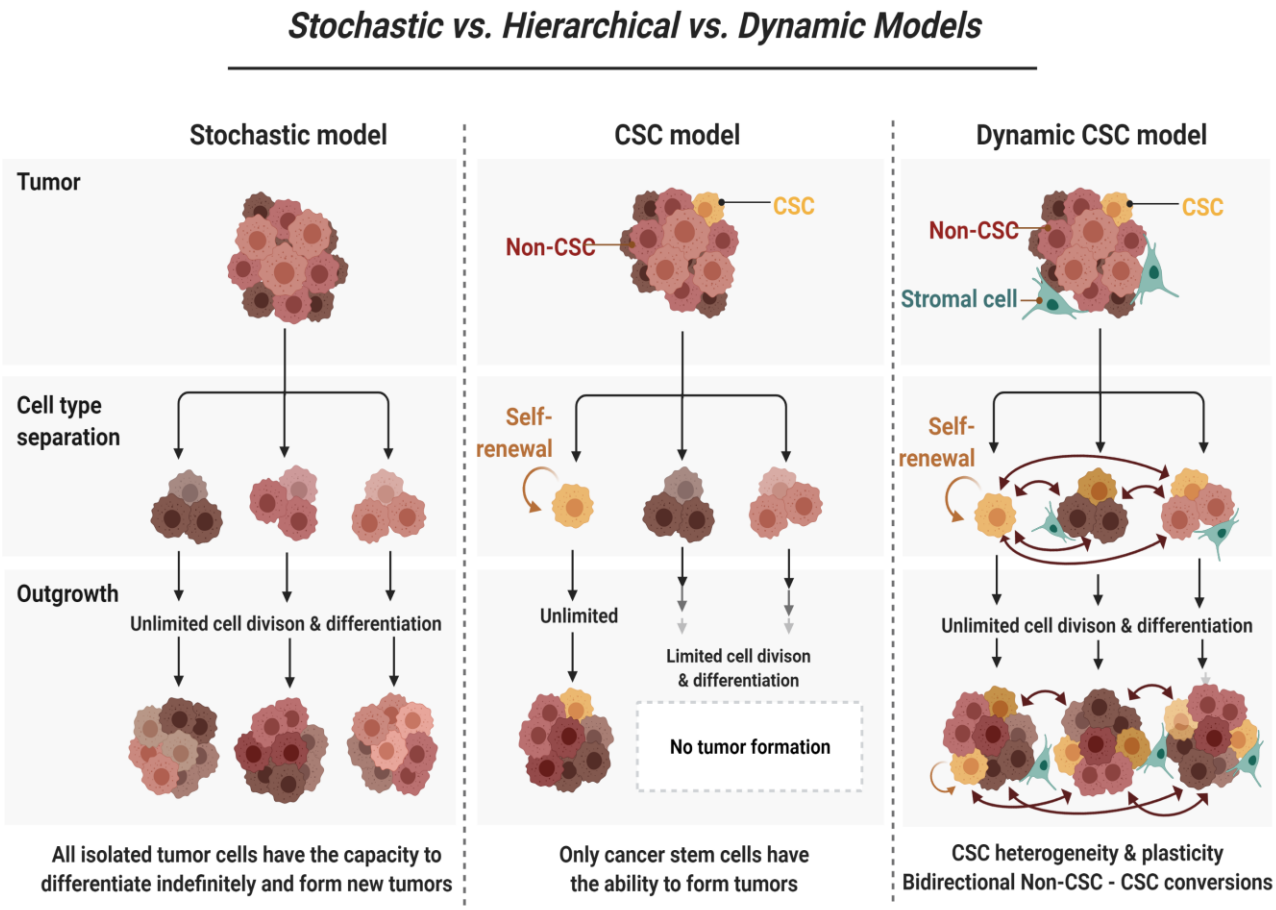

Figure 13. Theories about intratumoral heterogeneity: Stochastic, hierarchy and dynamic models. According to the stochastic or clonal evolution model (left), different populations of cancer cells within the bulk tumor are tumorigenic and thus have the capacity to proliferate uncontrollably, differentiate and form new tumors. According to the hierarchical or CSCs model (center), only certain subpopulations of undifferentiated cells (CSCs) have the capacity for tumor initiation, maintenance, and spreading. The dynamic CSCs model (right) takes into account recent findings about the remarkable heterogeneity and plasticity of cancer cells, and consider that bidirectional conversions between non-CSCs and CSCs are possible.

Given the current focus on therapeutic targeting of CSCs, this dynamic theory has important implications on the development of future therapies [63,72,78,83]. Actually, and based on this plastic CSC model, members of our research group have recently proposed a novel therapeutic approach focused on targeting those cells that are involved in the non-CSC and CSC conversion. They propose to specifically target some peripheral non-CSCs, located in the TME edges, which have the potential to give rise to CSCs with their corresponding properties and subsequent role in tumor growth, progression, TME formation, and eventually, distant metastasis [84]. Combined therapies should be focused not only against CSCs themselves, but also against these bidirectional switching between CSCs and non-CSCs in order to provide a more effective therapeutic treatment and ultimately improve patient survival.

3.2 Intertumoral heterogeneity

Regarding intertumoral diversity, there are also two theories attempted to explain the variability that can be observed between different tumors arising in the same organ. The first theory corresponds to the mutational model (**Figure 14**), which proposes that intertumor variability is a consequence of genetic and/or epigenetic mutations that shape the different tumor phenotypes [64]. The second theory corresponds to the cell-of-origin model, which puts forward the idea that different cancer subtypes within the same tissue or organ are caused by different oncogenic events in the hierarchy of the cell lineage (**Figure 14**). According to this theory, any type of cell within the organism is able to become cancerous after accumulating mutations, and different tumor phenotypes can be developed depending on the differentiation state of that initial cell. After the malignant transformation of that particular tumor initiating cell, and independently of its differentiation degree, the tumor progression can be fitted to the stochastic or the hierarchical model [64,85].

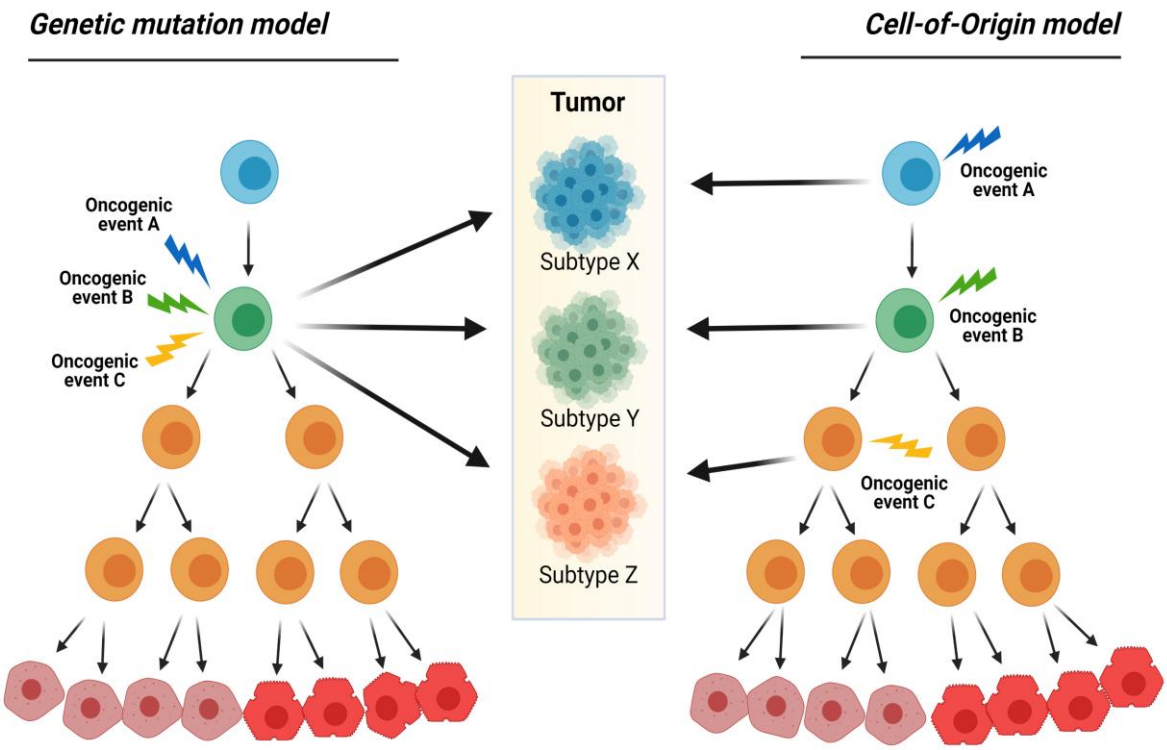

Figure 14. Theories of intertumoral heterogeneity: Mutational and cell-of-origin models. According to the mutational model, different genetic (and epigenetic) mutations primarily determine the different tumor phenotypes. According to the cell-of-origin model, different cell populations serve as cells of origin for the different cancer subtypes that arise in a tissue or organ.

4. CANCER STEM CELLS

As previously described, clonal evolution and CSC models have been classically proposed as drivers of intratumoral heterogeneity. However, these two theories are not necessarily mutually exclusive, and the concept of CSC plasticity and bidirectional switching between CSCs and non-CSCs has added more complexity to these highly debated paradigms, so it must be taken into account in order to explain the tumoral diversity observed within a given tumor [67,86].

The bulk of a solid tumor is composed not only by neoplastic cells, but also by a wide variety of surrounding non-tumorigenic cells within the TME, such us supporting vascular cells, diverse immune inflammatory cells, fibroblasts, as well as several stromal cells (**Figure 7**). In this context, tumor cells are hierarchically organized and sustained by a heterogeneous subpopulation of cells with stem-like functional properties, which are widely known as Cancer Stem Cells (CSCs), Tumor Initiating Cells (TICs) or Tumor Stem Cells (TSCs) (**Figure 15**) [87–89].

First evidence of the existence of this fraction of cells came from the study carried out by Bonnet and Dick in 1997. In their study, the authors successfully isolated a specific cell subpopulation from acute myeloid leukaemia (AML) patients. To their surprise, those cells showed functional properties similar to haematopoietic stem cells, and actually they were able to give rise to novel AML after implanted into immunodeficient mice [90]. After that, first evidence of CSCs found in solid tumors was reported in breast cancer [91].

Those early studies laid the groundwork for the subsequent investigations and accumulating evidence in favor of the CSC concept. To date, not only the existence of CSCs has

been widely reported, but also their primary role in driving tumorigenesis, progression, metastasis, therapeutic resistance and recurrence of tumor [67,72,86,92–94], as a consequence of their unique characteristics (**Figure 15**).

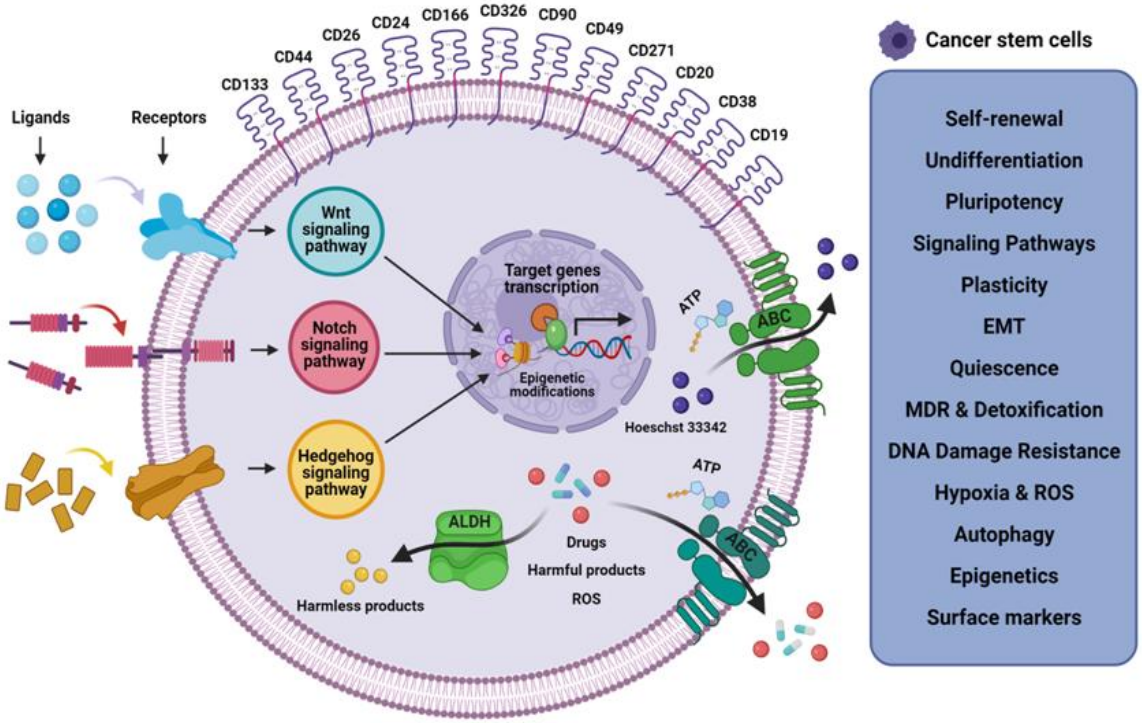

Figure 15. Schematic representation of the main hallmarks of CSCs: stemness capacities, such as self-renewal, undifferentiation and pluripotency, as a consequence of a noteworthy deregulation of several signaling pathways such as Wnt/β-catenin, Notch, or Sonic Hedgehog, among others; ability of stay quiescent for long periods; plasticity and capacity to undergo EMT; Therapeutic resistance, as a consequence of several properties and protective mechanisms, including the overexpression of MDR (ABC transporters) or detoxification proteins (ALDH), resistance to DNA damage-induced cell death or oxidative damage, and autophagy activation, among others; All these traits, as well as other environmental and epigenetic factors, make influence one another. Also, specific surface markers allow the isolation and characterization of different types of CSCs.

4.1. CSC characteristics

4.1.1. Self-renewal and pluripotency

Stem cells and CSCs are both characterized by their capacity for self-renewal and their potential for differentiation. On the one hand, the self-renewal ability allows them to give rise to indefinitely more cells of the same cell type, perpetuating the stem cell pool and maintaining their undifferentiated state. On the other hand, they are also able to differentiate into several types of more specialized cells. These traits in specific lineages of stem cells are orchestrated by environmental signals coming from their niche [83,86].

However, CSCs differ from normal stem cells in several traits that contribute to their malignant phenotype. For instance, they present differences in the way of dividing and replicative potential, cell cycle properties, DNA damage repair mechanisms [95]. Additionally, they also present a noteworthy deregulation of several signaling pathways, such as Wnt/β-catenin, Notch, or Sonic Hedgehog, which are involved in self-renewal, differentiation and survival [87,96,97]

4.1.2. Plasticity

In the last years, accumulated evidence has shed light on CSC heterogeneity and plasticity in several types of cancer, such as glioblastoma [98–101], melanoma [102,103], breast cancer [104,105] or colorectal cancer [106,107], proving that there are different subsets of CSCs displaying extensive metabolic and phenotypical plasticity. In addition to the aforementioned dynamic switching ability between CSC and non-CSC subsets, they also show biochemical and biophysical diversity, resulting in drug-resistance potential and/or varied dissemination to distant organs [108,109]. This CSC plasticity is orchestrated by cell-intrinsic factors such as epigenetic

modifications, transcription factors or mutations, and also by cell-extrinsic factors like physical and chemical conditions of the TME and molecules produced by its associated cells [84,110].

4.1.3. CSCs and the Epithelial-to-Mesenchymal Transition

The epithelial-to-mesenchymal transition (EMT) is a highly dynamic and staggered process by which a polarized epithelial cell that normally interacts with basement membrane via its basal surface, undergo several changes at different levels that allow it to adapt a mesenchymal phenotype (**Figure 16**). Throughout this process, epithelial cells loss of epithelial apico-basal cell polarity, detach from each other by breaking cell-cell junctions and from the underlying basement membrane as a consequence of ECM remodeling, and mesenchymal fate is determined by the activation of a new transcriptional program, meaning that several EMT-inducing transcription factors are activated. Subsequently, some specific epithelial markers are lost while some other specific markers of mesenchymal cells are acquired [111,112].

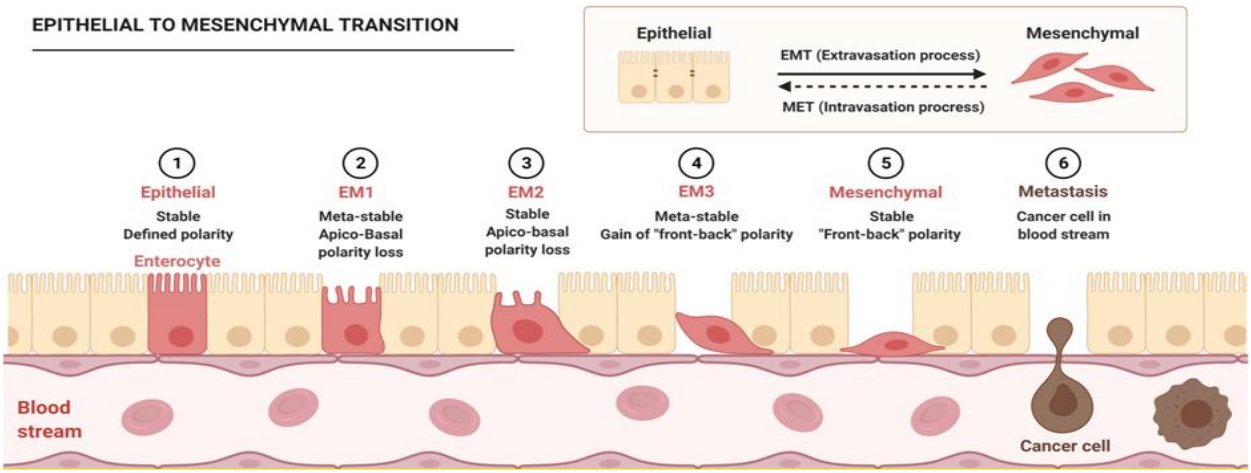

Figure 16. Schematic representation of Epithelial-to-Mesenchymal Transition (EMT). This is a biological process by which epithelial cells undergo to multiple biochemical changes that make them lose their cell polarity, break cell–cell and basement membrane adhesions, as well as some specific epithelial markers, and acquire a mesenchymal cell phenotype with migratory capacity, invasiveness, resistance to cell death, increased production of extracellular matrix components and specific mesenchymal markers.

EMT normally takes place during normal embryonic development, tissue regeneration, organ fibrosis, and wound healing. However, in the context of cancer, there is strong evidence that EMT is also involved in tumor formation, progression, metastasis, and the generation of tumor cells with stem cell properties that play a major role in resistance to cancer treatment [75,89,111,113]. The reverse process, mesenchymal-to-epithelial transition (MET), seems to play an important role final steps of malignant progression and metastasis in distant organs, but it still remains to be further studied in greater detail [114–116].

4.1.4. Quiescence

The ability to stay quiescent, which is the reversible state of a cell in which it does not divide but retains the ability to re-enter cell proliferation, is another major trait of CSCs. This cellular state, also known as dormancy, confers them an important resistance to most anticancer treatments and it is highly related to tumor recurrence [87,89,117].

4.1.5. Therapeutic resistance

CSCs are also characterized by their remarkably resistance to the majority of the anticancer drugs and therapeutic treatments, which still represents an ongoing challenge in cancer treatment and is undoubtedly one of the main reasons for treatment failure and cancer relapse. This property is a consequence of several properties of CSCs, such as those previously reviewed (self-renewal and differentiation capacity, plasticity, or their ability to undergo EMT or stay quiescent), it is also attributable to other intrinsic resistance mechanisms that CSCs harbor against radiation and chemotherapy at a much higher rate than non-CSC, differentiated tumor cells (**Figure 15**) [94].

4.1.5.1. High expression of multidrug resistance (MDR) or detoxification proteins

CSCs present a remarkable overexpression of drug-efflux pumps such as ATP-binding cassette pumps (ABC transporters), such as MDR1, ABCG1, ABCG2 or ABCB1, which allow them to expel multiple citotoxic drugs or harmful products from their cytoplasm [118]. For instance, ABG2 and P-Glycoprotein drive out the fluorescent Hoeschst 33342 dye, which allow the isolation of the CSC-enriched side population [119–121]. In addition, the cytosolic enzyme aldehyde dehydrogenase (ALDH), which is one of the most widely known CSC markers, also plays a protective role by oxidizing intracellular aldehydes which could be potentially toxic [122].

4.1.5.2. Resistance to DNA damage-induced cell death

CSCs also harbor several mechanisms that allow them to avoid DNA damage-induced cell death and thus contribute to their strong therapeutic resistance. For example, they have an enhanced DNA repair capacity. It has been proved that these cells present an enhanced DNA repair capacity after radiation, since they have significantly increased expression levels of certain genes involved in DNA damage response, as well as higher activation of checkpoint mechanisms when double and single DNA breaks are produced, inhibiting the cell cycle progression in order to repair the damage [123,124]. Additionally, in response to oxidative DNA damage, it has also been reported an enhanced reactive oxygen species (ROS) scavenging as well as increased activation of anti-apoptotic signaling pathways such as PI3K/Akt, WNT/b-catenin or Notch [125].

4.1.5.3. Autophagy

Autophagy is a regulated self-degradative mechanism of the cell that allows the orderly degradation and recycling of dysfunctional cellular components. Therefore, it is an important process for balancing sources of energy under several stressful conditions. Although autophagy plays dual roles in tumor suppression and promotion in many cancers, it is involved in the regulation of some of the CSC properties and takes an important part in their stemness maintenance, recurrence induction, and treatment resistance [123,126].

4.1.5.4. Hypoxia and ROS

Hypoxia plays a key role not only in the stemness maintenance of CSCs, but also in their drug resistance capacity. Indeed, they are commonly located nearby hypoxic zones within tumors [127]. Mainly, there are two mechanisms by which hypoxia takes part in drug resistance: Activation of stem-related pathways and quiescence promotion. On the one hand, activation of HIF1α induces the expression of several EMT and stemness activators, such as Wnt, Hedgehog and Notch pathways alongside other stemness-specific markers [128]. On the other hand, hypoxia promotes cancer cell quiescence, as it represents a restrictive stressful context for cellular growth [129].

At the same time, the HIF1α signaling pathway also induces a decreased formation of ROS, which has also been reported to be essential for preserving important stemness CSC properties, including drug resistance, as well as promoting quiescence. As previously mentioned, ALDH is one of the culprits of ROS decreased levels [130,131].

4.1.5.5. Tumor environment

As previously mentioned, TME makes a huge impact on tumor biology. Accumulated evidence supports that multiple cell interactions within the TME, as well as the physical and chemical conditions of TME, play important roles in CSC dynamics and properties, including their treatment resistance [132].

Cancer-associated fibroblasts (CAFs) have been reported to stimulate the secretion of specific cytokines and chemokines involved in CSC maintenance, self-renewal and invasion capacity [79,80]. Regarding immune cells, it has been indicated that tumor-associated macrophages (TAMs) also promote some of these CSCs properties which confer them chemoresistance [81,82].

In addition, some of the previously mentioned signaling pathways and autophagy mechanism are activated in the hypoxic context within the TME [133,134], and several inflammatory processes that take place in this environment have been also associated to CSCs and their chemoresistance [135].

4.1.5.6. Epigenetics

CSC-mediated drug resistance is also modulated by epigenetic mechanisms, such as DNA methylation or histone modifications. For instance, it has been demonstrated that several changes in chromatin methylation contribute to chemoresistance in CSCs [136]. Some epigenetic silencer proteins of the Polycomb group like BMI1 or EZH2 have also been indicated to be involved in CSC self-renewal and resistance to chemotherapy and radiation-induced cell death [137,138]. Moreover, histone acetylation seems to play an important role in regulation of transcriptional activation and CSC treatment resistance too [139].

4.2. CSC isolation and characterization

Traditionally, isolation and characterization of CSCs have been widely carried out by using biochemical methods, which are based on some of the specific characteristics of these cells previously described. For instance, one of the most commonly applied method is to sort CSCs based on their differential expression of multiple surface markers (CD133, CD44, CD34, CD26, CD24, CD166, CD326 (EpCAM), CD271, CD20, CD90, CD49, CD184, CD38, CD19, among others) (**Figure 15**) [86,140,141]. In fact, it is a common practice to use specific patterns of surface markers in order to perform a more accurate and specific selection of different CSC subsets in different types of tumors, such as $CD34^{+}/CD38^{-}$ in leukemia [142] or $CD44^{+}/CD24^{-}$ in prostate cancer [143].

Another commonly applied method is the determination of ALDH activity, typically measured with the Aldefluor® assay kit. An increased enzymatic activity of this intracellular protein detected by fluorescence-activated cell sorting (FACS) has been correlated with CSC-enriched populations in several cancer types [144–146]. Also, the detection of the side population (SP) phenotype by Hoechst 33342 dye exclusion is widely used [147].

In addition, there are several functional assays that can be applied for CSC characterization. On the one hand, there are several *in vitro* assays for proliferation, colony forming units, sphere formation, or adhesion, migration and invasion capacity. On the other hand, *in vivo* tumorigenicity assays for testing carcinogenesis and tumor progression can also be carried out [148].

Besides these traditionally applied methods, novel approaches and methodologies have been proposed and in order to better isolate and characterize different types of CSCs. Emerging

technologies are currently being applied in this regard, including biophysical methods such as microfluidic chips, trypsin deadhesion or atomic force microscopy [149–151]; single-cell methods like FACS, single-cell OMICS or single-cell imaging [152–154]; and computational methods, which represent the latest *in silico* approaches being taken for characterizing CSC plasticity [77,155].

4.2.1. Malignant Melanoma CSCs

In like manner, isolation and characterization of malignant melanoma cancer stem cells (MM-CSCs) are based on the same methods described for CSCs in general, including surface markers, drug resistance-associated markers and intercellular markers.

As previously mentioned, specific marker signatures are typically used to identify tumor-specific CSCs. In the case of melanoma, there is still controversy about the existence of a unique and specific pattern of surface marker for melanoma stem cells. This is mainly due to the high degree of cellular plasticity and the multiple mechanisms that might be driving the progression of this type of tumor [156]. Despite of that, some combinations of surface markers has been proposed to specifically isolate MM-CSCs, such as $CD133^{+}/CD20^{+}$ or $CD44^{+}/CD20^{+}$ [140].

In the last decade different biomarkers have been proposed for the identification of this subtype of CSCs [157], including some related to melanocyte undifferentiated state (CD133, CD271), MDR mechanisms (ATP-binding cassette transporters), or to metabolic traits (ALDH activity) [158–160]

Regarding surface markers, the most consistently used to identify MM-CSCs are CD133, CD20 and CD271. In the last years, some conflicting results have cast some doubts on its role in specifically defining the CSC fraction in MM [160]. In particular, the use of CD271 remains

controversial, due to its highly variable expression and several results that have cast some doubts on its reliability and high variability observed in its expression levels [159]. However, there is also accumulating evidence supporting their use for MM-CSCs identification. For instance, recent studies have proved that CD271 and CD133 seem to be involved in MM aggressiveness, progression and prognosis [161–163].

About markers associated to MDR mechanisms, ABC transporters responsible for drug efflux can be also used for specific MM-CSCs identification. For instance, ABCB5, that has been associated with higher cellular tumorigenic ability and also correlated with tumor progression in melanoma patients, or ABCG2, which has been found significantly co-expressed with other MM CSC-specific surface markers such as CD133 [164–166].

With regards to intracellular markers, some of the previously detailed methods for general CSC isolation are also applied in case of MM-CSCs identification, such as ALDH activity assessment or side population detection [167].

In addition, some other functional assays generally applied for CSC characterization can be carried out in MM-CSCs, both *in vitro* (colony forming units or sphere formation capacity under conditioned media) and *in vivo* (tumorigenicity assays) [148].

5. BIOMARKERS

In the last years, the American National Institute of Health (NIH) and Food and Drug Administration (FDA) has reviewed biomarker definitions, as part of their common resource "Biomarkers, EndpointS, and other Tools (BEST)", created with the aim of unifying the definition of biomarker and their different types, among other related purposes [168]. According to this joint FDA-NIH resource place, a biomarker is "*A defined characteristic that is measured as an indicator of normal biological processes, pathogenic processes or responses to an exposure or intervention*".

Besides the general definition, there are different classes of biomarkers also defined according to their potential applications and usefulness in patient counseling and care, clinical research, or therapeutic development, including diagnostic, monitoring, pharmacodynamics/response, predictive, prognostic, safety and susceptibility/risk biomarkers. A particular biomarker might be included in two or more of those categories and some definitions may overlap, but all of them present particularities in their clinical use that distinguish them from each other [169].

In this era of precision medicine and multiple effective treatments highly dependent of early and accurate detection, such as targeted therapies or immunotherapies, designing the optimal personalized therapy strategy demands the development of sophisticated clinically useful biomarkers of several types, for the sake of earlier cancer detection, better treatment response, and improved patient survival [169–172].

In this regard, the perfect biomarker would be a metabolically and analytically stable molecule detectable and/or quantifiable in body fluids such as blood, urine, or saliva, through

minimally invasive techniques. To date, no such a flawless biomarker exists for this disease. However, circulating biomarkers in several body fluids take on a remarkable importance in this context, and they have currently become a major trend in this field of research.

5.1. Biomarkers in malignant melanoma

Melanoma biomarkers can be classified into different categories of those previously mentioned. In general, the majority of them are being used as diagnostic biomarkers, since they are overexpressed in MM cells. Other biomarkers show higher expression in advanced stages of disease and serve as indicators of therapy response or risk of recurrence, so they are considered prognostic or predictive. Some serologic and histologic markers typically associated to MM include lactate dehydrogenase (LDH), tyrosinase, S100 family of calcium-binding proteins, cyclooxygenase-2 and matrix metalloproteinases. Actually, some MM-CSCs markers are also used to identify some cell subpopulations that show significant potential for driving carcinogenesis, metastasis and drug resistance [170,173].

Despite all the significant advances made in the last years in order to provide insights into MM behavior and outcome, this disease is still unpredictable. Hence, more efforts still need to be made in finding out fitting biomarkers for early detection, correct staging, avoidance of overdiagnosis and discrimination of other skin malignancies, and also benefit patients' prognosis and personalized treatments.

5.2. Circulating/Liquid biomarkers

Liquid biomarkers, such as tumor cells, tumor-derived metabolites, proteins, nucleic acids and extracellular vesicles, are commonly found in several body fluids like blood, urine, or saliva, among others. These circulating components are easily accessible through minimally

invasive methods such as liquid biopsies, and they can provide priceless diagnostic, prognostic and predictive information [174–176] (**Figure 17**). Liquid biopsies present certain advantages in comparison to tissue based profiling. For instance, they are minimally invasive and can be routinely performed in order to follow up tumor progression and patient's response to therapy [172]. In addition, since tumors exhibit genetic and phenotypic heterogeneity, liquid biopsies allow the collection of different molecules derived from multiple metastases [177], providing a more comprehensive profile of a patient's cancer.

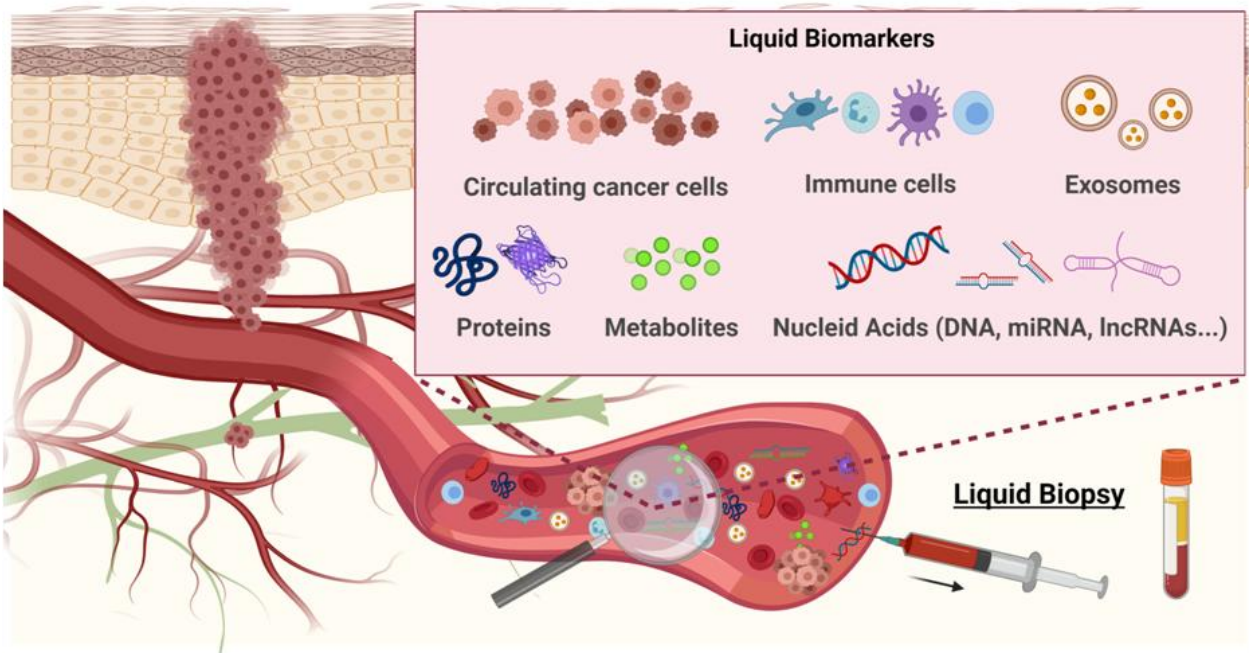

Figure 17. Different circulating cells and molecular compounds, such as tumor and immune cells, proteins, nucleic acids (ctDNA, miRNAs, lncRNAs…), metabolites and extracellular vesicles (which include exosomes), can be detected in the bloodstream by liquid biopsies and may serve as potential cancer biomarkers.

With regards to MM, in the last years several circulating biomarkers have been identified and proposed in pre-clinical models and clinical samples based on different strategies. For instance, there are some proteomics-based approaches, including mass spectrometry proteome profiling and affinity-based proteomic assays molecular and cellular profiling approaches [178–

181]. In addition, there are also molecular and cellular approaches for liquid biomarker discovery in MM. Molecular profiling methods are focused on circulating tumor DNA (ctDNA) (associated to BRAF and NRAS mutations or epigenetic changes) [182–184], microRNAs (miRNAs) and long noncoding RNAs (lncRNAs) [185,186], exosomes and exosomal miRNAs [187,188]. Cellular profiling methods look at circulating tumor cells (CTCs) [189] and several immune cells [190] (**Figure 17**).

Nonetheless, despite recent advances in these technologies and the considerable amount of potential biomarkers reported, their identification remains challenging and time-consuming. Only a few of them have been validated or FDA-approved for clinical use. Indeed, the only circulating biomarker with significant prognostic value in the updated version of the 8th edition AJCC melanoma staging system is lactate dehydrogenase (LDH) [191]. Increased LDH levels are associate with poor survival in stage IV melanoma [192] and poor outcome in patients treated with dabrafenib and trametinib [193]. Furthermore, significantly reduced LDH is associated with better response to immunotherapy [194]. Other circulating proteins have shown diagnostic and prognostic value for this disease, including S100B, C reactive protein (CRP), melanoma-inhibiting activity (MIA) protein, vascular endothelial growth factor and interleukin-6, but all of them have limitations for clinical application, regarding their sensitivity or specificity [173].

6. EXTRACELLULAR VESICLES

Besides the classical forms of cell communication like cell junctions, adhesion contacts, or soluble factors that can act in an autocrine, paracrine or endocrine manner, a novel mechanism of cell-to-cell communication called communication by extracellular vesicles (EVs) has emerged in the last few years [195]. The term "extracellular vesicle" is a generic term that refers to a heterogeneous population of endogenous nano-sized cell-derived membrane vesicles with pleiotropic functions, released by cells into the intercellular space and the bloodstream [196].

There are various subtypes of EVs, including exosomes (typically 30–150 nm), microvesicles (150–1,000 nm) and apoptotic bodies (1–5 μm) [197] (**Figure 18**). However, it should be noticed that the International Society for Extracellular Vesicles (ISEV) recently revised the nomenclature of these vesicles. According to the Minimal Information for Studies of Extracellular Vesicles ("MISEV") guidelines [198] they published in 2018, EVs should be discriminated depending on several distinctive traits, such as morphological aspects, biochemical composition, biogenesis, or cell of origin. For instance, according to their size, they should be termed as small EVs (sEVs) and medium/large EVs (m/lEVs), with ranges defined (<100nm or <200nm for sEVs and >200nm for m/lEVs). Therefore, conventionally termed "exosomes" could be also called "sEVs".

6.1. Exosomes (sEVs): biogenesis, structure and biological functions

Regarding its biogenesis, exosomes are originated by a sequential process of inward budding of late endosomes, producing multivesicular bodies (MVBs) that later fuse with the plasma membrane [199] (**Figure 18**).

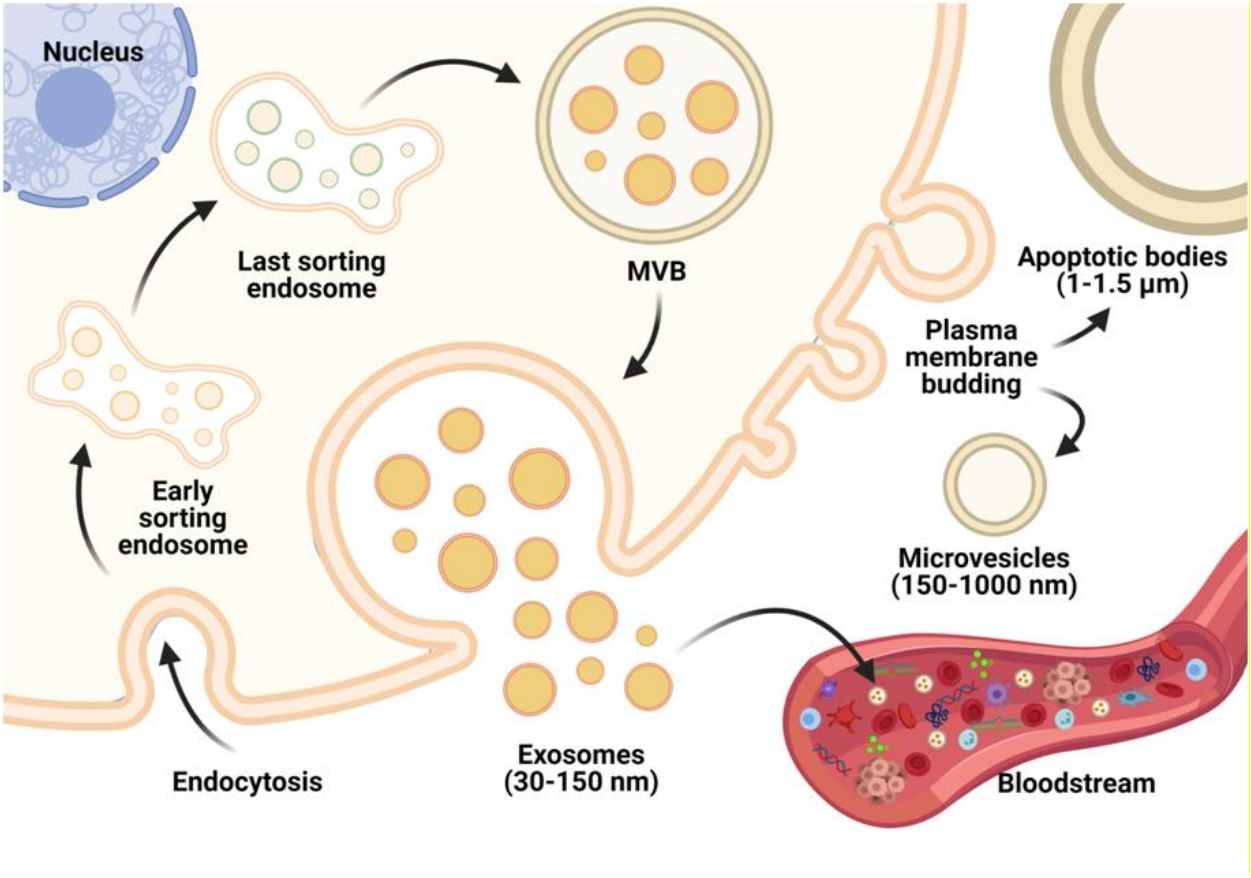

Figure 18. Schematic representation of the different types of EVs depending on their size and biogenesis processes. Exosomes correspond to a smaller subset of EVs (30–150 nm) that are originated by a sequential process of inward budding of late endosomes, producing multivesicular bodies (MVBs) that later fuse with the plasma membrane. This way, exosomes are released to the extracellular matrix and to the bloodstream, throughout which they disseminate to distant parts of the body.

This way, exosomes are released into the intercellular space and bloodstream by most cell types, being able to reach recipient cells, deliver their cargo and promote a wide spectrum of functional responses or phenotypic changes on them [196,200]. They contain and transfer a series of important bioactive molecules such as nucleic acids (DNA, mRNA, miRNA, non-coding RNAs) proteins, lipids and other metabolites, being this content dependent on cell types and conditions [199,201]. By transferring their cargo, exosomes mediate near and long-distance intercellular communication in health and disease and affect different aspects of target cells biology (**Figure**

19). In addition, these sEVs and their membrane are enriched in different molecules that can be used as exosomal markers: tetraspanins such as CD9, CD63 and CD81, proteins implicated in endocytosis and cargo sorting such as ALIX, flotillin and TSG101, integrins, major histocompatibility complex (MHC) classes I and II proteins and protein receptors, among others [196] (**Figure 19**).

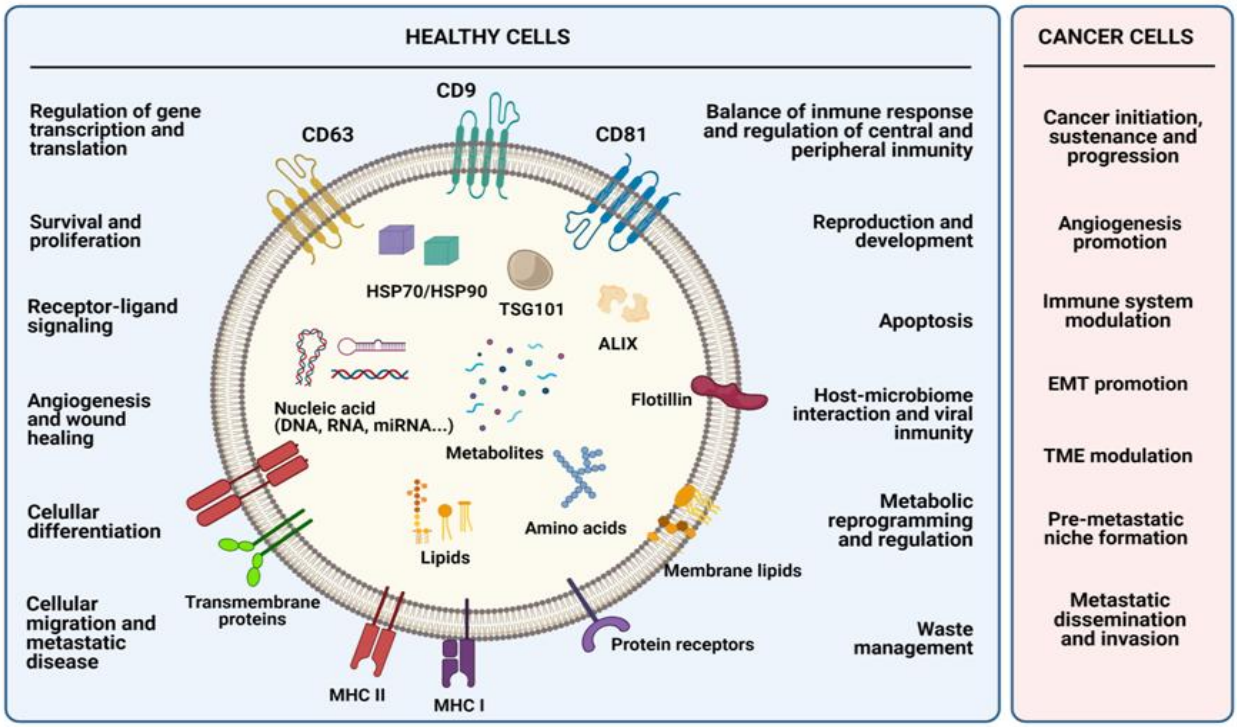

Figure 19. Schematic representation of exosomes' structure. These sEVs are generated by all cells and they carry nucleic acids, proteins, lipids, and metabolites. They act as messengers in near and long-distance cell-to-cell communication and exert pleiotropic functions in both normal and cancer cells.

6.2. Role in cancer, CSCs and MM

Regardless their nomenclature, accumulating evidence constantly confirms that EVs and exosomes, in particular, play a major role in cancer biology, including MM [187,202] (**Figure 19**). By transferring their cargo to target cells of different lineage, cancer cell-derived exosomes are able to induce pathways involved in cancer initiation, sustenance, progression and metastasis

[203,204]. They support tumor progression by promoting angiogenesis, immune system modulation and tumor parenchyma remodelling [205,206]. In addition, EVs are also released by CSCs, influencing their surrounding niche. Indeed, CSC-derived EVs can regulate direct crosstalk with other neoplastic cells or can modify normal surrounding cells to promote immune tumor escape, tumor growth and metastasis. Several studies have demonstrated that CSC-derived EVs play a key role in tumor progression [207].

In relation to MM, several studies reported different important roles of MM-derived exosomes in several processes and mechanisms underlying the tumorigenicity of this type of skin cancer (**Figure 19**). For instance, it has been reported that MM-derived sEVs are involved in the metastatic dissemination and invasion process from the primary location to regional lymph nodes [208] and distant organs by promoting the generation of pre-metastatic niches [209]. They also play an important role as promoters of EMT in primary melanocytes through paracrine and autocrine signaling in the tumor microenvironment [210]. Actually, it has been demonstrated that they contribute to metastatic invasion by carrying messenger proteins (e.g. the oncoprotein c-MET) educating bone marrow-derived cells towards a pro-metastatic phenotype or influencing the behaviour of immune cells [211,212]. Furthermore, exosomal miRNAs also play significant roles in tumor malignancy of this neoplasia [80,213].

As previously mentioned, the release of exosomes and other EVs into the different body biofluids allows their detection, being a major source of secreted biomarkers in circulation [214–217]. Since cancer cells exhibit enhanced production of exosomes, their concentrations are increased in body fluids of cancer patients compared to healthy controls [203]. Thus, exosomes (and other EVs) could represent a rich source of non-invasive biomarkers for the diagnosis and prognosis of cancers, including MM, as well as therapeutic targets [58,187,215,218,219].

7. METABOLOMICS

In this whole context, metabolomics takes on special importance, integrating all these topics, and it is one of the main pillars on which this thesis is based.

Metabolomics comprises a multidisciplinary set of sciences devoted to the systematic study of the chemical processes involving metabolites, the small molecule substrates, intermediates and end products of cell metabolism. Together, the whole set of metabolites and their interactions constitute the metabolome, which represents a complete set a faithful representation of cell physiology that, unlike genes and proteins, is not subject to epigenetic regulation or post-transcriptional/translational modifications [220,221].

Indeed, metabolomics is related to other genomic, proteomic and transcriptomic technologies in charge of the studying the whole set of genes (genome), proteins (proteome), and mRNAs (transcriptome), respectively. Indeed, it is often likened to its proteomic sibling, from which metabolomics has taken advantage of in terms of "inheriting" experience and methodologies, but also subsequent challenges and limitations, including the metabolite identification process. Actually, one of the major current challenges of systems biology and functional genomics is to integrate all the overwhelming amount of information coming from different omics technologies, in order to provide a better understanding of cellular biology [222,223].

In other words, metabolomics sheds light on the unique chemical fingerprints that specific cellular processes leave behind and provides a functional readout of the physiological state of an organism. It deepens into other aspects of cellular function, complementing other omics technologies, by allowing the description of metabolic patterns related to a certain disease

or a phenotype of interest, being its ultimate goal the comprehensive identification of key biological mechanisms underlying disease etiology and progression.

7.1. Metabolomics approaches, methodologies and challenges

Within metabolomics, untargeted and targeted studies represent the two main approaches. Targeted (or validation-based) metabolomic studies, aim to analyze previously well-known relevant metabolites, and often also obtain their absolute quantification. Generally, this type of approach focuses on identifying and quantifying a limited number of known metabolites, such as those commonly found in clinical analyses. Conversely, untargeted (or discovery-based) approaches are focused on the global detection and relative quantification of the whole set of metabolites within a sample. This type of approaches is commonly carried out in order to obtain data for as many species as possible, annotating both known and unknown metabolites as well as their changes [222,224,225] (**Figure 20**).

Regarding data acquisition, there are several separation [liquid chromatography (LC), gas chromatography (GC) and capillary electrophoresis (CE)] and detection [mass spectrometry (MS) and nuclear magnetic resonance (NMR)] methods that can be used in untargeted metabolomics studies [222]. Different combinations of those techniques can be applied, depending on the goals of the study. In particular, the combination on LC-MS-based metabolomics has become the leading technology for analyzing a wide coverage of metabolites [226]. Despite LC methods take longer (minutes to hours) than others like direct infusion or flow injection analyses (seconds to minutes), they are remarkably advantageous regarding selectivity, sensitivity and versatility, especially for complex biological samples like body fluids [224].

After separation, acquisition methods are based on the registration of accurate mass measurements of individual molecules by full scan MS1, followed by data dependent or independent acquisition of those compounds, defining those features with a mass-to-charge ratio (m/z) and retention time (RT). Additionally, specific MS/MS fragmentation patterns of selected features are also subsequently generated, which provide valuable information in terms of ultimate metabolite identification by using both compound and spectrum databases [222,224].

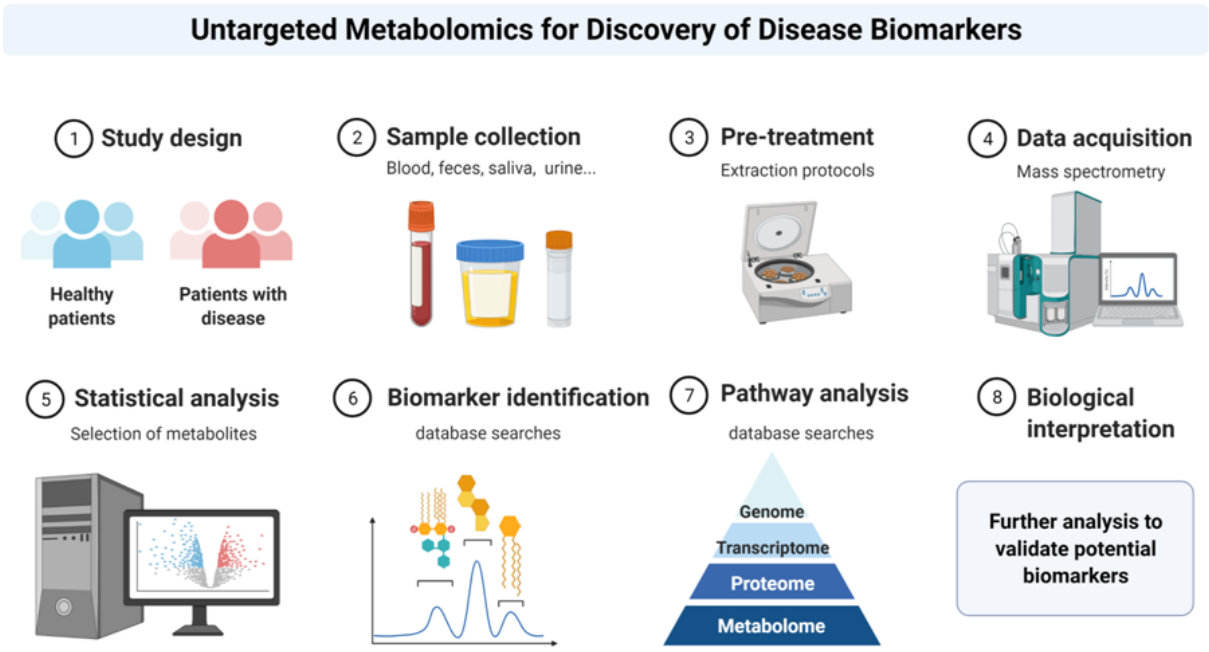

Figure 20. Overview of the workflow typically followed in untargeted metabolomics approaches, which normally includes an initial study design, sample collection from different biological sources, metabolite extraction protocols by using different solvents such as methanol (MeOH) or acetonitrile (AcN), data acquisition throughout different platforms such as LC/GS and MS/NMR, statistical analyses in order to select those differential features between the groups of comparison and identification of those selected compounds. Final steps comprise pathway analyses integrating data from different omics, biological interpretation, and ultimately, further studies for potential biomarkers validation.

The data processing workflow followed in untargeted approaches typically comprises several steps including, peak detection, filtering and alignment, and finally feature annotation and metabolite identification by using several public or private databases [222].

However, despite its multiple advantages and strengths, it should be also taken into account that metabolomics still has some weaknesses and there are several current challenges to overcome, such as the reproducibility of experiments, false discovery rates, lack of standard reference material for many metabolites, as well as lack of connection and integration among data bases and other omics, which makes of compound identification probably the major limitation of metabolomics.

7.2. Applications in cancer research

Over the last decade, metabolomic studies have made great contributions to cancer research, not only providing comprehensive insights into the complex biological mechanisms and deregulated pathways underlying cancer etiology and progression, but also leading to the discovery of novel diagnostic/prognostic/predictive biomarkers and personalized treatment [227,228] (**Figure 21**).

With regards to MM, several studies using omics technologies have reported many potential biomarkers clinically useful for this neoplasia [229]. Unfortunately, none of them has reached the clinical practice so far. In the last years, several metabolomic studies have evaluated metabolic changes in MM cells using various analytical techniques in both *in-vivo* and *in-vitro* models, but using other methodological platforms such as GC-MS [230] or NMR [231]. Only a few of them have been recently carried out in MM patients' serum samples [232] or using untargeted LC-MS approaches [233,234].

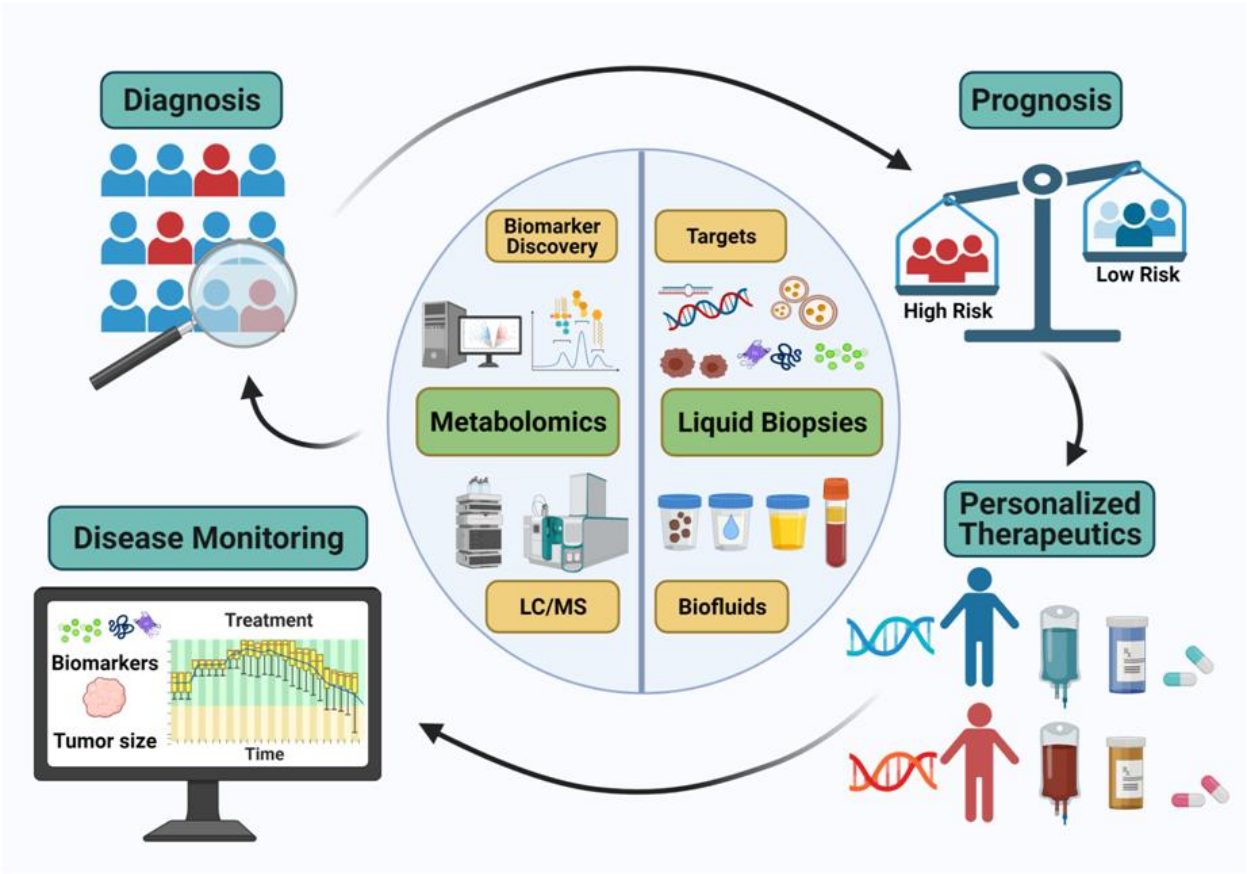

Figure 21. Clinical applications of liquid biopsies and metabolomics. Liquid biopsies include several body fluids, such as blood, urine, saliva, or stool, which contain cancer-derived cells and molecular components, including CTCs, nucleic acids, proteins, metabolites and exosomes. These targets circulate throughout the patient's body and can be detected and analyzed thanks to modern technologies such as metabolomics. The application of these types of technologies to liquid biopsies analysis offers a number of clinical applications: detection and quantification of potential biomarkers for early diagnosis of cancer, identification of aggressive subtypes of cancer and high-risk patients who require intensive treatment; design of optimal personalized therapies; as well as monitor in real time the treatment response of each individual.

Therefore, significant efforts still need to be made in finding suitable biomarkers that could aid or improve MM early and accurate diagnosis. In this regard, untargeted LC-MS-based metabolomics applied to liquid biopsies and circulating compounds could pave the way toward those achievements (**Figure 21**).

HYPOTHESIS

HYPOTHESIS

In this era of precision medicine and multiple effective treatments for cancer disease, such as targeted therapies or immunotherapies, the discovery, validation and implementation into clinic of novel reliable biomarkers is essential not only for early and accurate diagnosis, but also for designing the optimal personalized therapeutic strategy and, ultimately, for improving patients' survival. In this sense, MM is a clear example, representing a highly curable type of cancer, if detected early. If not, it is the most aggressive and deadliest form of skin cancer, showing an extraordinary metastasis capacity and chemotherapy resistance, which are partially due to CSCs. To date, unfortunately, there are no suitable clinical diagnostic, prognostic or predictive biomarkers for this disease. Therefore, significant efforts have been carried out in recent years and many sources of potential biomarkers are being researched by using different cutting-edge technologies.

In this context, our hypotheses were based on the following pieces of evidence:

1. CSCs are responsible for the tumor initiation, progression, therapy resistance, relapse and metastasis. However, despite their great potential, their isolation and characterization still remain challenging, and they are not currently being used as diagnostic and prognostic tools in the clinical practice.
2. Accumulating evidence supports the idea of the multiple roles that exosomes play in cancer's biology, including tumor progression and dissemination to distant organs. These sEVs are actively released by all cells, including CSCs, to the extracellular matrix and to the bloodstream.

Hypothesis

3. Circulating compounds, including exosomes, represent a novel source of biomarkers since they can be easily isolated from the different body fluids. Accordingly, liquid biopsies analysis using different omics technologies and analytical platforms, such as metabolomics and LC-HRMS, represent a powerful tool for biomarker discovery.
4. Currently, there are no suitable clinical diagnostic, prognostic or predictive biomarkers for MM, and the few which have been proposed neither take into account the CSCs nor the CSC-derived exosomes as a target.
5. The metabolomic characterization of exosomes derived from CSCs and serum of patients with MM might allow the identification of potential exosomal and serological biomarkers with diagnostic, prognostic or predictive value for this disease.

OBJECTIVES

OBJECTIVES

Based on our hypotheses, the main goal of this study was to identify potential CSC-derived exosomal and serological biomarkers using metabolomics techniques (LC-HRMS) with diagnostic value for malignant melanoma.

In order to achieve this general objective, several specific objectives were established:

1. To recruit patients with MM at several stages of disease, collecting both serum samples and clinical data.
2. To isolate, enrich and characterize CSC subpopulations in MM cell lines.
3. To isolate and characterize exosomes derived from both MM-CSCs and serum of patients with MM.
4. To analyze the metabolomic profile of both MM CSC-derived and serum-derived exosomes, as well as those of total serum of patients with MM by using a LC-HRMS analytical platform and following an untargeted biomarker discovery approach.
5. To detect those metabolites differentially expressed in exosomes derived from MM-CSCs and non-CSCs, as well as in patients with MM and healthy individuals, not only in their serum-derived exosomes but also in the total serum fraction.
6. To identify those differential compounds susceptible to being considered as potential biomarkers, and tentatively evaluate their potential clinical usefulness in terms of early diagnosis of MM.

MATERIALS AND METHODS

MATERIALS AND METHODS

1. MALIGNANT MELANOMA PRIMARY CELL LINE

1.1. Cell culture and CSC enrichment

The human primary Mel1 MM cell line comes from a malignant metastatic melanoma (stage M1a) skin biopsy (BBSPA-Mel#1) and was provided by the Biobank of the Andalusian Public Health System (Spain). This cell line is hipotriploid (complex karyotype with multiple numerical and structural chromosome abnormalities), MelA positive, p53 positive and S100 positive, and has high tumorigenic ability. Mel1 adherent cells were maintained in standard culture conditions. Enriched Mel1 CSC subpopulations were obtained after culturing as primary and secondary spheroids in serum-free medium and in anchorage-independent conditions [235]. Mel1 adherent cells were cultured in a humid incubator at 37°C and 5% CO_2, with DMEM (Dubelcco's Modified Eagle's medium) (Sigma-Aldrich, St. Louis, MO, USA) supplemented with 10% heat inactivated fetal bovine serum (FBS) (Gibco, Grand Island, NY, USA) and 1% Penicillin/Streptomycin (P/S) (Sigma-Aldrich) in 75 cm^2 flask culture (Nunc, Roskilde, Denmark), unless otherwise indicated. FBS was inactivated by heating at 56°C for 45 minutes. Cells were assayed for mycoplasma contamination. Enriched Mel1 CSC subpopulations were obtained as follow: for primary spheroids, culture cells were collected by centrifugation (1500 rpm for 10 min) and the pellet was resuspended twice in phosphate buffered saline (PBS). Then, resuspended cells were plated in serum-free sphere culture medium (DMEM:F12, 1% P/S, B27, 10 µg/mL ITS, 1 µg/mL Hydrocortisone, 4 ng/mL Heparin, 20 ng/mL EGF, 10 ng/mL FGF, 10 ng/mL IL6, 10 ng/mL HGF) in ultra-low adherence 6-well plates (Corning, Corning, NY, USA) for 72h. For the secondary sphere culture, cells from primary spheroids were collected by

centrifugation (1500 rpm for 10min), and then the pellet was resuspended in DMEM-F12 sphere medium mechanically disrupted with a pipette and by syringing three to five times through a sterile 25-gauge needle. After that, cells were plated, resuspended and incubated for 72h in sphere culture medium in ultra-low adherence 6-well plates.

1.2. Sphere-forming assay

To determine the self-renewal ability of the Mel1 CSCs population, a sphere-forming assay was performed [236]. Mel1 cells were grown as spheroids as described above: 2.5×10^5 cells were washed with PBS and resuspended in sphere culture medium in ultra-low adherence 6-well plates (Corning). Spheres > 75 μm diameter were counted after 3 days by light microscopy. For the secondary sphere-forming assay, 2.5×10^5 single cells derived from primary spheroids were plated and resuspended in sphere culture medium in ultra-low adherence 6-well plates. Diameters were measured using the ImageJ software.

1.3. Colony-forming assay

The clonogenic capability of Mel1 CSCs was determined by a colony-formation assay in soft agar as previously described [236] with minor modifications. Briefly, 10^4 cells coming from secondary spheroids were seeded in 0.4% cell agar base layer, which was on top of 0.8% base agar layer in 6-well culture plates. Then, cells were incubated for 23 days at 37°C and 5% CO_2, adding 100 μL of DMEM (10% FBS, 1% P/S) every 1-2 days. Cell colony formation was then examined under a light microscope after staining with 0.1% Iodonitrotetrazolium Chloride (Sigma-Aldrich). The size of colonies was measured using ImageJ software.

1.4. Aldefluor assay and phenotypic characterization by flow cytometry

The analysis of CD20 and CD44 surface markers and the ALDH1 activity were performed using a Becton Dickinson FACSCanto II flow cytometer from the CIC Scientific Instrumental Centre (University of Granada) as previously described [236]. Briefly, ALDEFLUOR assays (Stem Cell Technologies, Vancouver, Canada) to detect ALDH1 activity in viable cells were performed according to the manufacturer's instructions. Cells were suspended in aldefluor assay buffer containing ALDH1 substrate (BAAA, 1 μmol/l per 1×10^6 cells) and incubated for 45 minutes at 37°C in darkness. Dethylaminobenzaldehyde (DEAB) was used as an ALDH1 inhibitor to set ALDH1 gates. The brightly fluorescent ALDH1-expressing cells were detected in the green fluorescent channel (520-540 nm). Cell surface levels of CD44 and CD20 were determined with anti-human antibodies CD44-phycoerithrin (PE) and CD20-allopycocyanin (APC) (MiltenyiBiotec, BergischGladbach, Germany), respectively. The brightly fluorescent PE and APC were detected in red (564-606nm) and blue (650-670 nm), respectively. All samples were analysed on a FACS CANTO II (BD Biosciences, San Jose, CA, USA) using the FACS DIVA software.

1.5. Side population assay

Hoechst 33342 exclusion (Side Population) assays were carried out as previously described [237] to analyse cells overexpressing ABC transporters. Single cell suspension obtained from parental cell lines and melanospheres were stained with Hoechst 33342 (Sigma-Aldrich) dye. As negative controls, Verapamil (Sigma-Aldrich) was used for maintaining the efflux channel closed, inhibiting the capacity to efflux Hoechst 33342 by cells. The brightly fluorescent cells were measured by flow cytometry in Hoechst blue (440/40) and Hoechst red

(695/40) of a FACScan Aria III (BD Biosciences) using FACS DIVA software from the CIC Scientific Instrumental Centre (University of Granada). Cells with the ability to efflux Hoechst 33342 were considered as the side population (SP).

2. EXTRACELLULAR VESICLES: EXOSOMES

2.1. Isolation and purification

For exosome isolation, Mel1 cells were cultured in 75 cm^2 flasks culture in standard anchorage-dependent culture conditions with DMEM supplemented with 1% P/S and 10% heat inactivated exosome-depleted FBS, until 80% confluence. FBS was depleted of bovine exosomes by ultracentrifugation at 100,000g for 70 min [216]. Exosomes were also isolated from Mel1 CSCs: a total of 3×10^6 cells were cultured as primary and, then, as secondary spheroids in anchorage-independent and serum-free conditions, as described above. Supernatant fractions collected from cell cultures after 72 h were centrifuged at 500g for 10 min to remove any cell contamination and debris. Exosomes from cell-free culture supernatants were purified by sequential centrifugation as previously described by Costa-Silva et al. with minor modifications [238]. Briefly, to remove any possible apoptotic bodies, dead cells and large cell debris, the supernatants were first spun at 10,000g for 40 min. Exosomes were collected by ultracentrifugation at 100,000g for 80 min. Exosome pellets were washed in 35mL PBS and pelleted again by ultracentrifugation at 100,000g for 80 min (Beckman SW28 rotor). In addition, serum-derived exosomes from patients with MM and healthy individuals were isolated following the same protocol described above, but washing the exosome pellets in 10 mL PBS. The final pellet was resuspended in 100µL of PBS and stored frozen at -80˚C for further analyses. Repeated freezing and thawing of the exosome suspensions was avoided.

2.2. Characterization

2.2.1. Transmission and scanning electron microscopy

Transmission Electron Microscopy (TEM) and Scanning Electron Microscopy (SEM) analyses were performed at the Centro de Instrumentación Científica (CIC, University of Granada). For TEM and SEM, samples were negatively stained with uranyl acetate as follows: a 30 μL drop of the exosome sample was placed on a carbon-coated 300 mesh grid and allowed to adsorb at room temperature for 5 min. The grids were then washed in drops of ultrapure water for 1 min. Adsorbed exosomes were negatively stained by placing the grids on a drop of 1% uranyl acetate in aqueous suspension for 1 min. The excess fluid was slightly drained with filter paper, and then sample grids were dried at room temperature for 6 min. The preparations were examined with a LIBRA 120 PLUS transmission electron microscope (Carl Zeiss SMT, Oberkochen, Germany) at an acceleration voltage of 120 kV, and the HITACHI, S-510scanning electron microscope. Then, samples were determinate with the Edwin-Röntec microanalysis system.

In addition, pellets obtained from CSC cultures were immersed in 4% paraformaldehyde/0.1 M PBS for 4 hours at 4ºC and washed in sucrose in 0.1 M PBS overnight. The fractions were incubated by increased alcohol concentrations and were cut in semithin sections at 0.5 μm with tissue processor (TP1020, Leica, Germany).

2.2.2. Atomic force microscopy

Atomic Force Microscopy (AFM) analyses were performed at the Centro de Instrumentación Científica (CIC, University of Granada). For AFM, purified exosomes were diluted 1:10 in deionized water. A 10μL drop of exosome suspension was adsorbed to freshly

cleaved mica sheets at room temperature for 10 min and rinsed with deionized water to remove salt precipitates. The sheets were then completely dried under a gentle stream of argon gas (Ar). The preparations were examined with an NX20 Atomic Force Microscope (Park Systems, Suwon, South Korea) and images were visualized and processed using the Park Systems XEI software. Measurements were carried out with ACTA cantilevers (40 $N \cdot m^{-1}$) and in Non-Contact Mode.

2.2.3. Western blot analysis

Exosome pellets were isolated from 100 mL of cell culture supernatants of adherent cells and CSCs and from 600 µL of patients' serum. The final pellets were resuspended in 100 µL of PBS and stored at 4°C for further protein quantification. The protein concentrations were measured using the BCA Protein Assay Kit (Pierce, Rockford, IL, USA) according to the manufacturer's instructions. Proteins extracts (30µg) were denatured at 95°C for 5min in loading buffer (containing Tris – pH 6.8, SDS, glycerol, β-mercaptoethanol and bromophenol blue). Proteins were subjected to 4-20% Mini-PROTEAN TGX (Bio-Rad, USA) gel together with Precision PlusProteinTM Kaleidoscope Prestained Protein Standards (Bio-Rad, USA). The samples were transferred to a nitrocellulose membrane (Trans-Blot, Mini Format, Bio-Rad) using a transfer apparatus according to the manufacturer's protocols (standard program: 25 V for 30 minutes) (Bio-Rad). After incubation with 5% skimmed milk in PBS-Tween 0.1% for 1 h at room temperature, the membranes were incubated overnight with antibodies against CD9 (dilution 1/1500, eBioscience), CD63 (dilution 1/500, Santa Cruz Biotechnology), CD271 (dilution 1/500, Abcam) and Alix (dilution 1/1000, Cell Signaling). Membranes were then incubated with conjugated goat anti-mouse secondary antibody and goat anti-rabbit secondary

antibody for 2 h, and signals were detected using the ECL-PLUS y ECL PRIME (Amersham Biosciences). The bands were visualized with medicals photographic films (AGFA).

2.2.4. Exosome size analysis

Analyses were performed on NanoSight NS500 instruments (Malvern Instruments, UK). The instrument was equipped with a 488 nm laser, a high sensitivity CMOS camera and a syringe pump. Exosomes were diluted 1:1000 in PBS buffer to obtain a concentration range (1-10 x 10^8 particles/mL). The measurements were analysed using the NTA2.3 software (Malvern) after filming three 60-second videos.

2.2.5. Immunogold labelling by transmission electron microscopy

Immunogold labelling of exosomes was carried out at the Andalusian Centre for Nanomedicine (Bionand, Spain). Exosomes suspensions were put on copper grid with Formvar-Carbon and incubated for 15 min at RT. They were dried slightly and diluted in 15 µL of 2% paraformaldehyde in 0.1 M PBS and incubated for 10 min. The samples were transferred to a 15 µL drop of 2% BSA in 0.1 M PBS, plus the primary antibody Anti-Human CD63 Clone H5C6 (RUO) (Becton Dickinson) diluted 1/500 and incubated for 1.5 h at room temperature within a humid chamber. After several PBS washes, the grid was incubated with the Anti-Mouse IgG (Whole molecule)-gold 10 nm secondary antibody (Sigma Aldrich) and incubated 1 h at room temperature within a humid chamber. The samples were marked with a negative stain by using 15 µL of 1% uranyl acetate in Milli-Q water for 15 seconds. The preparations were examined with a LIBRA 120 PLUS transmission electron microscope (Carl Zeiss SMT, Oberkochen, Germany).

3. PATIENTS WITH MALIGNANT MELANOMA

3.1. Collection and preparation of serum samples

Serum samples were collected in the Oncology Service at the University Hospital Virgen de las Nieves of Granada and University Hospital San Cecilio of Granada (Spain). The ethics committee from both hospitals approved the study (number: 32140085), and all clinical investigations were conducted according to the principles expressed in the Declaration of Helsinki ("Ethical Principles for Medical Research Involving Human Subjects"). Written informed consent was obtained from all patients and controls before their enrolment in the study. Samples were collected in BD vacutainer SSTII advanced tubes (Becton Dickinson, Franklin Lakes, NJ) with silica to activate clotting of the specimen, incubated at room temperature for 30 min, and centrifuged for 10 min at 1400g. Afterwards, the supernatant (around 1 mL) was carefully aspirated and stored at -80ºC until the examination.

Regarding the experiments carried out in chapter 1, samples were obtained from serum of patients with MM (MMPs) (n=20) and healthy controls (HCs) (n=14). MMPs presented different stages of the disease, namely: Stage I (n=5), stage II (n=5), stage III (n=5) and stage IV (n=5).

For those experiments performed in chapter 2, a total of 105 serum samples were collected, containing 26 HCs and 79 MMPs. Regarding the stage of disease, MMPs presented different stages, namely: Stage I (n=22), stage II (n=22), Stage III (n=22) and stage IV (n=13).

In both cases, serum samples from the corresponding HCs were supplied by the Biobank of the Andalusian Public Health System and were collected and treated in the same manner as the patients' samples.

4. METABOLOMIC ANALYSES

The metabolomic analyses of exosomes isolated from cell culture supernatant and patients' serum samples were performed in Fundación MEDINA (Centro de Excelencia en Investigación de Medicamentos Innovadores en Andalucía) as described by García-Fontana, et al. with minor modifications [239].

4.1. Metabolite extraction

Exosome samples from both MM Mel1 cell line and MMPs' serum (chapter 1), as well as total serum samples from MMPs and HCs (chapter 2), were kept at 4˚C during the analytical process. Sample preparation for LC-HRMS analysis was performed as follows. Exosome samples were thawed on ice and vortexed. Proteins were removed from exosome suspension using an appropriate extraction solvent [methanol (1:3 exosomes:MeOH) for exosome samples and acetonitrile(1:8 serum/AcN) for total serum samples] and shaken (60 seconds), [Exosome samples were also sonicated (1 min) and shaken again]. Then, samples were centrifuged at 13,300 rpm for 15 min at 4°C. Supernatants were collected and dried under an N_2 air stream. Dried samples were reconstituted in mobile phase (MP) (50% H_2O and 50% AcN at 0.1% of formic acid), 90 μL or 250 μL for exosomes samples and total serum samples, respectively. Internal standards such as caffeine, creatine, L-Leucine, roxithromycine or L-Abrine were also added at 500 ppbs. Next, samples were transferred to the analytical vials. Samples were stored at 4°C and analysed within 24 hours of reconstitution.

4.2. High-Performance-Liquid-Chromatography/High-Resolution-Mass-Spectrometry analyses

HPLC/HRMS were carried out using an AB SCIEX TripleTOF 5600 quadrupole-time-of-flight mass spectrometer (Q-TOF-MS) (AB SCIEX, Concord, Canada) coupled to high performance liquid chromatography (HPLC) system, in positive electrospray ionization (ESI) mode.

Before HRMS analysis, chromatographic separation was performed by Agilent Series 1290 LC system (Agilent Technologies), equipped with a reverse phase Atlantis T3 HPLC C18 column (C18: 2.1mm x 150mm, 3mm) (Waters, Milford, MA, USA) kept at 25 ºC in ESI mode. Mobile phase was 0.1% formic acid-90:10 H_20/AcN (Eluent A) and 0.1% formic acid-90:10 AcN/H_20 (Eluent B). The gradient elution was: 0.00–0.50 min 1% eluent B, 0.50–11.00 min 99% eluent B, 11.00–15.50 min 99% eluent B, 15.50–15.60 min 1% eluent B, and 15.60–20.00 min 1% eluent. The elution flow rate was 300 µL/min. For each sample, 5 µL were injected into the HPLC system. Samples were injected randomly in order to prevent any possible time-dependent changes in the chromatographic profiling. Blank solvent (BS) and quality control (QC) samples were injected interspersed in the sequence run. The QC samples were prepared by pooling an equal volume of all samples and injected frequently across the sequence run in order to check the stability and performance of the system. The BS samples were also run interspersed in the sequence to identify possible impurities of the solvents or extraction procedure and to check carryover contamination from intense analytes.

For HRMS analysis, TripleTOF 5600 was operated using a TOF method in combination with information dependent acquisition (IDA) method, obtaining not only full scan mass spectra

acquisition but also simultaneous automatic acquisition of MS/MS fragmentation mass spectra for the most intense ions of each scan. Ion Source parameters and IDA conditions were: gas source 1: 50.00; gas source 2: 50.00; curtain gas: 45.00; temperature: 500.00 °C; ionspray voltage floating: 4500.00; TOF masses: Min = 80.0000 Da Max = 1600.0000 Da; accumulation time: 0.2500 sec, IDA accumulation time: 0.1000 sec. Mass calibration was automatically performed every 10 injections. The method consisted of high-resolution survey spectra from m/z 50 to m/z 1600 and the 8 most intense ions were selected for acquiring MS/MS fragmentation spectra after each scan. An Automated Calibration Delivery System performed an exact mass calibration prior to each analysis.

4.3. Data set creation

PeakView software (version 1.0 with Formula Finder plug-in version 1.0, AB SCIEX, Concord, ON) was used in order to assess the analytical drift in terms of mass and retention time shift, which is an essential step for a reliable processing of data. The variability of several known peaks (m/z and RT), corresponding to those analytical standards previously added, were evaluated. MarkerView software (version 1.2.1.1, AB SCIEX, Concord, ON) was used for processing the LC-HRMS raw data. This software performs peak detection, alignment and data filtering, generating a feature table which defines measured m/z, RT and integrated ion intensity for each peak. An automated algorithm in the RT range 0.8–19 min and m/z range 50–1600 was used for data mining.

For exosome samples, the intensity threshold of extraction was established at 100 counts per second, in order to avoid background noise. RT and m/z tolerances of 0.1 min and 15 ppm, respectively, were used for peak alignment. Background noise was removed by using a specific tool of MarkerView software. The analytical replicates of each sample were averaged.

For total serum samples, extraction intensity threshold was established in 50 counts per second. Peak alignment was achieved using RT and m/z tolerances of 0.07 min and 10 ppm, respectively. Based on the accuracy of mass measurement, the algorithm select true molecular features, and group ions related to charge-state envelope and isotopic distribution. Only features that were present at least in 60 samples were considered. In order to discard possible contaminants and background mass signals present in the BS, a filtering procedure with fold-change (FC > 2) and Student's *t*-test ($p < 0.05$) between BS and MMP/HC samples was applied.

Mass signals with an unacceptable reproducibility (RSD > 30%) with regards to the QC samples were also discarded. Subsequent statistical analyses were carried out using MetaboAnalyst 4.0 Web Server [240] as previously described [239].

4.4. Data pre-treatment

QC distribution on principal component analysis (PCA) plot was used for analytical validation prior to the following analysis. After that, different approaches of data normalization (normalization by a QC reference sample, sum and median normalization), data transformation (logarithmic and cubic root transformation) and scaling (auto scaling and Pareto scaling) were evaluated in order to define which combination provides a better grouping of QC samples on PCA plot and a normal distribution of the data. Variables with unacceptable reproducibility (RSD > 30%) or detected in less than 50% of QC samples, were also rejected from the data matrix.

4.5. Data treatment

Statistical analyses were carried out using MetaboAnalyst 4.0 Web Server. Briefly, after dataset creation, raw data were normalized, transformed, and scaled in order to achieve a more Gaussian type distribution [241]. Then, filtering according to significant differences was done based on statistical analysis including both univariate (UVA) and multivariate (MVA). Statistical analyses were carried out to filter variables (metabolites) that are significantly different between the groups compared. UVA assesses the statistical significance of each peak/variable separately, while MVA takes into account the combination of the effects of multiple variables. For UVA, a double filtering procedure with t-test (p-value < 0.05) and fold-change (FC > 1.5) was applied in order to identify differentially expressed mass signals between BS and biological samples. This first filtering allowed removing background noise and preserving the peaks from true biological samples. Then, UVA-based (ANOVA or t-test) filtering (p-value < 0.05) was used to detect differential metabolites between the sample groups. Thus provides a quality criterion to assess variable relevance for further data analysis. For MVA, principal component analysis (PCA) and partial least squares regression (PLS-DA) were carried out after UVA-based filtering. PCA was applied to assess quality of the analytical system performance. PLS-DA allowed discriminating variables that are responsible for variation between the comparison groups. For statistical validation, quality description by goodness of fit (R^2) and goodness of prediction (Q^2) was used. A powerful model for diagnostics should show high values of R^2 and Q^2 but also not vary more than 0.2–0.3. For metabolomics data, $R^2 > 0.7$ and $Q^2 > 0.4$ are considered acceptable values [241]. Selection of the metabolites with highest discriminatory power and therefore susceptible of being considered as potential biomarkers was based on their variable importance in projection

(VIP) score, which had to be >1, and on their fold change, which had to be <0.6–>1.5. The models were also validated using 10-fold cross validation (CV).

4.6. Biomarker identification

PeakView software was used to estimate the elemental formula of selected marker compounds from accurate mass, isotopic clustering, and fragmentation patterns. Next, accurate mass searching was performed in several compound databases (Metlin, Human Metabolome Database, Lipid Maps, PubChem, ChemSpider). The mass tolerance was established at 10 ppm. For automatic MS and MS/MS elemental formula estimation the Formula Finder plug-in of PeakView software (AB SCIEX) was used, and the mass tolerance was set at 10 mDa. For those tentatively identified compounds with a fragmentation spectrum available, similarities between the theoretical and the experimental fragmentation spectrum was assessed using both the fragmentation pane tool of PeakView software for *in silico* fragmentation and scientific literature search. Only candidates whose presence in humans was likely were selected as potential MM biomarkers.

4.7. Biomarker evaluation

Receiver operator characteristics (ROC) curve analyses were carried out in order to assess the clinical utility of the metabolites selected as potential biomarkers[221,242]. ROC curves are often summarized into a single metric known as area under the curve (AUC), which indicates the predictive and classificatory capacity of a specific biomarker (or model combining several ones). A general guide for assessing the utility of a biomarker based on its AUC is as follows: 0.5–0.6 = fail; 0.6–0.7 = poor; 0.7–0.8 = fair; 0.8–0.9 = good; 0.9–1.0 = excellent. ROC curves are generated by Monte Carlo cross validation (MCCV) using balanced sub-sampling. In

each CV, two thirds (2/3) of the samples are used to evaluate the feature importance. The top important features are then used to build classification models which are validated on the 1/3 of the samples that were left out. The procedure was repeated multiple times to calculate the performance and confidence interval of each model. The AUC provided in this work are flipped (1-AUC) and consequently they are always presented as being >0.5 independently of the case control ratios. Biomarker evaluation models were created using a linear SVM with different numbers of features (up to 10 in this case). ROC curves were generated using the predicted class probabilities from repeated cross validation for each model.

5. STATISTICAL ANALYSES

For Mel1 characterization, all data are presented as the mean ± standard deviation. Differences between groups were analysed for statistical significance using the two-tailed Student's t-test. P-value of 0.05 was accepted as the statistical significance level.

CHAPTER 1

Metabolomic profile of cancer stem cell-derived exosomes from patients with malignant melanoma

BACKGROUND

BACKGROUND

Malignant melanoma (MM) is the most aggressive and life-threatening form of skin cancer whose incidence continues increasing worldwide at a great rate. It is known that this aggressiveness is mainly due to intratumoral heterogeneity. In fact, tumor cells are hierarchically organized and sustained by cancer stem cells (CSCs), a subpopulation of cells with stem-like functional properties such as self-renewal ability and multipotency, among others [92,93]. This fraction of cells is highly responsible for tumor initiation, maintenance, progression, metastasis and recurrence. In addition, CSCs are remarkably resistant to radiotherapy and chemotherapy as a consequence of their particular biology [94]. Moreover, the CSC phenotype is not a rigid state and the intratumoral heterogeneity of cancer also extends to CSC characteristics, mainly due to tumor microenvironment (TME) [84]. In particular, malignant melanoma CSCs can be identified by the expression of specific markers and functional assays, and their stem-like properties have been demonstrated *in vitro* and *in vivo* [243,244].

Although significant efforts have been made in the last years, identification of useful diagnostic, prognostic and predictive biomarkers in MM remains challenging. Several candidate biomarkers have been proposed but few have reached clinical application [245]. Thus, it is important to discover specific useful biomarkers and develop methods that can sensitively detect this neoplasia at subclinical metastatic stages.

Recent investigations confirm that extracellular EVs and exosomes (sEVs), including those released by CSCs, play important roles in cancer's biology [203]. By transferring their cargo to different target cells, including surrounding TME cells, they promote multiple processes directly related with tumor initiation, sustenance, progression and metastasis, including angiogenesis, immune system modulation and avoidance, tumor growth, and tumor parenchyma

remodelling [204–207]. MM-derived exosomes are involved in the metastatic dissemination to regional lymph nodes [208] and distant parts of the body by promoting the generation of pre-metastatic niches [209,211].

Importantly, exosomes and other EVs represent an important source of circulating biomarkers, since they are released into the bloodstream and other body fluids, especially by cancer cells [203,214–217]. Therefore, they can be easily isolated by minimally invasive techniques such as liquid biopsies, representing a rich source of potential novel biomarkers for the diagnosis and prognosis of cancers, including MM, as well as therapeutic targets [215,246,247].

In this context, metabolomics as emerging "omic" research technology represents a powerful tool for biomarkers discovery. Metabolomics refers to the systematic identification and quantification of the complete set of low molecular weight metabolites, known as metabolome, which are context dependent and vary according to the physiology, developmental or pathological state of a cell, tissue or organism [248]. The study of the complete metabolome is technically challenging, due to its diversity, and multiple strategies are employed to provide a broad metabolic coverage. In this regard, MS is the gold standard analytical platform for metabolomics, as it provides high sensitivity, versatility and reproducibility [217,224,248]. In order to extract useful biological information from large and complex datasets generated by mass spectrometers, univariate (T-test, ANOVA) and multivariate (PCA, PLS-DA) statistical analyses are used [217,240].

Over the last decade, several studies using omics technologies have enhanced the development and validation of biomarkers currently used in the diagnosis, prognosis and

treatment response prediction in MM [229], but unfortunately none of the metabolites identified as potential biomarkers has been proven to be clinically useful so far.

In this work, we characterized a patient-derived MM cell population enriched in CSCs and analysed the metabolomic profile of exosomes derived from these MM cells and from serum of patients with MM using a high-resolution mass spectrometry untargeted approach (**Figure 22)**. To our knowledge, we reported for the first-time differences on exosome metabolomic profile from CSCs-enriched melanospheres versus MM differentiated cells. We also reported metabolomic differences between serum-derived exosomes from patients with MM at several stages of the disease compared to those derived from healthy controls.

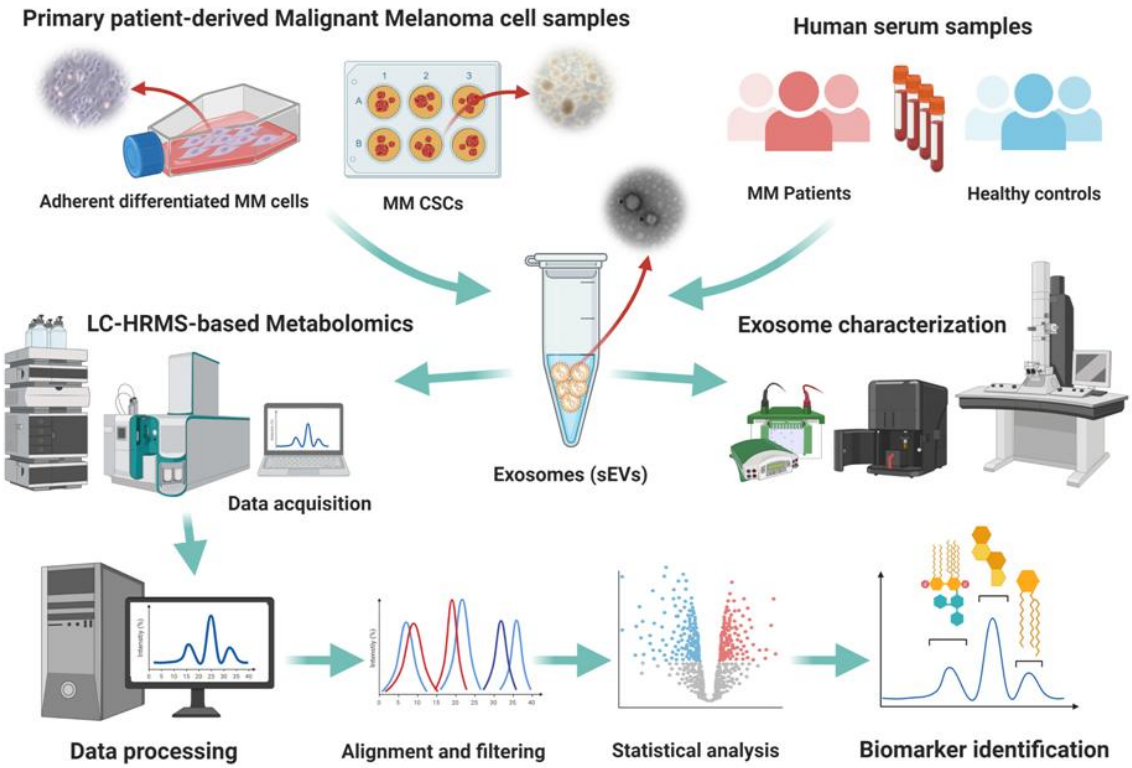

Figure 22. Graphical abstract representing the general workflow and the main assays performed in this study.

RESULTS

RESULTS

1. Characterization of primary Mel1 melanospheres

For the enrichment of melanoma CSCs, we used a primary patient-derived tumor cell line (Mel1) from an MM skin biopsy (stage M1a). We studied the anchorage-independent growth of Mel1 spheres in serum-free conditions [235] to determine their CSC characteristic phenotype by determining sphere forming ability, proliferation rate of primary and secondary melanospheres, clonogenic capacity by colony-formation assay in soft agar, side population, CD20 and CD44 cell surface markers expression and ALDH activity.

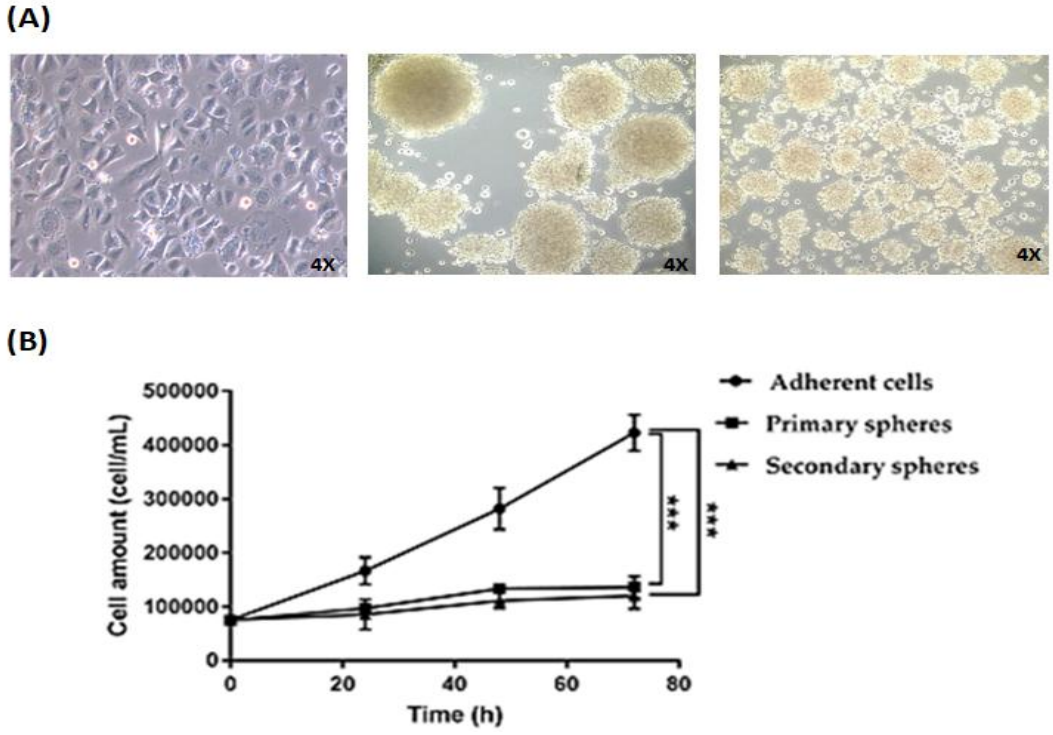

Figure 23. (A) Representative light microscopy (4x) images of primary (left) and secondary (right) melanospheres formed from Mel1 cell line; **(B)** Proliferation curves of Mel1 adherent cells and melanospheres cultured for three days and seeded with an equal number of cells at day 0.

Under anchorage-independent and serum-free conditions Mel1 cells had the capacity of self-renewal by the increased sphere number and size of melanospheres (**Figure 23A**).

Cells growing as melanospheres had a significantly lower proliferation rate when compared to the adherent cell culture of the same cell line, with a doubling time for adherent cells, primary and secondary spheres of 31.6, 51.7 and 65.1 h, respectively. Therefore, melanospheres showed the slow-cycling nature of stem cell populations (**Figure 23B**).

Although a significantly higher number of secondary spheres were observed in comparison with primary spheres (**Figure 24A**), the size was smaller in secondary spheres than in primary spheres, with average diameters of 5.6 and 0.8 mm, respectively (**Figure 24B**). Moreover, Mel1 melanospheres showed a high capacity to form colonies in soft agar (**Figure 24C**).

Accordingly, secondary spheres showed a significantly higher proportion of cells expressing both CD20+ and CD44+ markers with values of 29% and 14.5% respectively in comparison to primary melanospheres (CD44+: 14%, CD20+: 9%) and cells growing in adherent conditions, where only 1.5% and 5% were positive for CD20 and CD44 respectively (**Figure 25A-B**). Moreover, the rate of side population (SP) in melanospheres was significantly higher than in adherent cells (**Figure 25C**). Thus, adherent cells displayed a 9.7% of SP, whereas primary and secondary Mel1 melanospheres showed 17.5% and 24.5%, respectively. Regarding ALDH activity, both primary (8.1%) and secondary melanospheres (26.9%) displayed a significantly higher proportion of ALDH+ cells than the adherent ones (4.8%) (**Figure 25D**).

Altogether, these results indicate that Mel1 cells growing as primary and secondary melanospheres in anchorage-independent and serum free conditions constitute an enriched cell population with functional and phenotypic stemness properties. Since secondary melanospheres were most enriched in CSC properties they were used for subsequent studies.

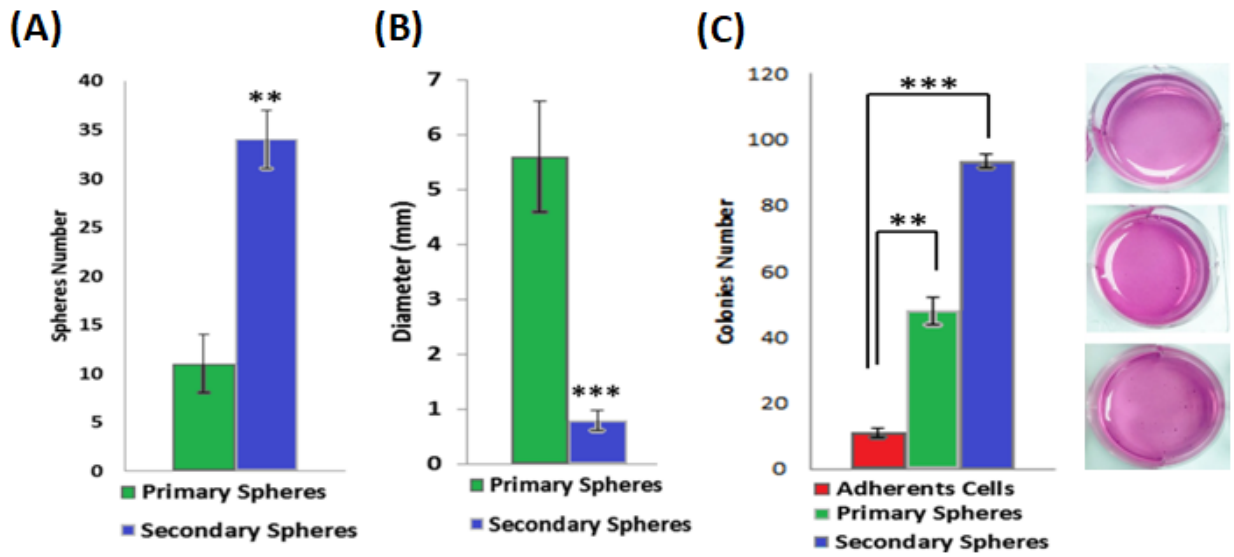

Figure 24. (A) Number of primary and secondary spheres formed by Mel1 cell line growing in anchorage-independent and serum-free conditions. Spheres were counted after 3 days under light microscopy; **(B)** Diameter of primary and secondary spheres, measured by ImageJ software; **(C)** Representative optical image of the colonies formed by Mel1 cells coming from adherents cells, primary and secondary spheroids after 37 days soft agar culture in P6 well plates; stained with 0.1% Iodonitrotetrazolium Chloride.

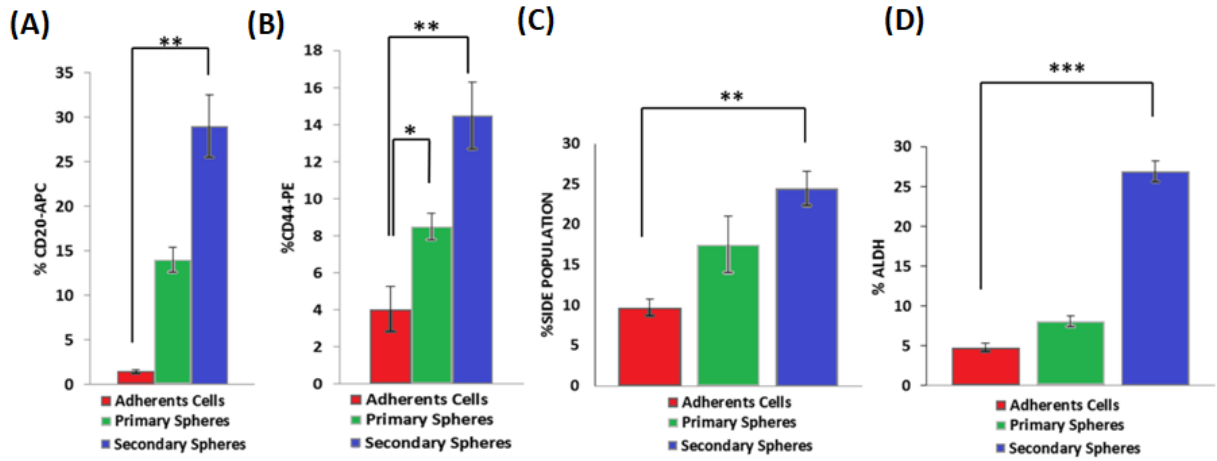

Figure 25. **(A)** Percentage of CD20+ and **(B)** CD44+ in adherent cells and primary and secondary melanospheres; **(C)** Side Population determined in the different culture types; **(D)** Percentage of ALDH+ cells measured by flow cytometry. Data are graphed as mean ± SD from experiments carried-out in triplicates (***P < 0.001; **P < 0.01; *P < 0.05).

2. Isolation and characterization of exosomes derived from primary patient-derived Mel1 CSCs and serum of patients with malignant melanoma

Based on their unique size and density, we isolated exosomes from the culture supernatant of Mel1 secondary spheres and MMP serum following the ultracentrifugation protocol described in the Material and Method section. Exosomes purification was confirmed by TEM, AFM, Western blot, NanoSight and SEM.

As shown in TEM images (**Figure 26A**) vesicles obtained from Mel1 secondary melanospheres (Figure 25A) have a characteristic saucer-like ultrastructure with diameters ranging from 40 to 210 nm and crescent shaped membrane invaginations limited by a lipid bilayer, while vesicles obtained from MMP serum had a diameter ranging from 30 to 140 nm. AFM images (**Figure 26B**) showed a heterogeneous organization of exosomes, in terms of the wide variation in shape and size as demonstrated in both 2-dimensional (2D) images and topographic profiles, regardless of their origin.

Western blot analysis (**Figure 27**) showed that these extracellular Mel1 vesicles were positive to known exosome classic markers including CD63, Alix and CD9. Moreover, we were able to detect the expression of the CD271 melanoma CSC marker in both exosomes and Mel1 secondary melanospheres. EVs isolated from serum of HCs and MMPs at different stages of the disease (stages I-IV) were also positive for Alix and CD9 markers.

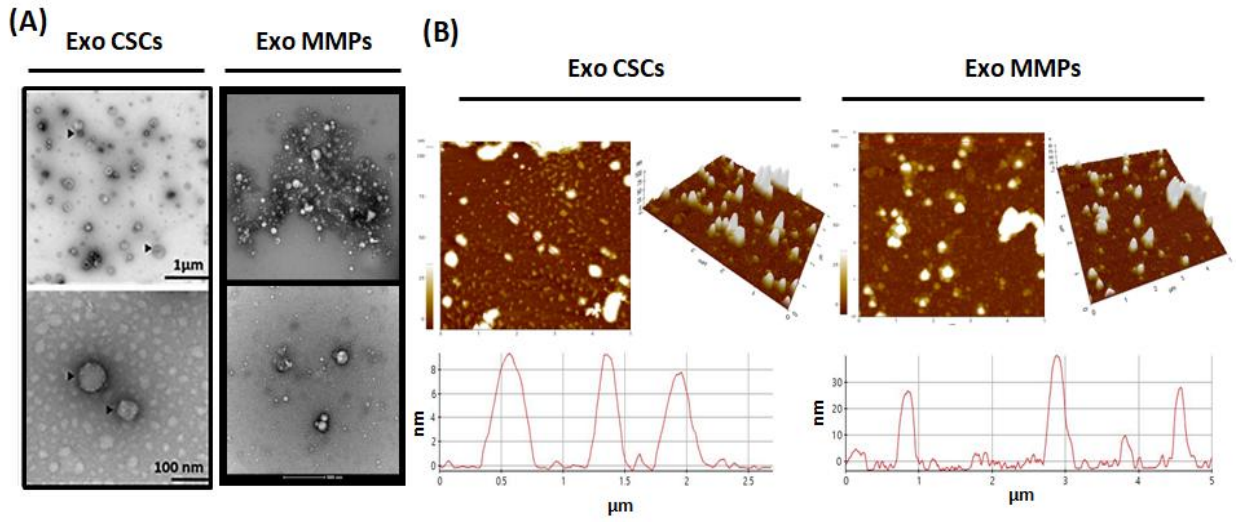

Figure 26. **(A)** Transmission electron microscopy images of isolated exosomes with a saucer-like shape limited by a lipid bilayer. EVs isolated from Mel1 secondary melanospheres culture supernatants had diameters ranging from ~40–210 nm; and those isolated from MMP in had a diameter ranging from ~30–140 nm. Images show exosomes derived from an MMP at stage IV. Black arrow heads point to exosomes; **(B)** Topography of exosomes derived from Mel1 secondary melanospheres and MMP serum observed under atomic force microscopy (AFM). Exosomes on a mica surface revealed heterogeneity in size and shape as well as forming aggregates in both 2-dimensional 2D (left) images and 3D profiles (right). Acquisition areas were 5 x 5 μm^2.

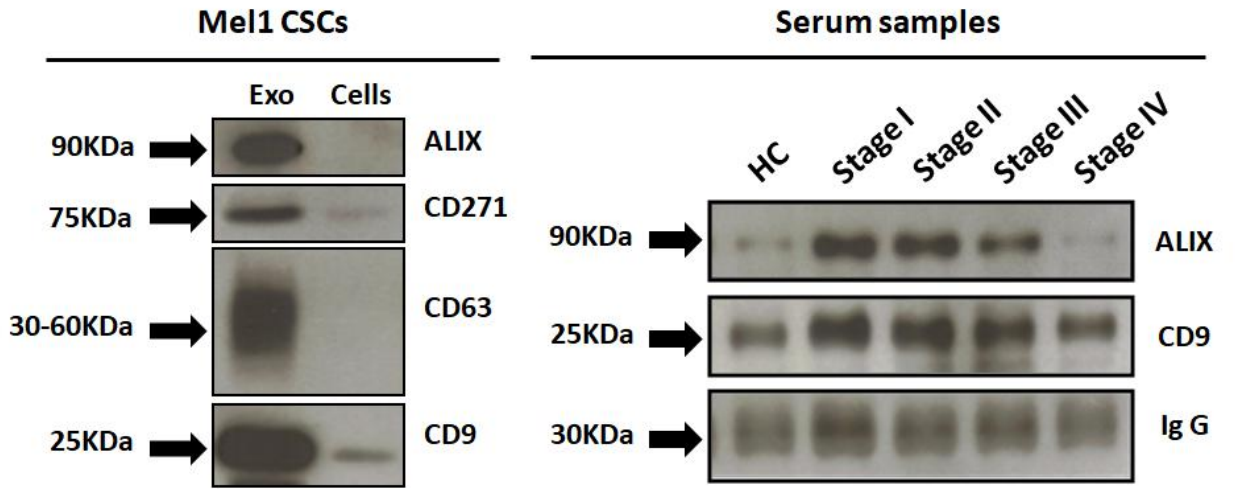

Figure 27. Western blot analysis of CD9, CD63, Alix exosomal surface markers and the CD271 melanoma stem cell marker in melanospheres-derived exosomes and Mel1 CSCs. The expression of CD9 and Alix are also shown as representative exosomal surface markers in MMP serum-derived exosomes. IgG was used as a positive control.

Exosome size distribution determined by NTA Software confirmed the presence of particles with nanometric size in both types of samples, and the average concentration was 5.48 x 10^8 particles/mL for Mel1 CSC-derived exosomes and 4.64 x 10^8 particles/mL for MMP serum-derived exosomes. Mel1 CSC-derived exosomes showed peaks around 115 nm corresponding to individual exosomes while larger size peaks were related to exosome aggregates (**Figure 28A**), which was also confirmed by SEM (**Figure 28B**). The micro-analysis determined that the majority component was carbon, which confirmed the organic origin of the samples (**Figure 28B**).

Furthermore, we were able to detect MVBs with spheroid structures inside surrounded by a phospholipid bilayer in Mel1 secondary melanospheres (**Figure 29A**). Finally, the morphology and size of exosomes were also verified by immunogold using beads coated with an anti CD63 antibody. Black punctate regions indicate a positive staining for CD63 around the exosome membranes from both Mel1 CSC-derived exosomes and MMP serum-derived exosomes (**Figure 29B**). Exosomes derived from Mel1 differentiated adherent cells were also isolated and characterized according to the same criteria (**Figure S1**).

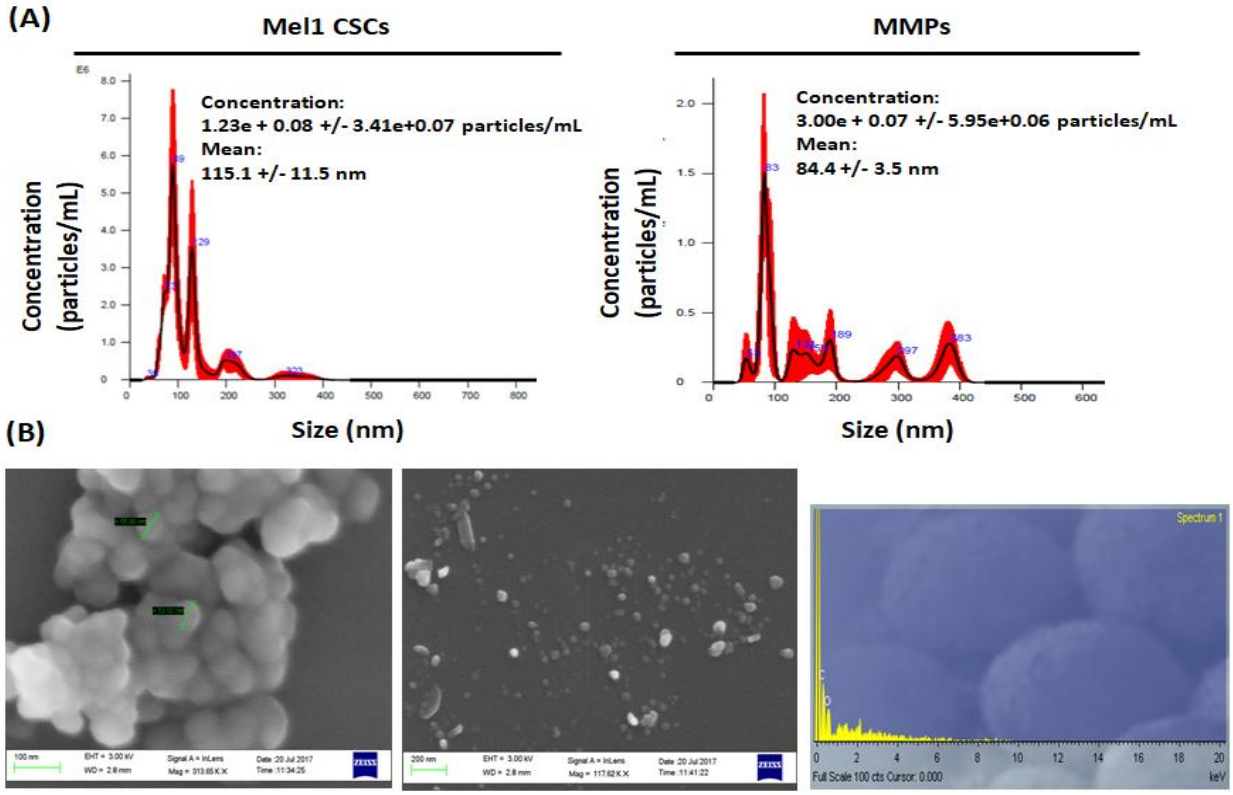

Figure 28. **(A)** The size distribution of exosomes obtained from Mel1 CSCs and MMPs serum was analyzed by NTA; **(B)** Scanning electron microscopy images of CSC derived-exosomes aggregated (left) and individualized (middle) and micro-analysis of particles (right) showing the particle composition.

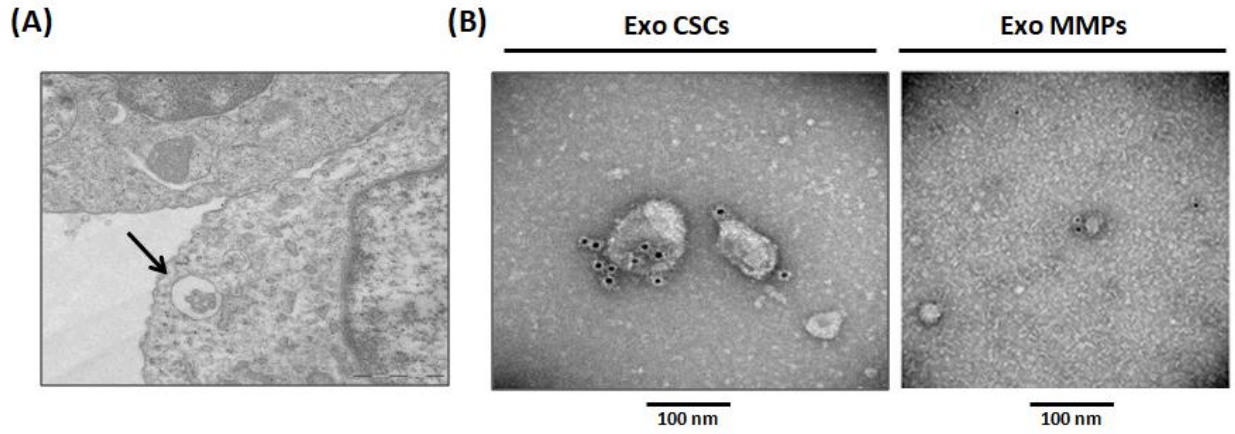

Figure 29. (A) Multivesicular bodies observed by electron microscopy in Mel1 CSCs. Image obtained from paraffin sections; **(B)** Immunogold using beads coated with an anti-CD63 antibody in exosomes derived from Mel1 secondary melanospheres cultures (left) and from a stage IV MMP serum (right).

3. LC-HRMS metabolomic analysis of primary patient Mel1-derived exosomes

Metabolomic characterization was first performed with exosomes isolated from adherent Mel1 tumor cells and from Mel1 CSCs. The LC-HRMS total ion chromatograms (TIC) observed in the positive ionization mode for the metabolites extracted from exosome samples showed excellent reproducibility in terms of retention time and signal intensity, suggesting a low analytical drift across the whole set of samples (**Figure 30**). A positive ionization data matrix of 2,486 mass signals was obtained as an outcome of the peak picking and alignment procedures. In order to filter the results and minimize the signal redundancy, only peaks representing monoisotopic ions (signals with the lowest m/z value within an isotope pattern) were selected (281 peaks) and subjected to the chemometric analysis. After that, raw data were normalized, transformed and scaled, and a first filtering by t-test and two-fold change was performed in order to discard mass signals present in blank solvent samples and, therefore, not exclusively present in biological samples.

After this filtering process, 138 candidates (5.5% of total mass signals) were considered and selected as differentially expressed in exosome samples versus mobile phase solvent samples. Next, ANOVA (p-value < 0.05) and fold change (FC) > 1.5 filtering was performed for multiple comparison on the 3 groups of samples (adherent cells, primary spheres and secondary spheres), and post hoc analysis using Tukey's Honestly Significant Difference (Tukey's HSD) were applied to identify significant metabolite changes. As an outcome, 19 differential m/z signals met these criteria (**Table 1**).

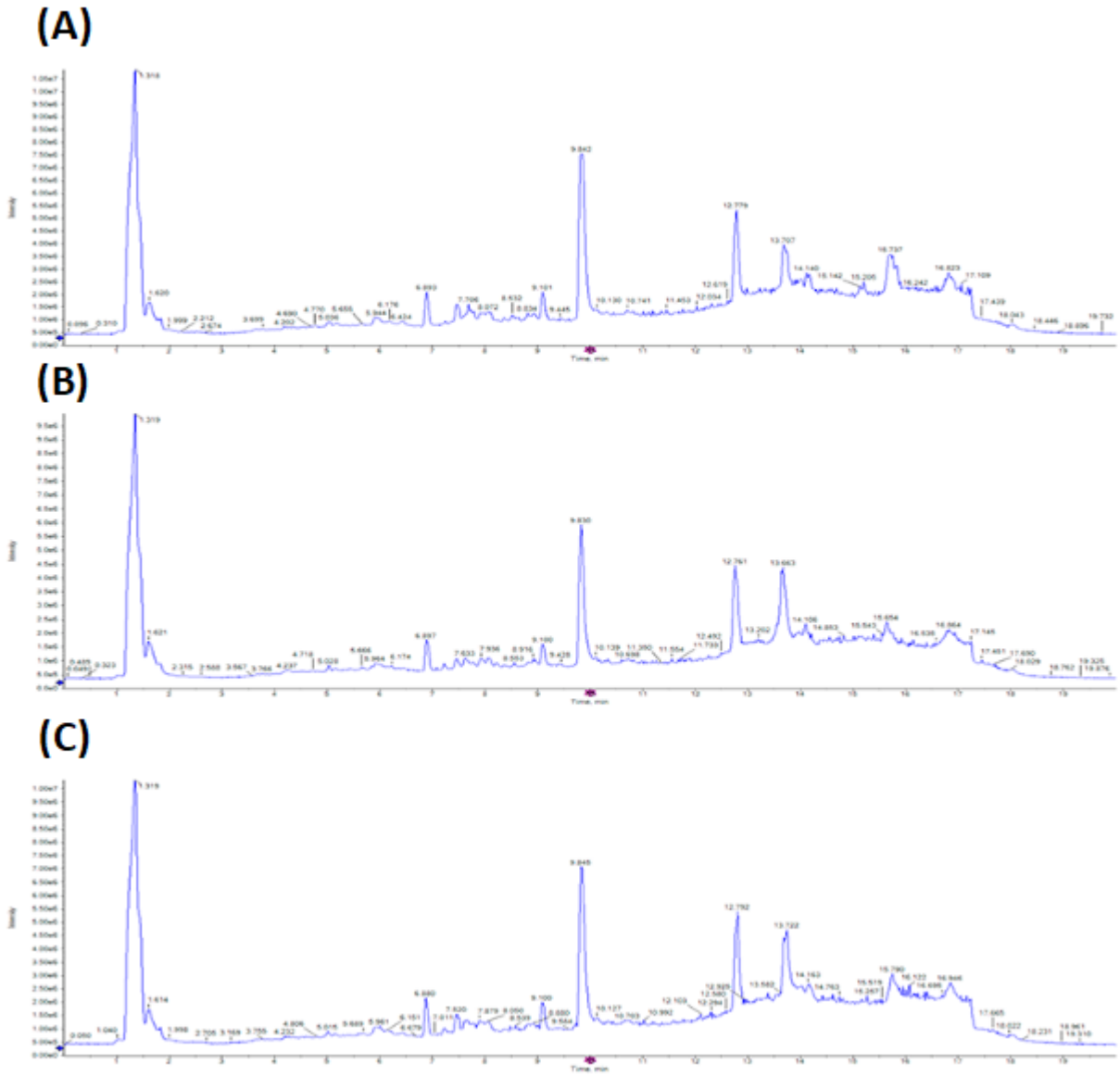

Figure 30. Representative LC-HRMS total ion chromatograms (TIC) of metabolites present in exosomes derived from Mel-1 cell line. TIC corresponding to representative exosome samples derived from **(A)** adherent cells, **(B)** primary melanospheres, and **(C)** secondary melanospheres, scanned by positive ion mode. The X axis represents the chromatographic retention time while the Y axis represents the intensity. Methanol was used for metabolite extraction.

Table 1. Significantly different metabolites found in the three-group comparison between adherent cells (AD), primary spheres (S1) and secondary spheres (S2), in Mel1 patient-derived cell line exosomes.

AD/S1/S2 [1]		
m/z [2]	RT [3]	P-value [4]
378.3214	12.6	$7.62x10^{-6}$
381.0997	5.1	0.001326
388.2521	4.2	0.0011
399.2608	15.2	0.00637
415.2359	15.2	0.006676
426.1372	7.0	0.000571
455.1165	7.7	0.000862
460.3096	4.4	0.005243
483.2172	15.7	0.00584
496.3409	11.6	$1.91x10^{-5}$
530.1469	8.6	$5.87x10^{-5}$
573.2039	5.4	0.006179
589.1461	5.2	0.001116
602.1573	5.1	0.001039
623.0031	1.3	$8.64x10^{-6}$
750.1882	7.7	0.000799
761.1923	5.1	0.00124
909.2258	7.7	0.000875
1206.827	1.3	0.000903

[1] Three-group comparison (ANOVA); [2] Mass-to-charge ratio; [3] Retention time (min); [4] p-value corresponding to univariate statistical analysis (ANOVA). Only peaks with a p-value < 0.05 were selected.

After the selection of those differential m/z signals, samples were analysed by principal component analysis (PCA) and partial least squares discriminant analysis (PLS-DA). The PCA score plots for all the analysed sample groups are shown in **Figure 31**. Blank solvent (BS) samples were clearly separated from biological samples (**Figure 31A**). Additionally, the close clustering of quality control (QC) samples reflected the quality of the analytical system performance (**Figure 31A-B**). Exosome samples derived from adherent cells, primary and secondary spheres were clearly separated from each other along the first principal component (PC1) and the second principal component (PC2), indicating a differential pattern of the metabolites found in exosomes isolated from adherent cells compared to primary and secondary spheres (**Figure 31B**).

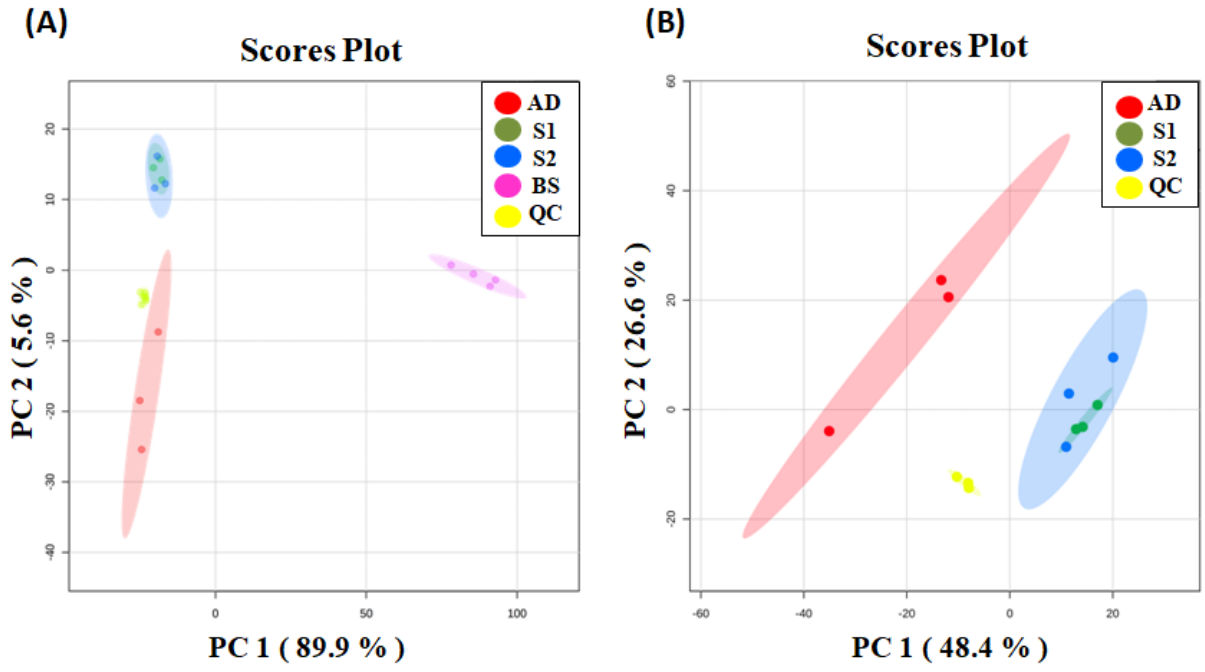

Figure 31. **(A)** PCA scores plot based on LC-HRMS data of all exosome samples derived from adherent cells (red), primary melanospheres (green), secondary melanospheres (blue), QC samples (yellow) and BS samples (pink). (**B**) Analytical validation based on the close clustering of QC samples (yellow) observed in the PCA scores plot.

However, as can be clearly seen in the PCA score plot, the greatest metabolic differences were found between adhered cells and CSCs melanospheres, but not between primary and secondary spheres. For that reason, a filtering by t-test (p-value < 0.05) and FC (FC > 1.5) was also performed comparing adhered cells with secondary spheres samples, as they were those that possessed more stemness properties (Figures 22-24). When comparing these two groups, 19 differential m/z signals also met these criteria (**Table 2**).

Based on PCA and PLS-DA models, exosome samples derived from adherent cells and secondary spheres were discriminated with a R^2 of 0.99 and a Q^2 of 0.97, exceeding the threshold values accepted in metabolomic experiments (R^2 > 0.7 and Q^2 > 0.4) (**Figure 32**) [241]. Accordingly, the heatmap displayed a clear differential pattern of metabolite expression across samples of exosomes derived from both Mel1 adherent cells and Mel1 secondary spheres (**Figure 33**). The corresponding PCA score plot for the three groups (Adherent cells, primary and secondary spheres) of comparison and the heatmap showing the differential abundance of those metabolites found as statistically different between them are shown in **Figure S1**.

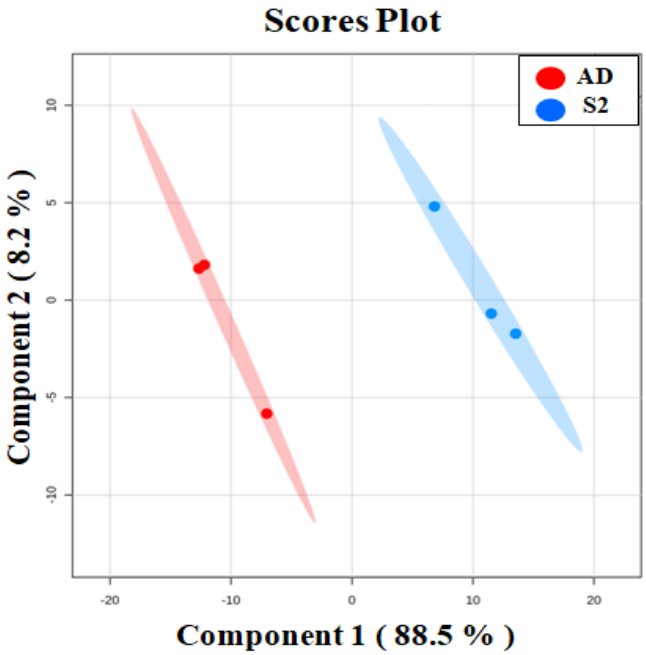

Figure 32. PLS-DA scores plot based on LC-HRMS data of exosome samples derived from adherent cells (red), and secondary melanospheres (blue). The two groups were discriminated with a R^2 of 0.99 and a Q^2 of 0.97, exceeding the threshold values accepted in metabolomic experiments (R^2 > 0.7 and Q^2 > 0.4).

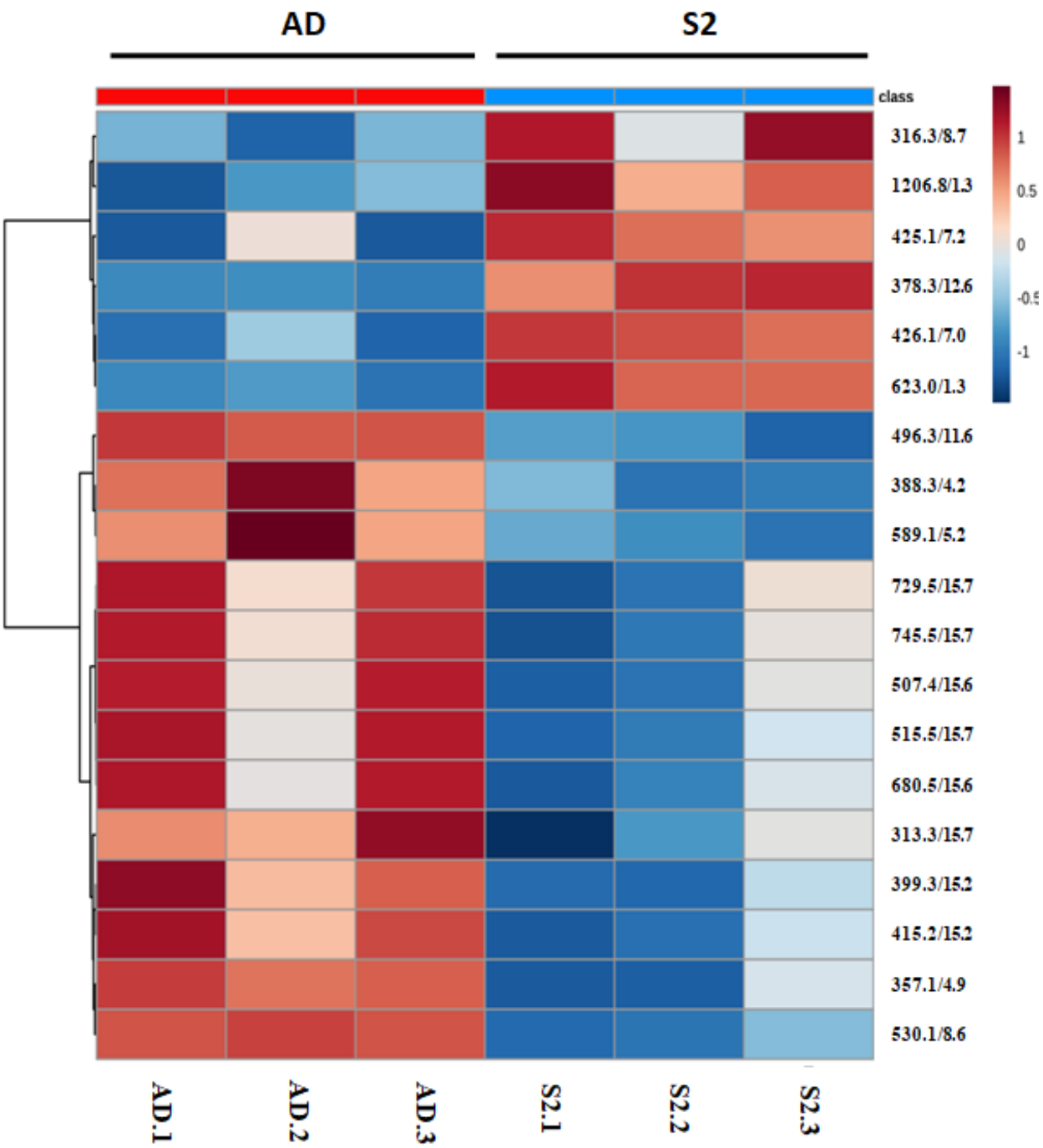

Figure 33. Heatmap showing the significantly different metabolites when comparing exosomes derived from adherent cells (red) and secondary melanospheres (blue). Each row on the heatmap represents a unique metabolite with a characteristic mass to charge ratio and retention time, while each column represents one exosome sample. The colour code represents the normalized intensity with which each metabolite is detected. Blue represents a decreasing trend, while red represents a rising trend.

Table 2. Differential metabolites found in the two-group comparison between exosomes derived from adherent cells (AD) and secondary spheres (S2), in Mel1 patient-derived cell line exosomes.

AD/S2 [1]			
m/z [2]	RT [3]	P-value [4]	FC [5]
313.2714	15.7	0.0318	1.7911 (↑)
316.3215	8.7	0.03372	0.6633 (↓)
357.1404	4.9	0.00163	11.1627 (↑)
378.3214	12.6	0.0008	0.3929 (↓)
388.2521	4.2	0.00685	1.5919 (↑)
399.2608	15.2	0.01546	1.8870 (↑)
415.2359	15.2	0.01587	1.8891 (↑)
425.136	7.2	0.01171	0.1966 (↓)
426.1372	7.0	0.00049	0.1124 (↓)
496.3409	11.6	$6.48x10^{-5}$	4.1367 (↑)
507.4077	15.6	0.04807	3.1055 (↑)
515.3962	15.7	0.04258	2.2071 (↑)
530.1469	8.6	$2.24x10^{-5}$	18.1682 (↑)
589.1461	5.2	0.04382	10.2656 (↑)
623.0031	1.3	0.00377	0.0106 (↓)
680.5277	15.6	0.04514	2.0574 (↑)
729.5293	15.7	0.04517	2.2063 (↑)
745.5143	15.7	0.04205	2.2513 (↑)
1206.827	1.3	0.009	0.4205 (↓)

[1]Two-group comparison (T-Test); [2]Mass-to-charge ratio; [3]Retention time (min); [4]p-value corresponding to univariate statistical analysis (T-Test). Only peaks with a p-value < 0.05 were selected; [5]Fold change expressed as the ratio of the two averages (AD/S2). Only peaks with a fold-change > 1.5 or < 0.66 were selected. The arrows indicate if the metabolite is increased (↑) or decreased (↓) in AD relative to S2.

4. Structural identification of selected differential metabolites in primary patient Mel1 cells

Metabolite identification was carried out according to the criteria explained in Materials and Methods section. In addition, we established 2 identification levels: (1) Molecular formula matched with isotopic profile and compound data-bases and (2) Experimental fragmentation spectrum matched in spectral data-bases. As a result, it was possible to assign the following tentative identifications for differential peaks between exosome samples derived from adherent cells and those derived from CSC melanospheres (**Table 3**): m/z 496.3381 corresponds to the glycerophosphocoline PC 16:0/0:0 (**Figure 34A**); m/z 515.3962 corresponds to the triacylglicerol TG(18:2/22:3/22:4) (**Figure 34B**); m/z 729.5293 corresponds to the diacylglycerophosphoglycerol PG(20:0/12:0) (**Figure 34C**); m/z 745.5143 corresponds to the glycerophosphoserine PS(P-16:0/15:1) (**Figure 34D**).

We were not able to identify the rest of m/z signals or assign them a biologically coherent molecular formula, according to the same mentioned criteria and the identification rules described by Kind and Fiehn [249].

The four tentatively identified and other nine unidentified ions have significant differences between the groups, being more abundant in exosome samples derived from adherent cells compared to those from secondary spheres. However, other 6 unidentified signals were more abundant in CSC Mel1-derived exosomes compared to those from adherent cells (**Figure 33**).

Table 3. Differential metabolites tentatively identified in Mel1 patient-derived cell line exosomes based on MS/MS fragmentation spectra and data-base search.

m/z[1]	RT[2]	Tentative ID[3]	Molecular Formula[4]	Mass error[5]	P-value[6]	FC[7]	IL[8]
496.3381	11.61	LPC (16:0)	$C_{24}H_{50}NO_7P$	3	$6.48x10^{-5}$	4.1367 (↑)	2
515.3962	15.72	TG(18:2/22:3/22:4)	$C_{65}H_{108}O_6$	0	0.04258	2.2071 (↑)	2
729.5293	15.71	PG(20:0/12:0)	$C_{38}H_{75}O_{10}P$	4	0.04517	2.2063 (↑)	2
745.5143	15.70	PS(P-16:0/15:1)	$C_{37}H_{70}NO_9P$	2	0.04205	2.2513 (↑)	2

[1]Mass-to-charge ratio; [2]Retention time (min); [3]Common name of the tentatively identified metabolite according to MS/MS fragmentation spectra and data-base search; [4]Molecular formula of the tentatively identified metabolite; [5]Mass error (ppm); [6]p-value corresponding to univariate statistical analyses (T-test). Only peaks with a p-value < 0.05 were selected; [7]Fold change expressed as the ratio of the two averages (AD/S2). Only peaks with a fold-change > 1.5 or < 0.66 were selected. The arrows indicate if the metabolite is increased (↑) or decreased (↓) in AD relative to S2; [8]Identification level: (1) Molecular formula matched in compound data-bases and (2) Experimental fragmentation spectrum matched in spectral data-bases.

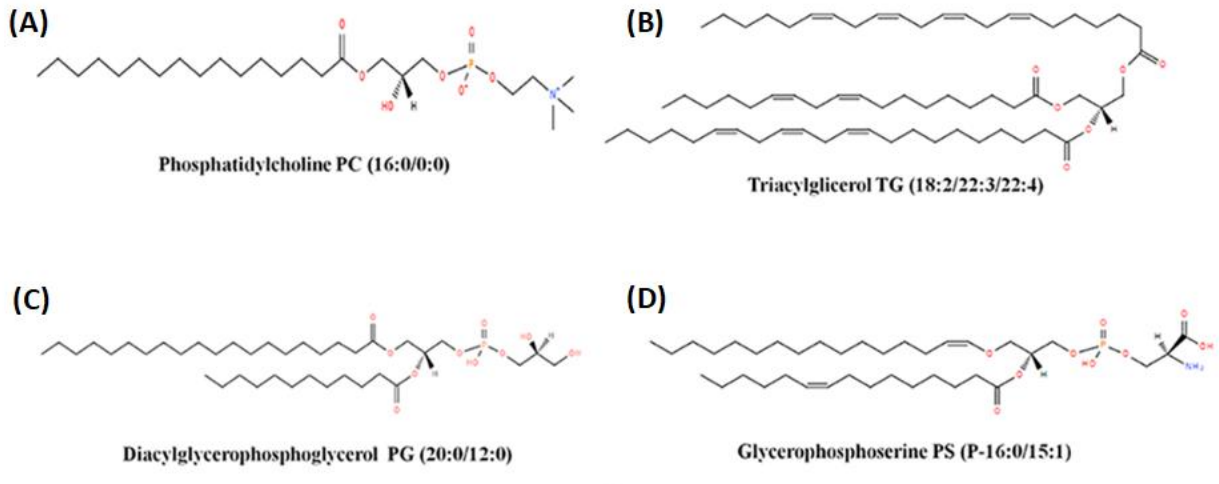

Figure 34. **(A)** Chemical structure of candidate biomarker 1-hexadecanoyl-sn-glycero-3-phosphocholine PC (16:0/0:0). **(B)** Chemical structure of candidate biomarker triacylglycerol TG (18:2/22:3/22:4). **(C)** Chemical structure of candidate biomarker diacylglycerophosphoglycerol PG (20:0/12:0). **(D)** Chemical structure of candidate biomarker glycerophosphoserine PS (P-16:0/15:1).

5. LC–HRMS metabolomic analysis of exosomes derived from serum of patients with malignant melanoma

Analogously to Mel1-derived exosomes, we carried out a metabolomic analysis in the same experimental conditions with the aim of exploring metabolomic differences between serum-derived exosomes from MMPs at different stages of the disease and HCs. As an outcome, 93 differential (T-test p-value < 0.05 and FC < 1.5) m/z signals were found. These signals were analysed by PCA and PLS-DA, obtaining a clear separation of exosome samples derived from MMP and HC serum within the PCA score plot along PC1 and PC2 (**Figure 35**). Again, it could be observed a clear separation of BS samples from biological samples (**Figure 35A**), and the close clustering of QC samples confirmed the quality of the analytical system performance (**Figure 35A-B**). In PLS-DA models, a clear separation of exosome samples derived from MMPs and HCs serum was observed, and they were discriminated with an R^2 of 0.99 and Q^2 of 0.98 (**Figure 36**).

Due to the greater complexity of the patient-derived serum composition, we found a larger number of differentially expressed metabolites compared to Mel1 primary cell line. Since metabolite identification is the most laborious and time-consuming task in the metabolomic workflow, we applied the variable importance in projection (VIP) technique as an additional independent variable selection method in order to achieve a more affordable set of metabolites in terms of identification [250]. Following the greater-than-one rule, which is usually considered for detecting variables with the greatest importance in the projection [250], 24 differentially expressed metabolites were selected (**Table 4**).

Table 4. Potential biomarkers differentially expressed in MMP compared to HC serum-derived exosomes based on MS/MS fragmentation spectra and data-base search.

m/z [1]	RT [2]	Tentative ID [3]	Molecular Formula [4]	Mass error [5]	P-value [6]	FC [7]	AUC [8]	VIP [9]	IL [10]
380.2551	9.64	Sphingosine-1-phosphate	$C_{18}H_{38}NO_5P$	2	$1.31x10^{-13}$	3.57 (↑)	1	1.03	2
400.3419	10.19	Palmitoylcarnitine	$C_{23}H_{45}NO_4$	1	$9.71x10^{-16}$	6.07 (↑)	1	1.26	2
426.3570	10.41	Elaidic carnitine	$C_{25}H_{47}NO_4$	2	$2.54x10^{-14}$	3.44 (↑)	1	1.13	2
438.2987	11.69	PE(P-16:0/0:0	$C_{21}H_{44}NO_6P$	2	$4.74x10^{-19}$	5.18 (↑)	1	1.33	2
454.2902	11.20	PE(16:0/0:0)	$C_{21}H_{44}NO_7P$	6	$1.99x10^{-09}$	3.72 (↑)	1	1.23	2
466.3302	13.55	Glycerophospholipid-related compound	$C_{23}H_{48}NO_6P$	2	$1.16x10^{-15}$	3.31 (↑)	1	1.18	1
477.2309	3.99	---	---	---	$2.33x10^{-24}$	9.84 (↑)	1	1.36	-
480.3080	11.64	PE(18:1/0:0)	$C_{23}H_{46}NO_7P$	1	$2.11x10^{-09}$	3.33 (↑)	1	1.23	2
482.3251	12.95	PE(18:0/0:0)	$C_{23}H_{48}NO_7P$	2	$5.19x10^{-10}$	3.71 (↑)	1	1.45	2
482.3585	11.71	PC(O-16:0/0:0)	$C_{24}H_{52}NO_6P$	4	$1.11x10^{-12}$	2.54 (↑)	1	1.1	2
496.3391	11.28	LPC (16:0)	$C_{24}H_{50}NO_7P$	1	$1.18x10^{-06}$	3.89 (↑)	0.99	2.28	2
502.2917	10.68	PE(20:4/0:0)	$C_{25}H_{44}NO_7P$	2	$1.24x10^{-10}$	3.25 (↑)	0.99	1.15	2
516.3009	4.17	Taurallocholic acid	$C_{26}H_{45}NO_7S$	4	$7.39x10^{-28}$	22.23 (↑)	1	1.72	1
521.2544	4.17	---	---	---	$3.90x10^{-27}$	22.86 (↑)	1	1.6	-
522.3551	11.47	PC(18:1/0:0)	$C_{26}H_{52}NO_7P$	1	$3.83x10^{-06}$	2.40 (↑)	0.96	1	2
524.3698	12.76	PC(18:0/0:0)	$C_{26}H_{54}NO_7P$	2	$3.95x10^{-08}$	4.00 (↑)	0.98	1.57	2
526.2902	10.47	PE(22:6/0:0)	$C_{27}H_{44}NO_7P$	5	$2.60x10^{-13}$	3.82 (↑)	1	1.06	2
564.3588	4.49	Ganglioside GM3 (d18:0/14:0)	$C_{55}H_{102}N_2O_{21}$	5	$5.80x10^{-12}$	2.19 (↑)	0.99	1.07	1
565.2809	4.32	---	---	---	$8.84x10^{-28}$	13.19 (↑)	1	1.58	-
604.3544	4.46	Presqualene diphosphate	$C_{30}H_{52}O_7P_2$	0.6	$4.46x10^{-29}$	24.62 (↑)	1	1.99	1
608.3849	4.61	---	---	---	$1.37x10^{-11}$	2.33 (↑)	0.99	1.08	-
632.3827	4.46	---	---	---	$1.20x10^{-28}$	44.92 (↑)	1	1.58	-
733.3346	4.15	---	---	---	$1.08x10^{-07}$	0.13 (↓)	0.95	1.02	-
736.4321	4.76	Glycerophospholipid-related compound	$C_{38}H_{68}NO_8P$	1	$4.47x10^{-29}$	52.18 (↑)	1	1.97	1

[1]Mass-to-charge ratio; [2]Retention time (min); [3]Common name of the tentatively identified metabolite according to MS/MS fragmentation spectra and data-base search; [4]Molecular formula of the tentatively identified metabolite; [5]Mass error (ppm); [6]p-value corresponding to univariate statistical analyses (T-test). Only peaks with a p-value < 0.05 were selected; [7]Fold change expressed as the ratio of the two averages (HC/MMP). Only peaks with a fold-change > 1.5 or < 0.66 were selected. The arrows indicate if the metabolite is increased (↑) or decreased (↓) in HC relative to MMP; [8]Area Under the Curve corresponding to ROC curve analyses; [9]VIP value corresponding to Variable Importance in the Projection selection technique; [10]Identification level: (1) Molecular formula matched in compound data-bases and (2) Experimental fragmentation spectrum matched in spectral data-bases.

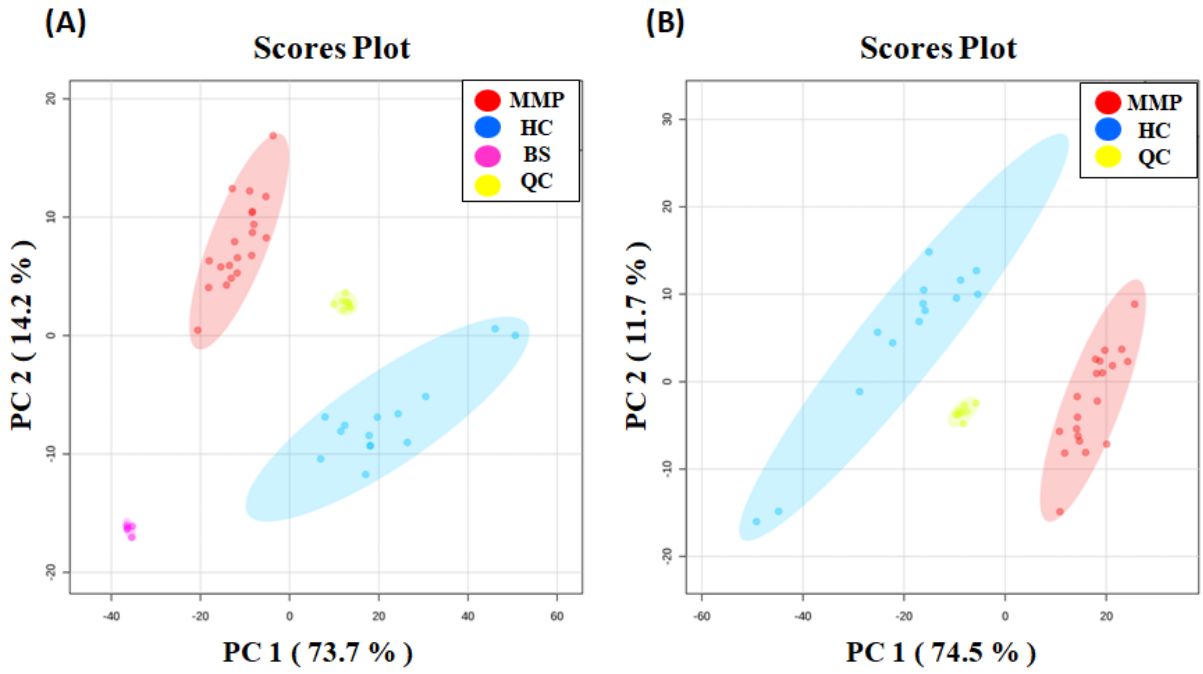

Figure 35. **(A)** PCA scores plot based on LC-HRMS data of all exosome samples derived from MMPs (red), HCs (blue), QC samples (yellow) and BS samples (pink). (**B**) Analytical validation based on the close clustering of QC samples (yellow) observed in the PCA scores plot.

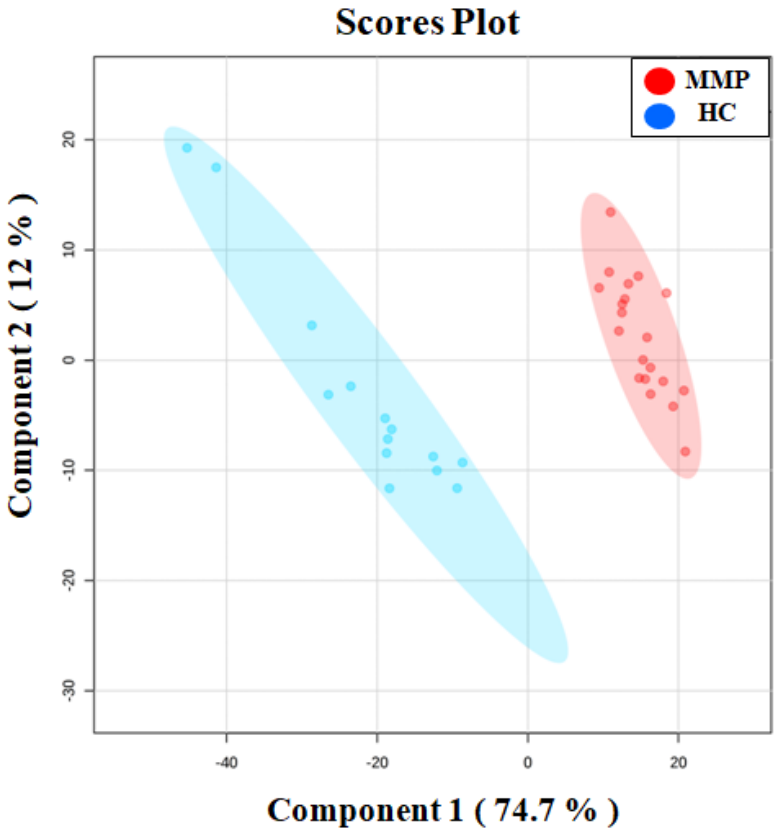

Figure 36. PLS-DA scores plot based on LC-HRMS data of exosome samples derived from MMPs (red), and HCs (blue). The two groups were discriminated with a R^2 of 0.99 and a Q^2 of 0.98, exceeding the threshold values accepted in metabolomic experiments ($R^2 > 0.7$ and $Q^2 > 0.4$).

The corresponding heatmap representing the differential abundance of these selected metabolites between exosome samples derived from MMPs and HCs is shown in **Figure 37**. As can be observed, 23 metabolites were more abundant in exosome samples derived from HCs, compared to those from MMPs, and only 1 metabolite (not identified) was higher in MMPs in comparison to HCs (**Figure 37, Table 4**).

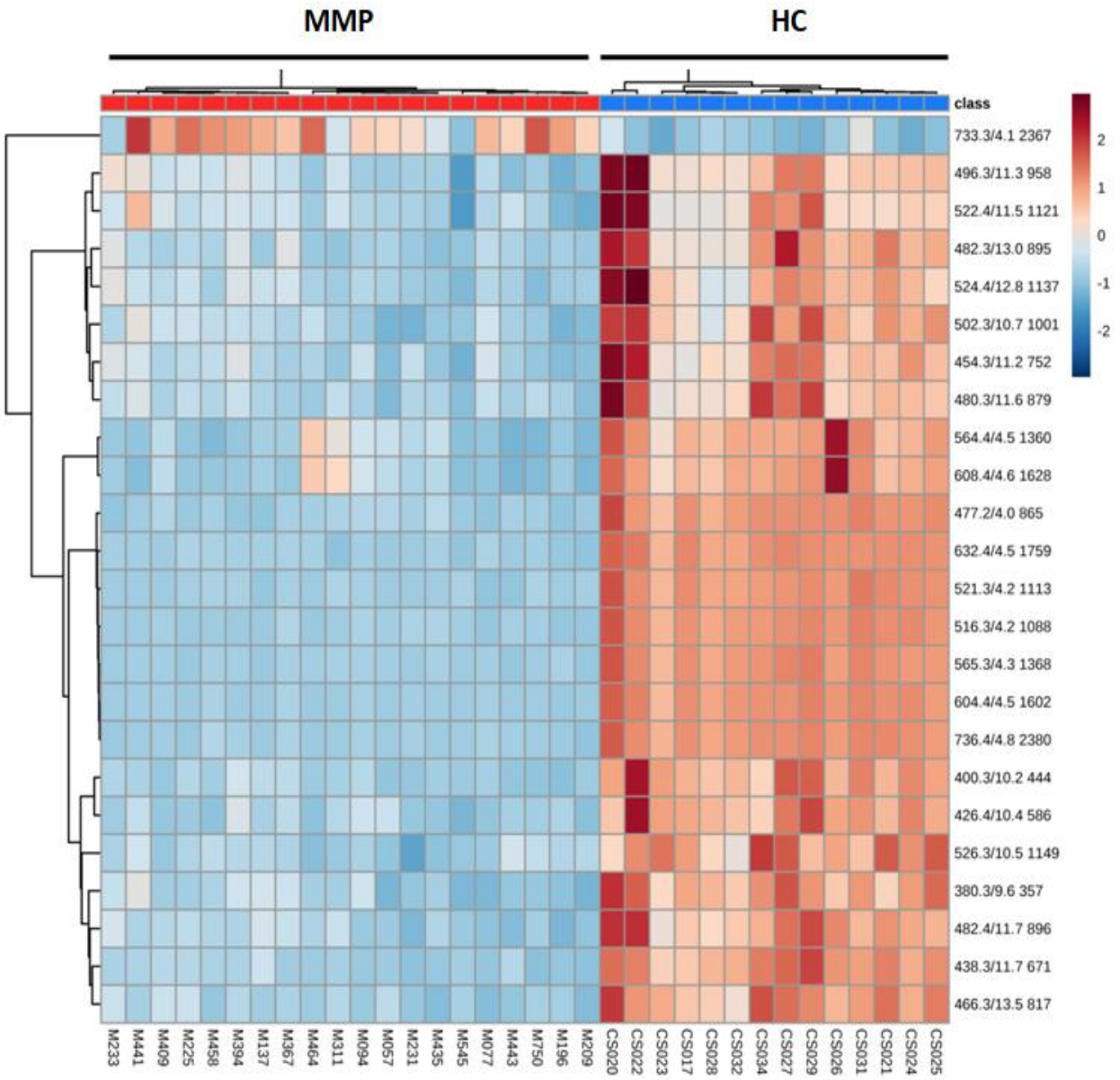

Figure 37. Heatmap showing the significantly different metabolites when comparing exosomes derived from adherent cells (red) and secondary melanospheres (blue). Each row on the heatmap represents a unique metabolite with a characteristic mass to charge ratio and retention time, while each column represents one exosome sample. The colour code represents the normalized intensity with which each metabolite is detected. Blue represents a decreasing trend, while red represents a rising trend.

Some of these selected differential peaks between the exosome samples derived from MMPs and those derived from HCs were tentatively identified (**Table 4**). Following the same

criteria previously described, we established 2 identification levels. In figure 37 it is represented the chemical structure and the corresponding interpretation of fragmentation spectrum of m/z 496.3381 identified as PC 16:0/0:0, as an example of one of those tentatively identified metabolites (**Figure 38**).

Additionally, the area under the curve (AUC) values were calculated from receiver operating characteristic (ROC) curve analysis in order to assess the potential clinical utility of the previously selected metabolites, displaying all values close or equal to 1, which suggest they could be considered as potential diagnostic biomarkers. Despite for some of the m/z signals a tentative identification was not possible following the same criteria [249], they could still be considered as potential biomarkers, since all of them showed high AUC values.

Interestingly, the metabolite corresponding to m/z 496.3381, identified as glycerophospholipid 1-hexadecanoyl-sn-glycero-3-phosphocholine (PC 16:0/0:0), was found to be not only overexpressed in exosomes derived from both HC serum and adherent Mel1 cells, compared to MMP serum and CSC Mel1 cells, respectively. Taken into account that this metabolite was not only tentatively identified, but also showed an excellent AUC value and discriminatory capacity between the two groups of samples (**Figure 39**), it could be considered a promising CSC-derived exosomal biomarker for MM.

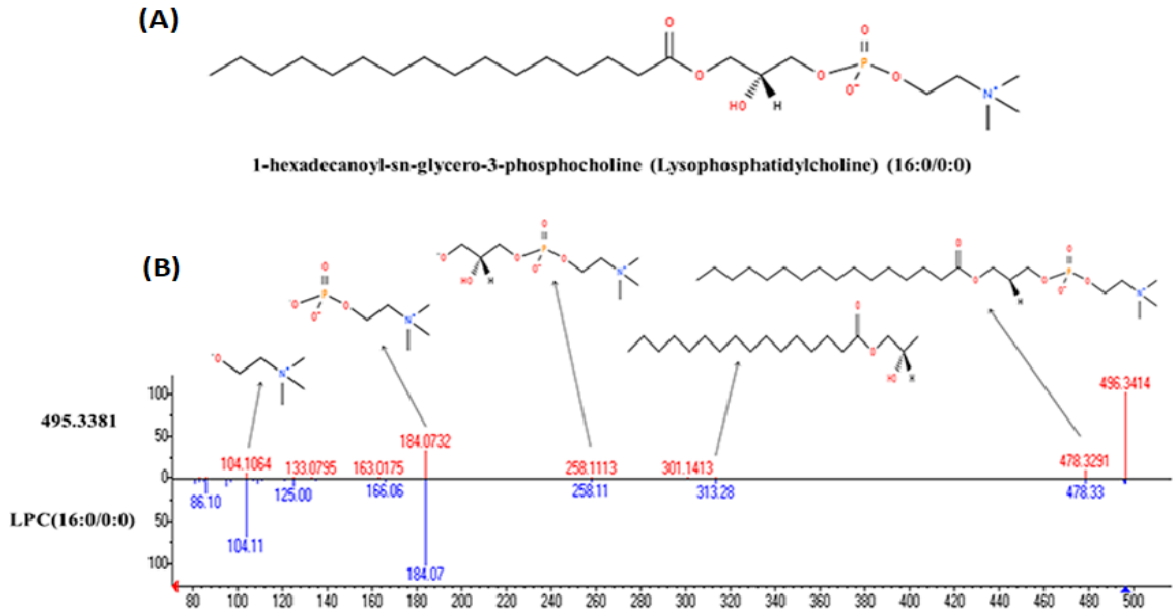

Figure 38. **(A)** Chemical structure of candidate biomarker 1-hexadecanoyl-sn-glycero-3-phosphocholine PC (16:0/0:0); **(B)** Representative fragmentation spectrum of candidate biomarker PC (16:0/0:0). Within the product ion spectra arising from the $[M+H]^+$ ions of this molecule, different specific fragments were found, such as the *m/z 184, 104, 258, 321 or 478* ions, corresponding to characteristic molecule fragments.

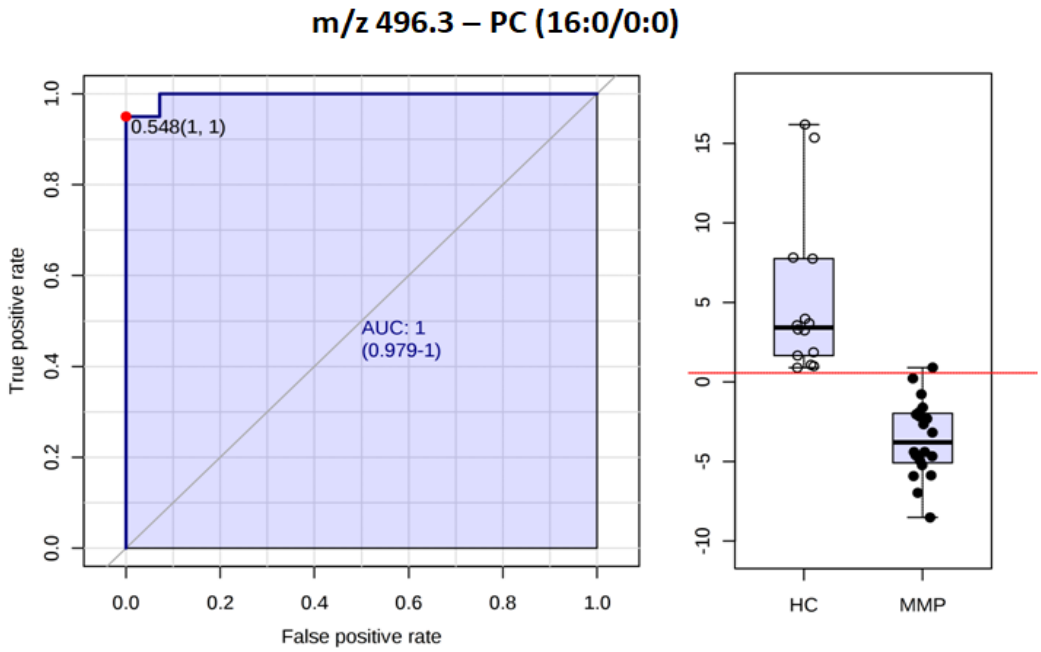

Figure 39. Receiver-operating characteristic (ROC) curve with the corresponding area under the curve (AUC) statistics and box-and-whiskers plot representing the relative abundance within MMP and HC serum-derived exosome samples for the metabolite corresponding to m/z 496.3381, identified as (PC 16:0/0:0).

DISCUSSION

DISCUSSION

As previously described throughout this whole dissertation, in the era of precision medicine and multiple effective treatments for cancer that we are living in, the necessity of developing sophisticated clinically useful biomarkers becomes more evident than ever. The design of optimal personalized therapy strategy absolutely depends on the earliest diagnostic, in order to achieve the subsequent best treatment response and, ultimately, improved patients' survival. In this regard, MM is one of the clearest examples.

In this context, circulating biomarkers represent an excellent source of biomarkers, easy to detect and/or quantify in body fluids such as blood, urine, or saliva, through minimally invasive techniques [175]. During the last decade, some of these circulating markers that has attracted the most attention of researchers in this field have been the EVs, and particularly the exosomes [251]. To date, it is known that the composition of sEVs is not a random sample of cell content, but rather is assembled by a highly selective process whose nature remains unclear [252]. Moreover, while in some instances the antigens found on the surface of microvesicles (e.g. lineage markers) could resemble those of their producing cells [253], several studies suggest that, especially exosomes, contain a more unique protein and RNA cargo. Thus, exosomes tend to be enriched in glycoproteins compared to the secreting cells [254]. In addition, sEVs imperatively comprise a lipid moiety, and their phosphatidylserine, cholesterol, sphingomyelin, and glycosphingolipid content is richer than their cellular sources [255,256]. Thus, the studies that originally reported their presence in blood determined that sEVs membrane could support the coagulation cascade by exposition on their surface of phosphatidylserine [257]. Furthermore, sEVs also interact with secreted phospholipases to generate eicosanoids, which regulate the transfer of cargo into a cellular recipient. Eicosanoids, potent bioactive lipid mediators, are

useful as biomarkers and contribute to a variety of biological functions, including modulation of distal immune responses, angiogenesis and tumor progression in cancer context [258]. The role of the various lipid pathways is crucial in the biogenesis and functions of microvesicles and exosomes. For instance, tumor-derived exosomes enriched in prostaglandins and free fatty acids (including arachidonic acid) participate in the formation of a favorable microenvironment for tumor growth [259]. In this context, sEVs contribute with their lipid molecules or their lipid-related enzymes to several pathophysiologies, playing an important role in cancer [260].

Exosomes are actively secreted by cancer cells at a higher rate than by normal cells. In particular, melanoma cells seem to produce a large quantity of these microvesicles [261], in contrast to normal melanocytes [262]. Moreover, a melanoma-specific exosomal signature, which correlates with tumor burden and metastasis, was identified in blood from patients with MM at stage IV [209]. Malignant melanoma is characterized by an extraordinary heterogeneity, propensity for dissemination to distant organs and resistance to chemotherapy, which results from the unique characteristics of melanoma CSCs [263].

In this study, we have set up a broadly applicable approach for metabolomic profiling of exosomes isolated from cell culture media of Mel1 melanoma CSCs and from serum of patients with MM at different stages in order to identify potential clinically useful biomarkers with prognostic/diagnostic value. First, we confirmed that the primary Mel1 cell line obtained from a metastatic MM growing in serum-free and anchorage-independent conditions displayed both CSC-like functional and phenotypic properties. Mel1 cells growing as spheres possess self-renewal ability and clonogenicity. The spheres were enriched in cells with high ALDH activity, overexpressing CD20 and CD44 surface markers and presenting a great SP rate. All these properties have been described as characteristics of CSCs [236]. The isolation of exosomes from

cell culture supernatant was performed by ultracentrifugation and confirmed by TEM, AFM and Western blot assays. Next, we characterized their size by NanoSight showing particles with diameters of around 100 nm, confirming the specific enrichment in exosomes [209,215]. Mel1 exosomes were positive for CD9, CD63 and Alix exosomal markers, and also for CD271 melanoma CSC marker. Previous studies on patients with melanoma have shown that CD271+ is a good candidate marker to unequivocally identify CSCs subpopulation [264]. However, it is important to highlight that, based on the exosome isolation and characterization protocols carried out in this study, the term "exosomes" applied in this work actually refers to sEVs, a general term proposed in the "MISEV" guidelines [198], comprising exosomes but also other vesicles which share size, density and markers.

The metabolomic profile of exosomes analysed through MS revealed significant differences in the metabolomic fingerprint of exosomes derived from CSCs as compared to tumor adherent (more differentiated) cells in Mel1 MM primary cell line and also in the exosomes derived from MMPs at different stages compared to HCs. ROC curves are frequently used in biomedical informatics research to evaluate classification and prediction models for decision support, diagnosis and prognosis. Thus, it is possible within a metabolomics study to calculate ROC curves for each potential biomarker in order to assess its potential clinical utility in terms of AUC [242]. In this regard, we calculated the AUC for each selected candidate biomarkers in patients' serum-derived exosomes, and we obtained values close or equal to 1. Considering that AUC values over 0.8 indicate a good predictor model, our results (**Tables 1** and **3**) suggest that these metabolites could be used as a panel of clinically useful biomarkers.

Metabolic reprogramming is firmly established as a hallmark of cancer [9] and lipids have been described to exert multiple biochemical functions during cancer development. Several

lipids, including sterols, di-/tri-acylglycerols and phospholipids are integral part of biological membranes and are also used for energy storage, production, and cellular signalling. Fatty acids (FA) are indispensable for lipid biosynthesis. Disruption of lipid metabolism, especially FA synthesis (FAS) and fatty acid oxidation (FAO) has become increasingly recognized as an important metabolic rewiring phenomenon in tumor cells [265]. Glycolipids and phospholipids (phosphatidylcholine and phosphatidylethanolamine) along with cholesterol are major components of biological membranes and markedly influence membrane fluidity [265]. In addition to their structural roles, lipids also orchestrate signal transduction cascades and can also be broken down into bioactive lipid mediators, which regulate several carcinogenic processes, such as cell growth, cell migration and metastasis [266].

In our study, we found a decreased expression between exosome samples derived from CSCs melanospheres and those derived from adherent-differentiated tumor cells of four tentatively identified metabolites from different lipid classes, such as glycerophosphoglycerols (PG(20:0/12:0)), glycerophosphoserines (PS(P-16:0/15:1)), triacylglycerols (TG(18:2/22:3/22:4)) and glycerophosphocholines (PC 16:0/0:0). Interestingly, we found that PC 16:0/0:0 expression was reduced in both Mel1 CSCs and MMPs in comparison to Mel1 differentiated tumor cells and HCs, respectively. In line with these results, previous studies reported the reduced expression of PC 16:0/0:0 associated with malignant diseases, such as colorectal cancer [267], digestive tract tumors or renal cell carcinoma [268]. Moreover, higher levels of other glycerophospholipids such as LysoPC 18:0/0:0 have been consistently related to lower risks of breast, prostate and colorectal cancer [269]. Other studies have shown that the serological lipidomic profile of prostate cancer patients revealed several putative lipids that might serve as diagnostic biomarkers of this neoplasm [270].

The metastatic potential of cancer cells correlates with the expression of genes involved in fatty acid synthesis, oxidation and intracellular lipid storage. It has been shown that enzymes involved in lipid metabolism play a role in metastasis. For example, stearoyl-CoA desaturase (SCD) and long chain fatty acyl synthetase (ACSL) 1 and 4 cooperate to induce epithelial to mesenchymal transition resulting in an increased invasion potential of colon cancer cells [271]. Furthermore, it has been suggested that the rapid extracellular hydrolysis of phospholipids like PC 16:0/0:0 by metastatic tumor cells and the subsequent cellular uptake of the resulting free fatty acids (FFA) seems to be a necessary prerequisite for metastatic potential of epithelial tumor cells, probably for generating pro-metastatic lipid second messengers [272].

In this work, we also detected significant differences in other metabolites in the serum-derived exosomes from HCs compared to MMPs. For example, we found lower levels of the lysophospholipid sphingosine 1-phosphate (S1P) in serum-derived exosomes from MMPs than in HCs. This is consistent with previous studies that had suggested this molecule as a potential serum biomarker for hepatocellular carcinoma (HCC) diagnosis, which was also found to be lower in HCC patients [273]. Other differential metabolites that were lower in MMP serum-derived exosomes were palmitoylcarnitine and elaidic carnitine. Recently, the role of the carnitine system has been described in the metabolic plasticity phenomenon, a mechanism through which cancer cells are able to become more aggressive and metastasize [274]. In agreement with our results, a similar previous study, aimed at characterizing the metabolomic serum profile of HCC patients in a Korean prospective cohort, also showed lower levels of palmitoylcarnitine in HCC patients, compared to HCs [275]. Another metabolomic study reported the potential use of this metabolite, among others, as a predictive serum biomarker in non-small cell lung cancer [276]. We also found lower levels of several phospholipid-related

compounds such as phosphatidylcholines (PCs) and phosphatidyletanolamines (PEs) in MMP exosomal extracts versus HC extracts (see Table 3). Changes in specific phospholipid (PL) levels in tissues, cells, and body fluids like urine, plasma or serum, have clearly been demonstrated to be associated with cancer [277]. Yang *et al.* suggested that specific differential PLs found in the plasma of breast cancer patients could be useful for diagnosis purposes [278] and Waki *et al.* also reported PL differences in breast CSCs and non stem cancer cells [279]. In colorectal cancer, decreased LPC levels in serum patients have potential for use as diagnosis biomarkers [280], since lower LPC levels could be associated with the loss of body weight and inflammation, but could also indicate a higher LPCs decomposition rate to support cancer metabolism. Another study showed that some PL species, including LPC(16:0), LPC(18:0), PC(16:0), and PC(18:0) were significantly less present in HCC and LC (liver cirrhosis) patients, compared to HCs [281]. Another tentatively identified metabolite, also found at lower levels in serum-derived exosomes from MMPs, is the glycosphingolipid Ganglioside GM3 (d18:1/16:00), a component of cell plasma membrane that modulates cell signal transduction events. It has been reported that GM3 downregulates the invasiveness capacity of human bladder cancer cells and also that exogenously added GM3 can prevent haptotactic cell migration in colorectal cancer cell lines [282]. For the rest of metabolites, it was not possible to give an accurate mass or MS/MS spectra-based putative identifications using several data-bases. This still represents a major challenge in the field of metabolomics. However, it could be clinically useful to explore exosome-associated metabolomic m/z signatures related to several stages of MM.

All these results found in both patients and CSCs suggest the importance of structural lipids detected in exosomes of patients with MM and their potential as useful diagnostic, prognostic, or predictive biomarkers for this disease.

CHAPTER 2

Untargeted LC-HRMS-based metabolomics to identify novel biomarkers for early diagnosis of malignant melanoma

BACKGROUND

BACKGROUND

Despite MM is the least common of all skin cancers, representing only about 1% of them, it accounts for the highest number of deaths by far [28]. According to the latest data [3], in 2020 there were reported 324,635 new cases (1.7% of total cancers) and almost 57,043 deaths (0.6% of total) caused by MM worldwide. Its incidence and mortality rates are steadily increasing every year and it is expected to continue to do so over the next decades. In general, the 5-year survival rate is elevated, as long as it is localized and early detected. However, this rate significantly drops when the disease is spread to regional lymph nodes or when it metastasizes to distant organs [28,30,57].

Currently, methods employed for MM diagnosis include visual assessment, biopsies, dermoscopies and histopathological examinations, in order to determine the malignancy of a suspicious cutaneous melanocytic lesion. However, diagnosis of skin lesions remains challenging, since relies on pathologist's interpretations, which are subjective, and neither accurate nor reproducible, especially in early stage invasive MM cases [58,59]. This underscores the necessity of new innovative diagnostic tools to support pathologists and compliment visual assessments, since diagnostic errors lead not only to under or overtreatment, but also to a higher economic cost of MM management.

Indeed, this justifies all the efforts made in recent years to further understand the mechanisms underlying this disease, as well as to discover biomarkers clinically useful for diagnosis, prognosis and prediction, for patient counsel and for appropriate management. In particular, an early diagnosis is crucial in this type of skin cancer, since an earlier stage at diagnosis improves survival [57,283].

Serum based biomarkers represent an ideal, non-invasive and easy to collect source of biomarkers. Unfortunately, only a few of them have been proven to be clinically useful. Indeed, the only circulating biomarker with significant prognostic value in the updated version of the 8th edition AJCC melanoma staging system is LDH [191]. Other circulating proteins have also been reported as potential diagnostic or prognostic biomarkers, but their low sensitivity or specificity limit its clinical application [173]. Therefore, MM diagnosis remains challenging, and further research is needed in order to discover reliable serologic biomarkers.

As previously discussed in the chapter 1 of this work, metabolomics and mass spectrometry represent an excellent and powerful tool for biomarker research. In this regard, several studies have proved in the last years their usefulness for biomarker discovery in various cancer types such as breast, gastric, lung, and colorectal cancer [284–288].

Considering the poor prognosis of advanced MM and the lack of reliable serologic biomarkers for the early detection of melanoma or prognostic markers for early-stage patients, and after having obtained the results previously described in chapter 1, the aim of this second study was to compare the metabolomic profile of serum samples derived from MMPs versus those derived from HCs. Therefore, this time we performed a similar metabolomic study but analyzing the whole serum, not only EVs, in a larger number of patients with MM, framed in the same context and main goal of this thesis and attempting to discover new potential biomarkers for diagnosis MM. In this regard, we report for the first time, some differentially expressed metabolites in serum from MMP and HC that could be considered as potential biomarkers for early diagnosis of this disease.

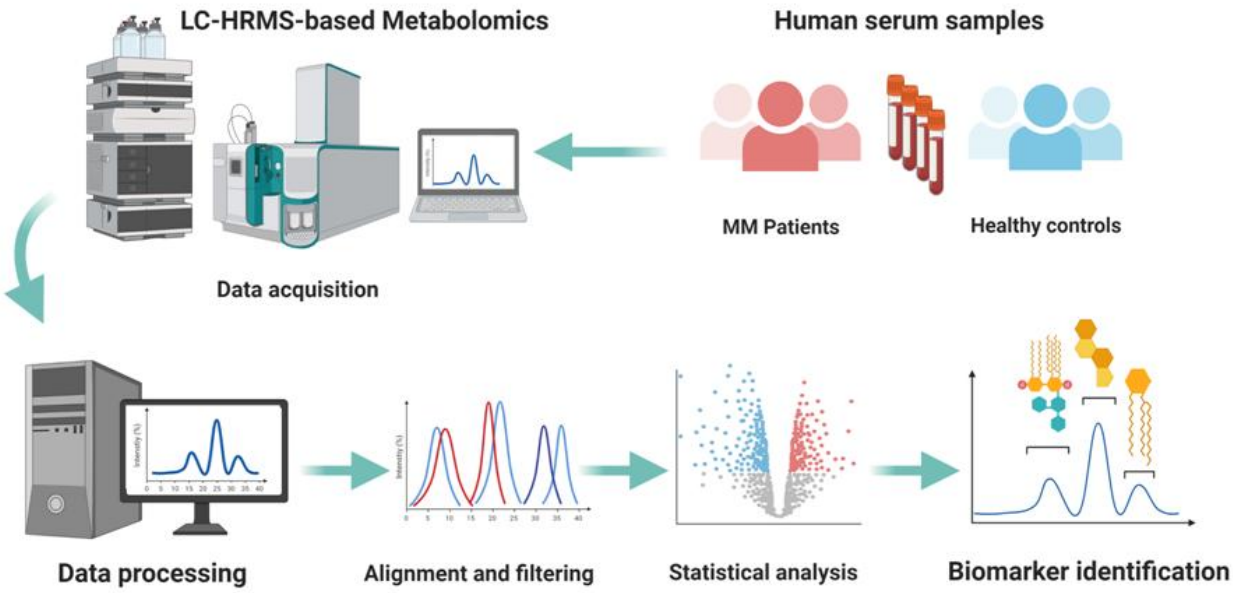

Figure 40. Graphical abstract representing the general workflow and the main assays performed in this study.

RESULTS

RESULTS

1. LC-HRMS metabolomic analysis of serum of patients with malignant melanoma

In this study, a total of 105 serum samples (79 MMPs and 26 HCs) were analysed following an untargeted metabolomic approach, using an LC-HRMS platform and an AcN-based metabolite extraction protocol. For nontargeted metabolomics, protein removal using an organic solvent-based metabolite extraction protocol is often performed. In particular, AcN-based extraction methods have been proven to be the one of the most effective in terms of obtaining information for lipid low-molecular-weight species [289].

Total ion chromatograms (TICs) of MMP and HC serum samples (**Figure 41**) revealed a good reproducibility in terms of retention time and signal intensity, a clear separation among [290]: medium-polar metabolites (e.g., phospholipids, lysophospholipids, and steroids), eluted between minutes 6 and 14; very polar metabolites (e.g., some amino acids and sugars), eluted in the first 5 minutes; and non-polar metabolites, eluted between minutes 14 and 17, and also significant differences between MMP and HC TICs.

After peak alignment and filtering procedures, a positive ionization data matrix of 1670 mass signals was obtained. In order to filter the results and minimize the signal redundancy, only peaks representing monoisotopic ions were selected (521 peaks) and subjected to the chemometric analysis. After that, raw data were normalized, transformed and scaled, and a first filtering by Student's *t*-test ($p < 0.05$) and fold-change (FC > 1.5) was performed in order to discard mass signals present in blank solvent samples and, therefore, not exclusively present in biological samples. After this filtering process, 133 candidates were considered and selected as differentially expressed in serum samples versus blank solvent samples. In addition, 4 features

were excluded for unacceptable variability (RSD > 30%); As a result, 129 variables were selected and evaluated in the PCA and PLS-DA.

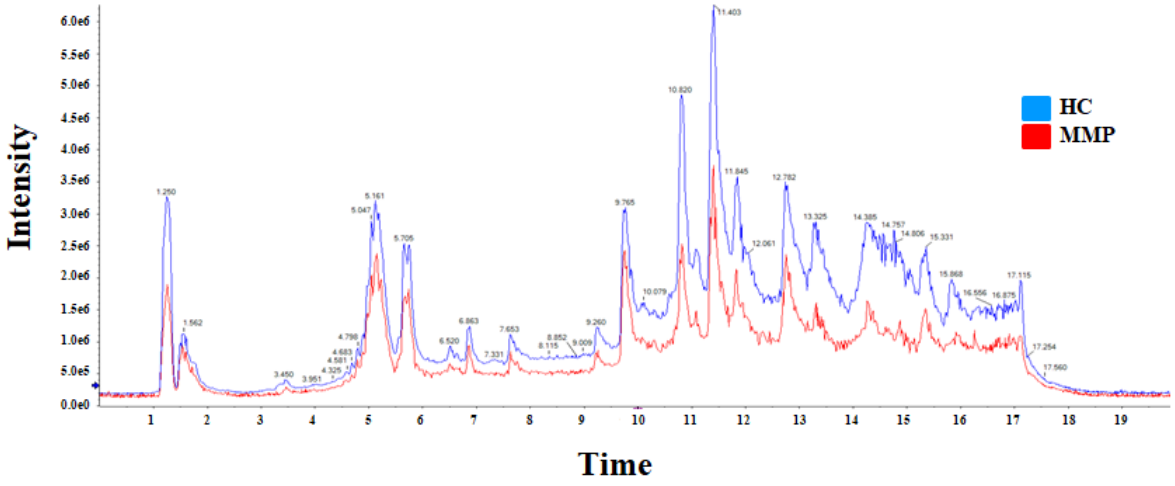

Figure 41. Representative LC-HRMS total ion chromatograms (TICs) of metabolites present in a HC (blue) and MMP (red) serum samples. The X axis represents the chromatographic retention time (RT) while the Y axis represents the intensity. Acetonitrile was used for metabolite extraction. A significant difference between HC and MMP TICs can be observed at 6–17 minutes, when most lipids elute.

The PCA score plot (**Figure 42A**) revealed a close clustering of QC samples and a clear separation of BS samples, confirming the quality of the analytical system performance and indicating that the separation observed between MMP and HC groups was mainly due to biological reasons. Additionally, the PLS-DA score plot (**Figure 42B**) suggested that it might be possible to discriminate between MMP and HC samples. The predictive ability of the PLS-DA model to discriminate between these groups was assessed, but the present model did not meet the threshold values accepted in metabolomic experiments of $R^2 \geq 0.7$ and $Q^2 \geq 0.4$, with no variation > 0.2–0.3, at least when all MMPs at different stages were considered in the analysis.

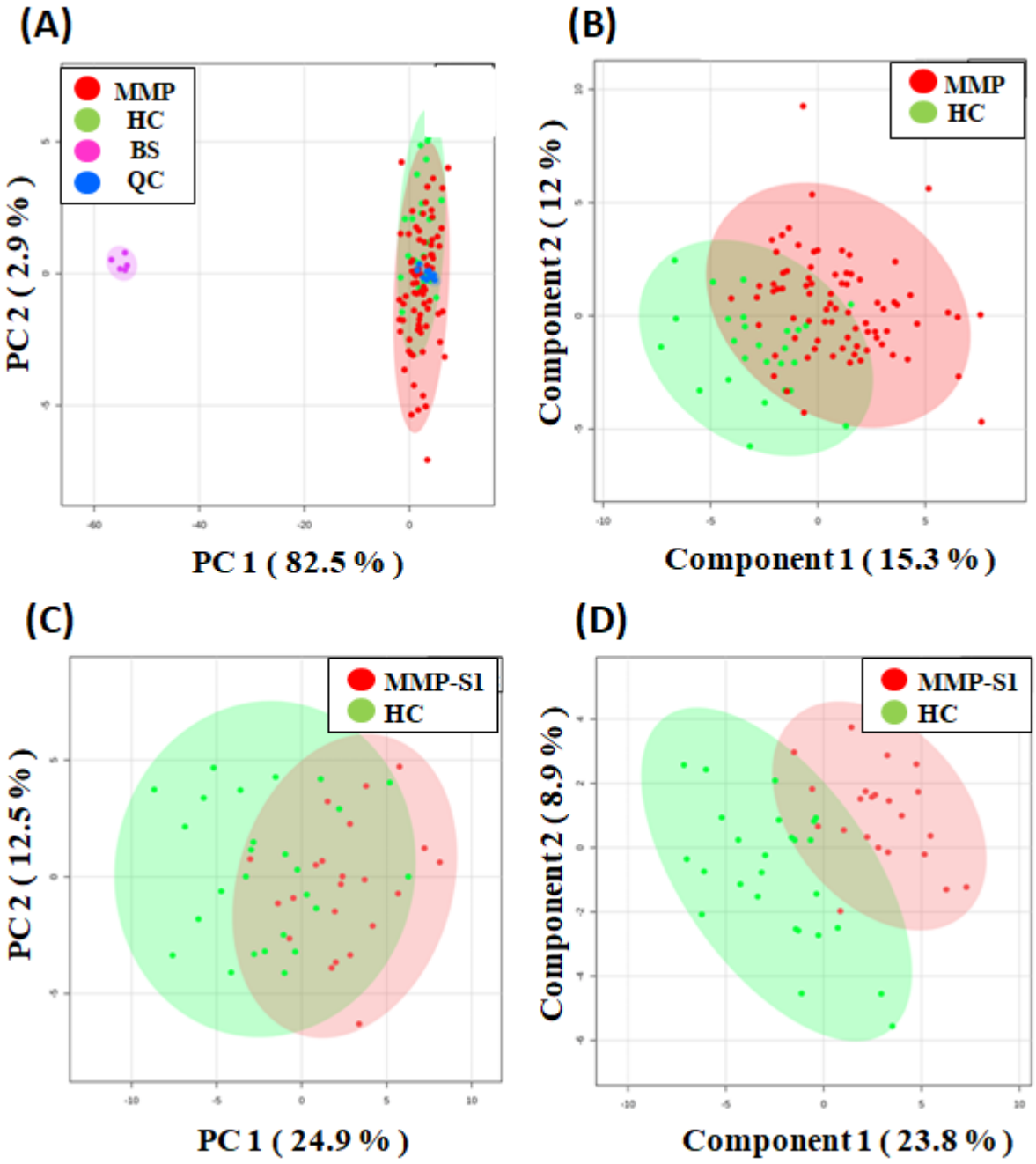

Figure 42. PCA (**A**) and PLS-DA (**B**) scores plot based on LC-HRMS data of serum samples from total MMPs (red), and HCs (green). QC samples (blue) and BS samples (pink); PCA (**C**) and PLS-DA (**D**) scores plot based on LC-HRMS data of serum samples from MMP–Stage 1 (red), and HCs (green).

However, based on the same approach and applying the same statistical analyses, we also carried out multiple comparisons between the HC group and the different MMP groups separately, according to their stage of the disease. No significant differences were found when comparing the different MMP groups (Stages I, II, III and IV). But interestingly, the PCA (**Figure 42C**) and PLS-DA (**Figure 42D**) score plots revealed a clear group separation when comparing the HC and the MMP-S1 (Stage I) groups, which is the most interesting and relevant comparison in terms of biomarker discovery for early diagnosis. Based on the PLS-DA model, the values obtained for R^2 and Q^2 were 0.82 and 0.56, respectively, which demonstrates the suitability of this model for discriminating between HC and MMP-SI groups.

In order to select those features susceptible of being considered as potential biomarkers, we applied a filtering process based on Student's t-test (FDR-corrected $p < 0.05$), the variable importance in projection (VIP) technique (VIP > 1) and a fold-change (FC > 1.5). As an outcome, 10 metabolites met these criteria and were consequently selected (**Table 5**).

Table 5. Potential biomarkers differentially expressed in MMP (Stage I) compared to HC serum samples based on MS/MS fragmentation spectra and data-base search.

m/z [1]	RT [2]	Tentative ID [3]	Molecular Formula [4]	Mass error [5]	P-value [6]	FC [7]	AUC [8]	VIP [9]	IL [10]
319.1932	15.75	---	---	---	$3.64x10^{-3}$	0.63 (↓)	0.77	1.59	-
478.2926	10.50	PE(18:2/0:0)	$C_{23}H_{44}NO_7P$	0	$6.42x10^{-7}$	1.78 (↑)	0.89	2.14	2
500.2737	10.72	PE(20:5/0:0)	$C_{25}H_{42}NO_7P$	7	$8.77x10^{-5}$	1.55 (↑)	0.79	1.68	2
520.3398	10.74	PC(18:2/0:0)	$C_{26}H_{50}NO_7P$	1	$1.73x10^{-7}$	1.80 (↑)	0.90	2.20	2
531.3236	10.83	---	---	---	$7.90x10^{-7}$	1.75 (↑)	0.88	2.17	-
539.3174	10.81	CDP-DG (18:0/22:3)	$C_{52}H_{91}N_3O_{15}P_2$	1	$5.85x10^{-8}$	1.95 (↑)	0.90	2.45	1
542.3222	10.83	PC(20:5/0:0)	$C_{28}H_{48}NO_7P$	3	$1.16x10^{-6}$	1.54 (↑)	0.87	1.89	2
604.2886	10.58	POB-PS	$C_{26}H_{48}NO_{11}P$	5	$5.09x10^{-8}$	1.62 (↑)	0.91	2.07	2
610.3136	10.62	---	---	---	$1.20x10^{-7}$	1.69 (↑)	0.9	2.12	-
640.3431	10.26	PKOHA-PG	$C_{29}H_{51}O_{12}P$	4	$1.17x10^{-3}$	2.03 (↑)	0.73	2.09	2

[1]Mass-to-charge ratio; [2]Retention time (min); [3]Common name of the tentatively identified metabolite according to MS/MS fragmentation spectra and data-base search; [4]Molecular formula of the tentatively identified metabolite; [5]Mass error (ppm); [6]p-value corresponding to univariate statistical analyses (T-test). Only peaks with a p-value < 0.05 were selected; [7]Fold change expressed as the ratio of the two averages (HC/MMP). Only peaks with a fold-change > 1.5 or < 0.66 were selected. The arrows indicate if the metabolite is increased (↑) or decreased (↓) in HC relative to MMP; [8]Area Under the Curve corresponding to ROC curve analyses; [9]VIP value corresponding to Variable Importance in the Projection selection technique; [10]Identification level: (1) Molecular formula matched in compound data-bases and (2) Experimental fragmentation spectrum matched in spectral data-bases and *in silico* fragmentation tools.

The heatmap representing the differential abundance of these potential biomarkers between MMP (Stage I) and HC is shown in **Figure 43A**. As can be observed, there is a clear pattern with 9 of these metabolites being more abundant in HC samples in comparison with those serum samples derived from MMPs, and only 1 metabolite was higher in MMPs compared to HC samples (**Figure 43A**). A heatmap representing the intensity average of the different compounds in each group of samples (MMP-S1 and HC) brings out this pattern more clearly (**Figure 43B**).

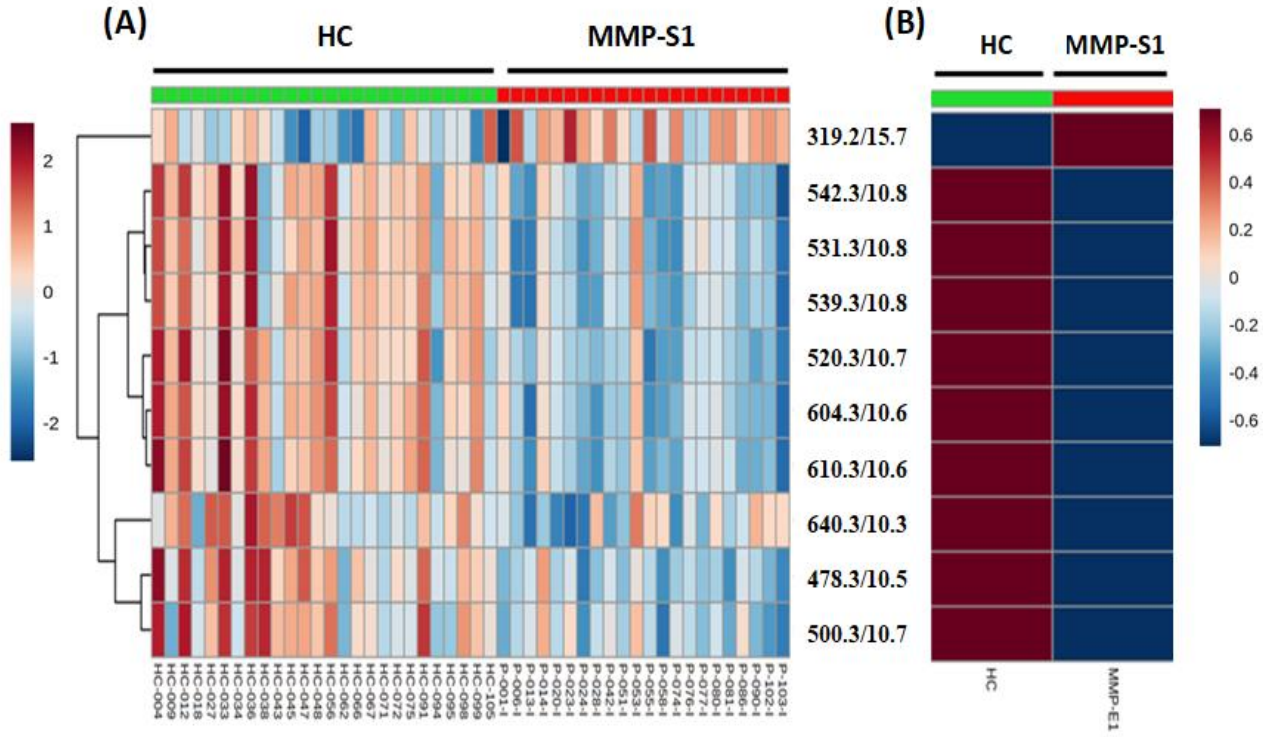

Figure 43. Heatmaps showing the differential metabolites between MMP-State I (red) and HC (green) serum samples. (**A**) Each row represents the intensity of each metabolite selected as potential biomarker with its characteristic mass to charge ratio and retention time, while each column represents each of the serum samples. (**B**) Each row represents the intensity average of each metabolite, while each column represents each group of samples. The colour code represents the normalized intensity with which each metabolite is detected. Blue represents a decreasing trend, while red represents a rising trend.

2. Evaluation of potential biomarkers

In order to evaluate the potential clinical utility of the previously selected compounds, the area under the curve (AUC) values were calculated from receiver operating characteristic (ROC) curve analysis. ROC curves represent a frequently used in metabolomics and biomarker research studies to assess classification and prediction models. Features with AUC values between 0.7-0.8 (fair), 0.8-0.9 (good) and 0.9-1 (excellent) are susceptible of being considered as potential diagnostic biomarkers [221]. In this study, AUC values calculated for all the 10 selected compounds ranged from 0.73 to 0.92 (**Table 5** and **Figure 44**).

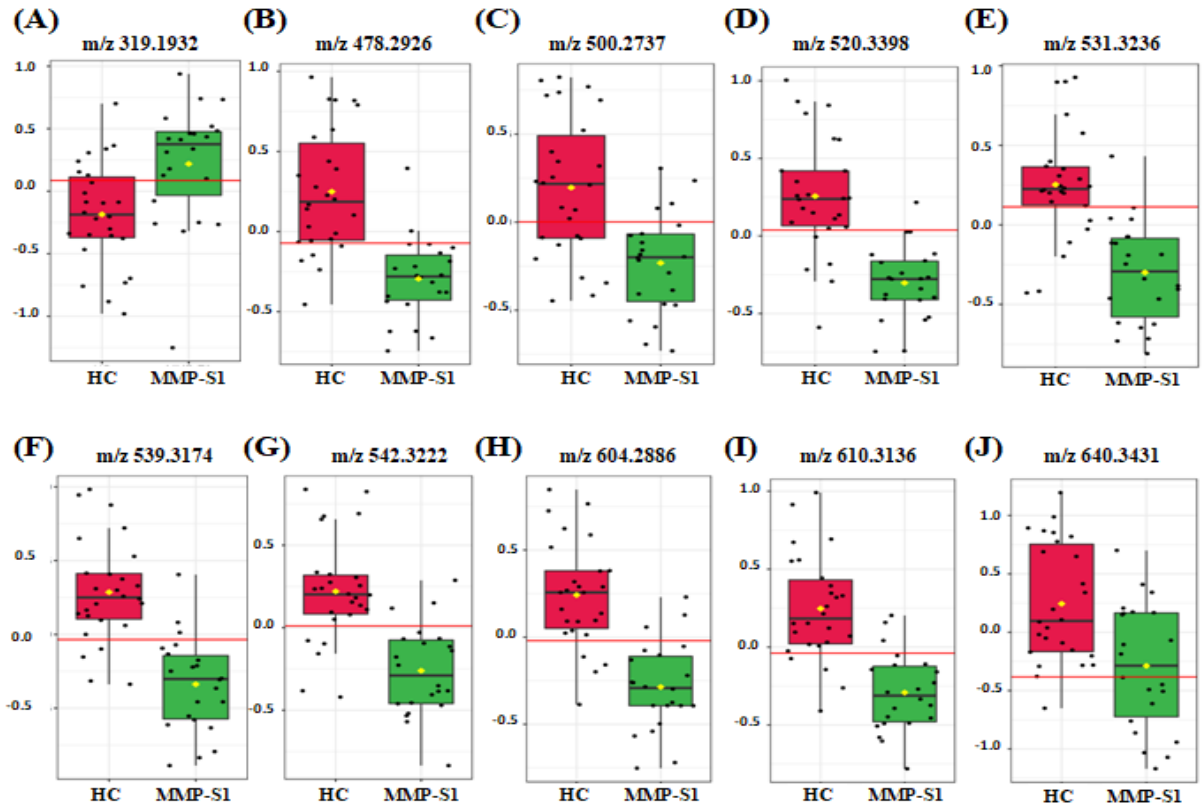

Figure 44. Box-and-whiskers plots representing relative abundance of those metabolites corresponding to m/z signals: (**A**) 319.1932, (**B**) 478.2926, (**C**) 500.2737, (**D**) 520.3398, (**E**) 531.3236, (**F**) 539.3174, (**G**) 542.3222, (**H**) 604.2886, (**I**) 610.3136 and (**J**) 640.3431 differentially expressed in serum samples from MMPs and HCs. The relative abundance of metabolites was significantly lower (nine of them) and higher (only one of them) in serum of MMPs, compared to HC serum samples.

Multivariate models combining several individual biomarkers are often generated in multifactorial diseases diagnosis studies, in order to improve discrimination and confidence levels. In these models, a multivariate mathematical equation is obtained, which provides a single score derived from several biomarkers that can be evaluated by ROC curve analysis as previously described [221]. In this regard, several biomarker models were created taking into account different subsets of the selected features (2 to 10). All of them displayed AUC values higher than 0.88 (**Figure 45A**) and showed a more than acceptable discriminatory capacity, since most of the samples were correctly classified in their correct class (MMP or HC).

In particular, the model created considering the 10 selected metabolites displayed an AUC value of 0.881 (95% CI: 0.753-1) and its corresponding ROC curve and prediction overview are shown in **Figure 45B-C**. Taking into account all these results, based on the ROC curves analyses, AUC values and biomarker model obtained, the 10 selected metabolites may be taken into consideration as potential serological biomarkers for early diagnosis of MM.

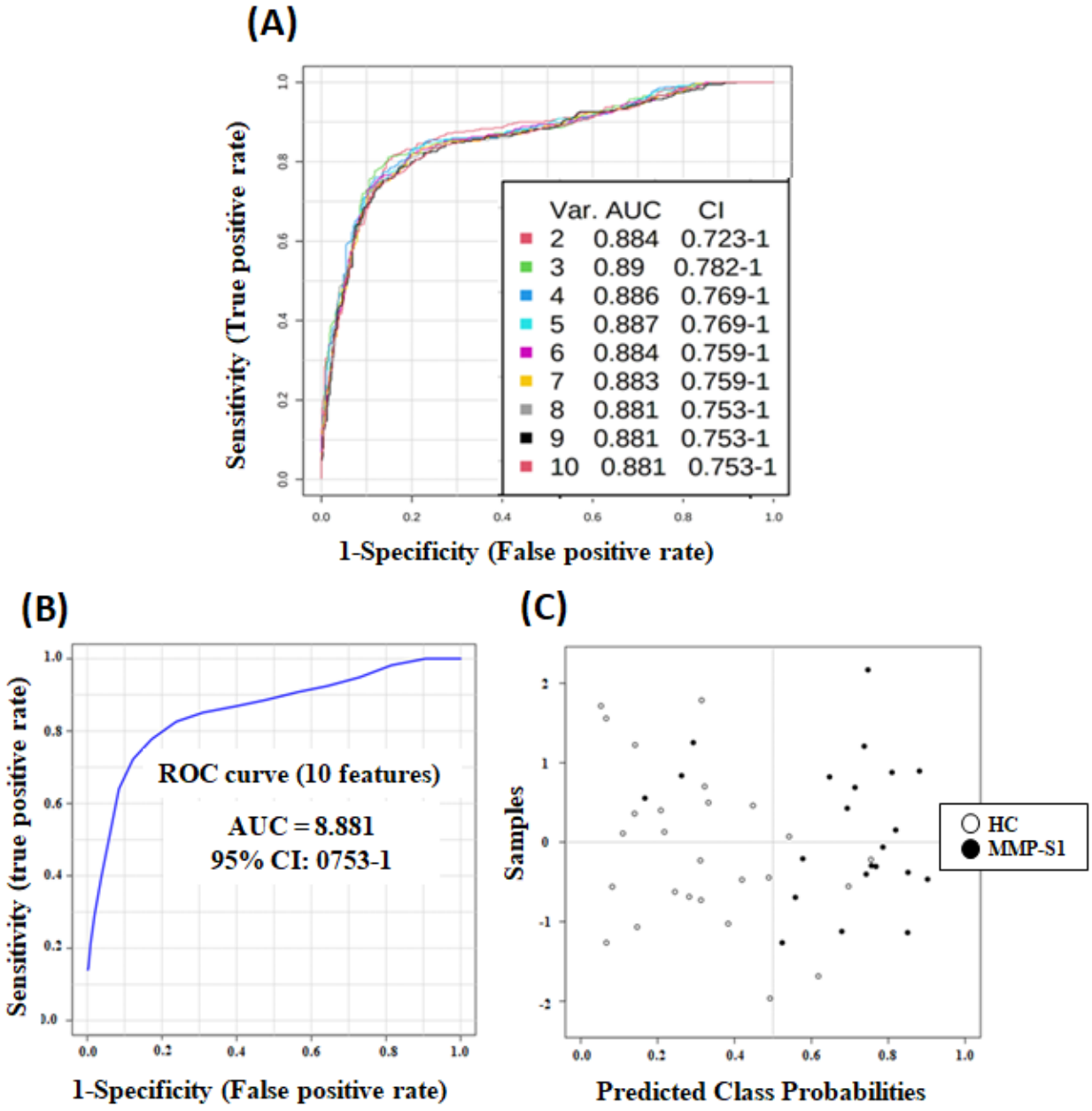

Figure 45. (**A**) Comparison of different models based on ROC curves. Nine biomarker models were created considering different combinations of the 10 selected metabolites. The legend shows the feature numbers, the AUCs (and CIs) of the 9 models. (**B**) ROC curve for combined (10 features) biomarker model; 100 cross-validations were performed and the results were averaged to generate the plot. (**C**) Average of predicted class probabilities of each sample across the 100-fold cross validations. The corresponding confusion matrix provided shows that 22/26 HC samples and 19/22 MMP samples were correctly classified.

3. Identification of potential biomarkers

Identification of selected metabolites was performed based on the assessment of the molecular formula from accurate mass, isotopic clustering and experimental fragmentation spectra interpretation and comparison in spectral databases (see Materials and Methods section for more details). Additionally, we established 2 identification levels: (1) Molecular formula matched with isotopic profile and compound data-bases and (2) experimental fragmentation spectrum matched in spectral data-bases and *in silico* fragmentation tools. As a result, tentative identifications for 7 of the selected potential biomarkers were achieved (**Table 5** and **Figure 46**): m/z 478.2926 corresponds to the glycerophosphoethanolamine PE(18:2(9Z,12Z)/0:0); m/z 500.2737 corresponds to the glycerophosphoethanolamine PE(20:5(5Z,8Z,11Z,14Z,17Z)/0:0); m/z 520.3398 corresponds to the glycerophosphocholine PC(18:2(9Z,12Z)/0:0); m/z 539.3174 corresponds to cytidine diphosphate diacylglycerol CDP-DG (18:0/22:3(10Z,13Z,16Z)); m/z 542.3222 corresponds to the glycerophosphocholine PC(20:5(5Z,8Z,11Z,14Z,17Z)/0:0); m/z 604.2886 corresponds to the oxidized glycerophosphoserine POB-PS; m/z 640.3431 corresponds to the oxidized glycerophosphoglycerol PKOHA-PG.

According to the same followed criteria and the identification rules described by Kind and Fiehn [249], we were not able to assign biologically coherent molecular formulas for 3 of the selected metabolites (**Table 5**).

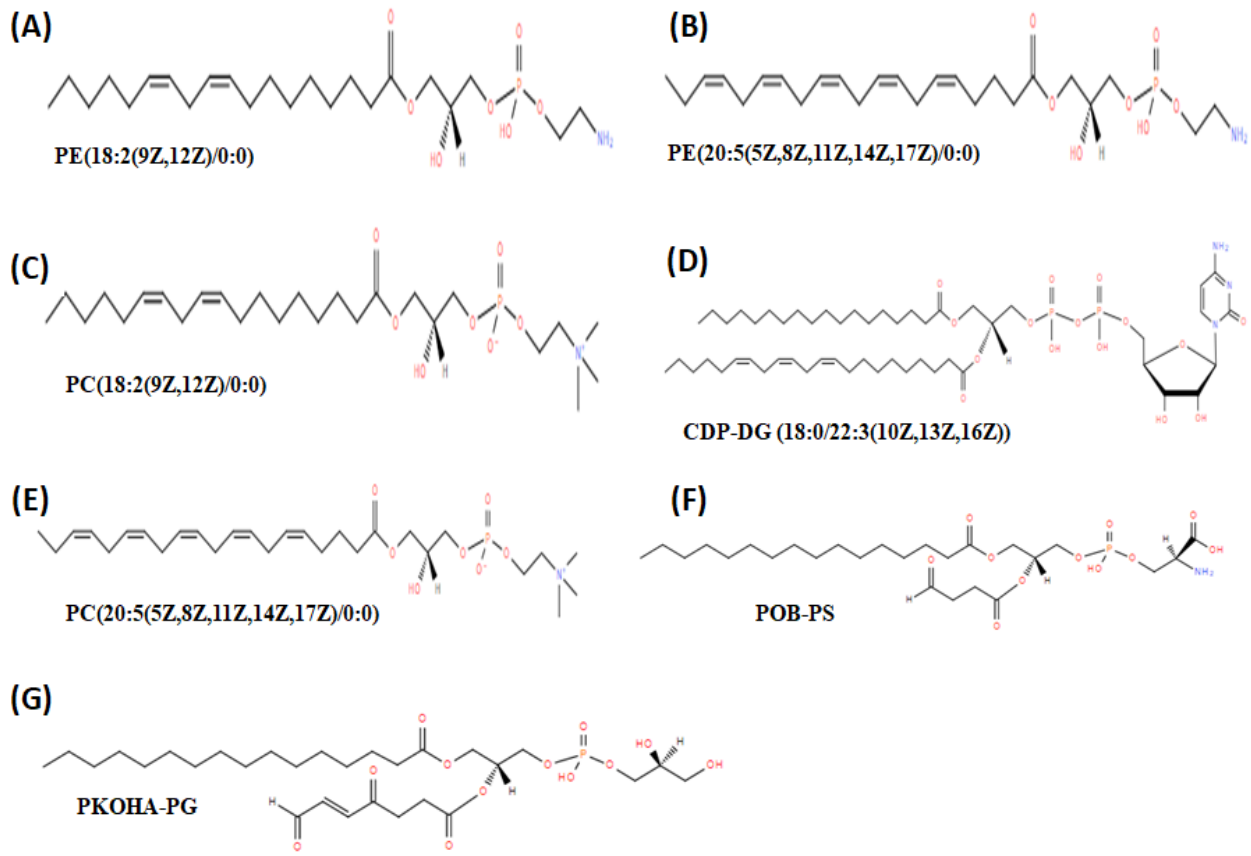

Figure 46. Chemical structures of candidate biomarkers tentatively identified as:

(**A**) glycerophosphoethanolamine PE(18:2(9Z,12Z)/0:0);

(**B**) glycerophosphoethanolamine PE(20:5(5Z,8Z,11Z,14Z,17Z)/0:0);

(**C**) glycerophosphocholine PC(18:2(9Z,12Z)/0:0);

(**D**) cytidine diphosphate diacylglycerol CDP-DG (18:0/22:3(10Z,13Z,16Z));

(**E**) glycerophosphocholine PC(20:5(5Z,8Z,11Z,14Z,17Z)/0:0);

(**F**) oxidized glycerophosphoserine POB-PS;

(**G**) oxidized glycerophosphoglycerol PKOHA-PG.

DISCUSSION

DISCUSSION

Despite advances in its treatment, MM is still the most life-threatening form of skin cancers, and its incidence rate and mortality have continued increasing worldwide over the past few decades. The diagnosis of this disease remains challenging and the procedure is still invasive, costly and takes too long, since it implies the removal and evaluation of the primary tumor, identification of high risk markers, and sentinel lymph node biopsy in order to check potential metastasis [291]. To date, several tissue and serological biomarkers for predicting MM progression and overall patient survival have been proposed [292]. However, only S100 calcium-binding protein B (S100B) and lactate dehydrogenase (LDH) are the serological markers proved to have some predicting value for disease progression to an advanced, but their translation into adequate therapeutic intervention and survival have not been achieved [293]. Hence, there are currently no single reliable serum-derived markers for early detection, prognosis prediction, treatment response or patient survival. This underscores an urgent need to discover reliable blood-based markers that may lead to a minimally-invasive, simple, economical and standardized test for detection of MM in its earliest stages, when disease is more amenable to treatment and the successful patient outcomes are more likely.

Here, LC-HRMS untargeted metabolomics was carried out in order to identify a molecular signature capable to discriminate between MMPs at different stages of disease and HC, illustrating the potential of this approach for biomarker discovering. According to our results, the chromatographic process was satisfactory and a significant difference between MMP and HC TICs was observed between minutes 6 and 14, when most lipids elute [290]. Univariate and multivariate analyses allowed the selection of 10 differentially expressed metabolites in serum from MMPs in stage I of disease and HCs, most of which were downregulated in patient

samples. Some of those selected compounds were tentatively identified and belong to different classes of glycerophospholipids (GP), such as glycerophosphoethanolamines, glycerophosphocholines, CDP-Diacylglycerols and oxidized glycerophospholipids. Phospholipids (PL) like phosphatidylcholines and phosphatidylethanolamines, along with other glycolipids and cholesterol are major components of biological membranes and greatly influence their fluidity [265]. As previously discussed, one of the most steadily established hallmarks of cancer is metabolic reprogramming [9] and lipids have been demonstrated to play multiples biochemical roles in cancer development [266,277].

In our study, nine of those metabolites selected as potential biomarkers (including the seven compounds tentatively identified as GPs) were found less expressed in MMP serum samples, while only one metabolite was found at higher levels in MMPs, compared to HCs. In accordance with these results, a reduced expression of specific PL-related compounds has been previously associated with different types of cancer such as colorectal cancer (CRC) [267] digestive tract tumors or renal cell carcinoma (RCC) [268]. Higher levels of other glycerophospholipids have also been related to lower risks of breast (BC), prostate (PC) and CRC [269]. CDP-diacylglycerols, which is another lipid metabolite that we found downregulated in MMPs, are important branchpoint intermediates and also key regulatory molecules in PL metabolism. Decreased levels of these molecules might be related with low PLs levels [294]. We also found lower levels of two oxidized PLs in MMP serum samples, which are another subtype of PLs that play an important role as endogenous pattern recognition ligands in innate immunity [295]. Therefore, they are also thought to be associated with pathogenesis of several diseases, including cancer [296–298].

Regarding diagnosis, decreased levels of this type of PLs in body fluids could be used for diagnostic purposes in different malignancies such as CRC [280], hepatocellular carcinoma (HCC) [273], liver cirrhosis (LC) [281]. This is consistent with the idea suggested by Raynor *et al.* that the fast extracellular hydrolysis of phospholipids by metastatic tumor cells and the subsequent cellular uptake of the resulting free fatty acids (FFA) seems to be indispensably necessary for epithelial tumor cells, probably for generating pro-metastatic lipid second messengers involved in their metastatic potential [272]. In addition, Tang *et al.* suggested that lower levels of PL-related compounds could be associated with the loss of body weight and inflammation, but could also indicate a higher LPCs decomposition rate to support cancer metabolism [280]. Moreover, elevated levels of specific PLs in body fluids have also been correlated with lower risk of BC, PC and CRC [269]. Another possible explanation for these findings could be the uncontrolled cell proliferation, which leads to PL degradation in order to generate energy for expansion and dissemination [299]. Other studies have also demonstrated that variations in the serological lipidomic profile and combinations of several putative PLs differentially found in body fluids might serve as diagnostic biomarkers of PC [270] and BC [278,298].

For diagnostic purposes, single biomarkers are often insufficiently sensitive or specific for clinical use. Thus, current research focuses on finding combinations of several biomarkers in order to improve clinical accuracy and predictive capacity. In this regard, ROC curves analyses are frequently used in biomedical informatics research to assess classification and prediction models. Here, we conducted this type of analysis and AUC values were calculated for each selected candidate, obtaining values that ranged from 0.73 to 0.92. The biomarker model utilizing those markers showed a more than acceptable classificatory capacity, being its

corresponding AUC value was 0.881 (95% CI: 0.753-1). Considering that AUC values over 0.8 indicate a good predictor model, our results suggest that these compounds might be considered to be used as a panel of clinically useful biomarkers for early diagnosis of this disease.

This study sets an open door to many other potential issues to further explore, and we are also aware that there are some limitations, being probably the most important one the sample size. While the total set of samples initially addressed (105, considering MMPs at Stage I, II, III, IV and HCs) could be considered more than acceptable for a metabolomic study, no significant metabolomic differences were found when comparing those samples from MMPs at different stage of disease. The most interesting results were obtained from a smaller sample size (22 Stage I MMPs vs 26 HCs), limiting the power of the study and the conclusions drawn. Therefore, this study could be considered a pilot, and further studies performed with larger sample sizes would be necessary in order to address models validation.

Despite instrumentation advances and better understanding accomplished in the last years in metabolomics, analysis of complex nature of biological samples (body fluids in particular), characterized by the huge amount of metabolites that can be detected and their highly wide dynamic range of their expression levels still remains challenging in metabolomic studies. The results obtained depend on several factors, including the sample type, cohort composition, analytical procedure, data treatment workflow, and cohort composition. Moreover, the difficulty to accurate metabolite identification by stepwise search in several molecular weight and fragmentation spectrum databases still represents one of the major limitations in the field. However, as previously discussed, not only identified molecules but also m/z signals could make up clinically useful metabolomic signatures, as long as they display suitable discrimination capacity in the corresponding biomarker evaluation models.

In this study, the 10 selected metabolites found differentially expressed in MMP-SI and HC serum samples displayed excellent discrimination capacity between those groups according to ROC curves analyses and the corresponding biomarker model assessment. Thus, these metabolites are susceptible of being considered as potential biomarkers and could represent a novel metabolomic signature, suitable and applicable for early diagnosis of MM. Taking into account the crucial importance of early detection of this type of skin cancer, in terms of treatment management and improved patient outcomes, these results provide valuable knowledge in this regard.

Further avenues to exploit could include complementary "omics" analyses, which will probably add new insights into the MM pathophysiological changes, as well as further complementary studies evaluating other easily collectible body fluids including saliva or urine, that might contribute to the discovery of additional potential diagnostic biomarkers.

Significant efforts still need to be made in the next years in order to find suitable biomarkers that could aid or improve MM early diagnosis, its correct staging, the discrimination of other pathological conditions, as well as indicate patients' prognosis or the most appropriate personalized therapeutic regimes. In this regard, studies like the one herein presented could pave the way for those goals, by suggesting novel potential biomarkers for early cancer detection. Furthermore, this study represent an excellent example of the potential role that untargeted LC-MS-based metabolomics applied to liquid biopsies and circulating compounds could play in biomarkers discovery for their use in translational research and precision medicine in oncology.

CONCLUSIONS

1. A patient-derived MM cell subpopulation enriched in CSCs was characterized by assessing the expression of specific markers and their stem-like properties.

2. Exosomes derived from CSCs and serums from patients with MM were isolated, characterized and their metabolomic profile was analyzed by LC-HRMS following an untargeted approach and applying univariate and multivariate statistical analyses.

3. Significant metabolomic differences were found in exosomes derived from MM-CSCs compared to those from MM differentiated cells. In particular, 19 metabolites were selected according to statistical criteria. They showed a clear differential pattern of expression across the two groups of comparison and 4 of them were tentatively identified as structural lipids of different types.

4. Additionally, some differences were also found in the metabolomic profile of serum-derived exosomes from patients with MM at several stages of disease, compared to those from healthy individuals. In particular, 24 metabolites were selected according to statistical criteria. They also showed a clear differential pattern of expression across the two groups of comparison and 18 of them were tentatively identified. According to ROC curve analyses, they all showed excellent discrimination capacity between the two groups of samples, suggesting that they could be considered potential exosomal biomarkers for MM.

5. Similarities in some structural lipids from both CSC-derived exosomes and those derived from patients with MM were also detected. In particular, the glycerophosphocoline PC 16:0/0:0 was commonly found to be overexpressed in exosomes derived from both HC serums and MM differentiated cells, compared to MMP serum and MM CSCs, respectively.

Conclusions

6. Significant metabolomic differences were found between patients in stage I of MM and HCs. In particular, 10 metabolites were selected according to statistical criteria. They also showed a clear differential pattern of expression across the two groups of comparison and 7 of them were tentatively identified as different structural lipids that belong to different classes of glycerophospolipids such as glycerophosphoethanolamines (PEs), glycerophosphocholines (PCs), cytidine diphosphate diacylglycerol (CDP-DG), or oxidized glycerophospholipids (POB-PS and PKOHA-PG).

7. Those selected differential metabolites were suggested as potential serological biomarkers for early diagnosis of MM, since they all yielded remarkable discrimination capacity between the two groups of samples, according to ROC curve analyses.

8. To our knowledge, this is the first reported evidence of differences in exosome metabolomic profile from CSCs-enriched melanospheres versus MM differentiated cells and serum samples from patients with MM and healthy individuals.

9. All together, the results presented herein provide evidence that metabolomics and LC-HRMS analytical platforms, represent a powerful tool to identify and quantify metabolites in liquid biopsies, which could serve as potential biomarkers for diagnosis of not only MM, but also for other types of cancer and diseases.

CONCLUSIONES

1. Se caracterizó una subpoblación celular enriquecida en CMCs en una línea celular primaria derivada de un paciente con MM mediante la evaluación de la expresión de marcadores específicos y de sus propiedades características.
2. Los exosomas derivados de CMCs y sueros de pacientes con MM fueron aislados, caracterizados, y su perfil metabolómico fue analizado por cromatografía líquida acoplada a espectrometría de masas de alta resolución (LC-HRMS) siguiendo una aproximación no dirigida y aplicando análisis estadísticos univariados y multivariados.
3. Se hallaron diferencias metabolómicas significativas entre los exosomas derivados de CMCs de MM y aquellos derivados de células cancerígenas diferenciadas. En concreto, se seleccionaron 19 metabolitos en base a criterios estadísticos. Todos ellos mostraron un claro patrón de expresión diferencial entre los grupos comparados y 4 de ellos fueron tentativamente identificados como lípidos estructurales de diferentes clases.
4. Además, también se encontraron diferencias en el perfil metabolómico de los exosomas derivados del suero de pacientes con MM en distintos estadios de la enfermedad, comparados con aquellos derivados de individuos sanos. En concreto, 24 metabolitos se seleccionaron en base a criterios estadísticos. Todos ellos también presentaron un claro patrón de expresión diferencial entre los grupos comparados y 18 de ellos fueron tentativamente identificados. De acuerdo con los análisis de curvas ROC, todos ellos presentaban una excelente capacidad de discriminación entre los dos grupos de muestras, lo cual sugiere que podrían ser considerados como potenciales biomarcadores exosomales de MM.

5. También se detectaron similitudes en algunos lípidos estructurales tanto en exosomas derivados de CMCs como en aquellos derivados de pacientes con MM. En particular, la glicerofosfocolina PC 16:0/0:0 se halló comúnmente sobre-expresada en exosomas derivados tanto de sueros de individuos sanos como en células diferenciadas de MM, en comparación con aquellos derivados de suero de pacientes con MM y CMCs de MM, respectivamente.

6. Se hallaron diferencias metabolómicas significativas entre pacientes en estadio I de MM e individuos sanos. En concreto, se seleccionaron 10 metabolitos en base a criterios estadísticos. Todos ellos presentaban un claro patrón de expresión diferencial entre los grupos comparados y 7 de ellos se identificaron tentativamente como lípidos estructurales pertenecientes a distintas clases de glicerofosfolípidos, como glicerofosfoetanolaminas (Pes), glicerofosfocolinas (PCs), citidín difosfato diacilglicerol (CDP-DG) o glicerofosfolípidos oxidados (POB-PS y PKOHA-PG).

7. Todos esos metabolitos diferenciales seleccionados fueron sugeridos como potenciales biomarcadores serológicos para el diagnóstico precoz del MM, puesto que todos presentaron una notable capacidad de discriminación entre los dos grupos de muestras, de acuerdo con los análisis de curvas ROC.

8. Hasta donde sabemos, esta es la primera evidencia reportada sobre diferencias en el perfil metabolómico de exosomas derivados de melanosferas enriquecidas en CMCs respecto a los de células diferenciadas de MM, así como en exosomas derivados de sueros de pacientes con MM respecto a los de individuos sanos.

9. En conjunto, los resultados presentados en este trabajo demuestran que la metabolómica y las plataformas analíticas LC-HRMS representan una poderosa herramienta para identificar y cuantificar metabolitos en biopsias líquidas, que podrían servir como potenciales biomarcadores para el diagnóstico no solo del MM, sino también para otros tipos de cáncer y otras enfermedades.

GLOSSARY

AFM: Atomic force microscopy

AJCC: American Joint Committee on Cancer

ALDH: Aldehyde dehydrogenase

AUC: Area under the curve

BCC: Basal cell carcinoma

BS: Blank solvent

CAF: Cancer-associated fibroblast

CE: Capillary electrophoresis

CSC: Cancer stem cell

CTC: Circulating tumor cell

ctDNA: Circulating tumor DNA

CV: Cross validation

DMEM: Dulbecco's modified eagle's medium

ECM: Extracellular matrix

EMT: Epithelial-to-mesenchymal transition

ESI: Electrospray ionization

EV: Extracellular vesicle

FACS: Fluorescence-activated cell sorting

FBS: Fetal bovine serum

FDA: Food and Drug Administration

GS: Gas chromatography

HC: Healthy control

HDI: Human development index

IDA: Information dependent acquisition

ISEV: International Society for Extracellular Vesicles

LC: Liquid chromatography

LDH: Lactate dehydrogenase

lncRNA: Long noncoding RNA

m/lEV: medium/large extracellular vesicle

m/z: mass-to-charge ratio

MDR: Multidrug resistance

MET: Mesenchymal-to-epithelial transition

MHC: Major histocompatibility complex

MIR: Mortality-to-incidence ratio

miRNA: microRNA

MISEV: Minimal information for studies of extracellular vesicles

Glossary

MM: Malignant melanoma

MM-CSC: Malignant melanoma cancer stem cell

MMP: Malignant melanoma patient

MP: Mobile phase

HRMS: High resolution mass spectrometry

MVA: multivariate analysis

MVB: Multivesicular body

NCD: Noncommunicable diseases

NIH: National Institute of Health

NMR: Nuclear magnetic resonance

NMSC: Non-melanoma skin cancer

PBS: Phosphate buffered saline

PC: Phosphatidylcholine

PCA: Principal component analysis

PE: Phophatidyletanolamine

PL: Phospholipid

PLS-DA: Partial least squares regression

QC: Quality control

Q-TOF: Quadrupole-time-of-flight

ROC: Receiver operator characteristics

ROS: Reactive oxygen species

RT: Retention time

SC: Skin cancer

SCC: squamous cell carcinoma

SEM: Scanning electron microscopy

sEV: small extracellular vesicle

SP: Side population

TAM: Tumor-associated macrophages

TEM: Transmission electron microscopy

TIC: Total ion chromatogram

TME: Tumor microenvironment

UV: Ultraviolet

UVA: Univariate analysis

VIP: Variable importance in projection

WHO: World Health Organization

BIBLIOGRAPHY

[1] Boyle P, Levin B. World Cancer Report 2008. 2008. https://doi.org/10.1016/j.cma.2010.02.010.

[2] McGuire S. World Cancer Report 2014. Geneva, Switzerland: World Health Organization, International Agency for Research on Cancer, WHO Press, 2015. Adv Nutr 2016;7:418–9. https://doi.org/10.3945/an.116.012211.

[3] Sung H, Ferlay J, Siegel RL, Laversanne M, Soerjomataram I, Jemal A, et al. Global cancer statistics 2020: GLOBOCAN estimates of incidence and mortality worldwide for 36 cancers in 185 countries. CA Cancer J Clin 2021. https://doi.org/10.3322/caac.21660.

[4] Wild CP. International Agency for Research on Cancer. Encycl. Toxicol. Third Ed., 2014. https://doi.org/10.1016/B978-0-12-386454-3.00402-4.

[5] Baba A, Câtoi C. Comparative Oncology. Chapter 3, TUMOR CELL MORPHOLOGY. Comp. Oncol., 2007.

[6] Roy D, Dorak MT. Environmental factors, genes, and the development of human cancers. 2010. https://doi.org/10.1007/978-1-4419-6752-7.

[7] Merlo LMF, Pepper JW, Reid BJ, Maley CC. Cancer as an evolutionary and ecological process. Nat Rev Cancer 2006. https://doi.org/10.1038/nrc2013.

[8] Dong LM, Potter JD, White E, Ulrich CM, Cardon LR, Peters U. Genetic susceptibility to cancer: The role of polymorphisms in candidate genes. JAMA - J Am Med Assoc 2008. https://doi.org/10.1001/jama.299.20.2423.

[9] Hanahan D, Weinberg RA. Ha1. Hanahan D, Weinberg RA. Hallmarks of cancer: The next generation. Vol. 144, Cell. 2011. p. 646–74. llmarks of cancer: The next generation. Cell 2011;144:646–74. https://doi.org/10.1016/j.cell.2011.02.013.

[10] Kroemer G, Pouyssegur J. Tumor Cell Metabolism: Cancer's Achilles' Heel. Cancer Cell 2008;13:472–82. https://doi.org/10.1016/j.ccr.2008.05.005.

[11] Negrini S, Gorgoulis VG, Halazonetis TD. Genomic instability an evolving hallmark of cancer. Nat Rev Mol Cell Biol 2010;11:220–8. https://doi.org/10.1038/nrm2858.

[12] Heldin CH. Autocrine PDGF stimulation in malignancies. Ups J Med Sci 2012. https://doi.org/10.3109/03009734.2012.658119.

[13] Aharinejad S, Sioud M, Lucas T, Abraham D. Targeting stromal-cancer cell interactions with siRNAs. Methods Mol Biol 2009. https://doi.org/10.1007/978-1-60327-547-7_12.

[14] Chial BH, Write PD, Right S, Education N. Proto-oncogenes to Oncogenes to Cancer. Nat Educ 2008.

[15] Gariglio P. Oncogenes and tumor suppressor genes. Mol. Oncol. Princ. Recent Adv., 2012. https://doi.org/10.2174/978160805016111201010064.

[16] Valeri N, Gasparini P, Fabbri M, Braconi C, Veronese A, Lovat F, et al. Modulation of mismatch repair and genomic stability by miR-155. Proc Natl Acad Sci U S A 2010. https://doi.org/10.1073/pnas.1002472107.

[17] Nagy JA, Dvorak HF. Heterogeneity of the tumor vasculature: The need for new tumor

blood vessel type-specific targets. Clin. Exp. Metastasis, 2012. https://doi.org/10.1007/s10585-012-9500-6.

[18] Valastyan S, Weinberg RA. Tumor Metastasis: Molecular Insights and Evolving Paradigms The Invasion-Metastasis Cascade. Cell 2011.

[19] Talmadge, Fidler. The Biology of Cancer Metastasis: Historical Perspective. Cancer Res 2010.

[20] Yanumula A, Cusick JK. Biochemistry, Extrinsic Pathway of Apoptosis. 2020.

[21] Plati J, Bucur O, Khosravi-Far R. Apoptotic cell signaling in cancer progression and therapy. Integr Biol 2011. https://doi.org/10.1039/c0ib00144a.

[22] Grivennikov SI, Greten FR, Karin M. Immunity, Inflammation, and Cancer. Cell 2010. https://doi.org/10.1016/j.cell.2010.01.025.

[23] Colotta F, Allavena P, Sica A, Garlanda C, Mantovani A. Cancer-related inflammation, the seventh hallmark of cancer: Links to genetic instability. Carcinogenesis 2009. https://doi.org/10.1093/carcin/bgp127.

[24] Martínez P, Blasco MA. Telomeric and extra-telomeric roles for telomerase and the telomere-binding proteins. Nat Rev Cancer 2011. https://doi.org/10.1038/nrc3025.

[25] Kruger S, Ilmer M, Kobold S, Cadilha BL, Endres S, Ormanns S, et al. Advances in cancer immunotherapy 2019 - Latest trends. J Exp Clin Cancer Res 2019. https://doi.org/10.1186/s13046-019-1266-0.

[26] Marie-Egyptienne DT, Lohse I, Hill RP. Cancer stem cells, the epithelial to mesenchymal transition (EMT) and radioresistance: Potential role of hypoxia. Cancer Lett 2013;341:63–72. https://doi.org/10.1016/j.canlet.2012.11.019.

[27] Foundation SC. Skin Cancer Facts and Statistics. Ski Cancer Inf 2019.

[28] American Cancer Society. Facts & Figures 2019. Am Cancer Soc 2019.

[29] Stratigos AJ, Forsea AM, Van Der Leest RJT, De Vries E, Nagore E, Bulliard JL, et al. Euromelanoma: A dermatology-led European campaign against nonmelanoma skin cancer and cutaneous melanoma. Past, present and future. Br J Dermatol 2012;167:99–104. https://doi.org/10.1111/j.1365-2133.2012.11092.x.

[30] National Cancer Institute. SEER Cancer Stat Facts. Natl Institutes Heal 2019.

[31] Bray F, Ferlay J, Soerjomataram I, Siegel RL, Torre LA, Jemal A. Global cancer statistics 2018: GLOBOCAN estimates of incidence and mortality worldwide for 36 cancers in 185 countries. CA Cancer J Clin 2018;68:394–424. https://doi.org/10.3322/caac.21492.

[32] Cormier J, Voss R, Woods T, Cromwell K, Nelson K. Improving outcomes in patients with melanoma: strategies to ensure an early diagnosis. Patient Relat Outcome Meas 2015. https://doi.org/10.2147/prom.s69351.

[33] Matthews NH, Li WQ, Qureshi AA, Weinstock MA, Cho E. Epidemiology of Melanoma BT - Cutaneous Melanoma: Etiology and Therapy. Cutan. Melanoma Etiol. Ther., 2017.

[34] Brenner M, Hearing VJ. The protective role of melanin against UV damage in human skin. Photochem Photobiol 2008. https://doi.org/10.1111/j.1751-1097.2007.00226.x.

[35] Khazaei Z, Ghorat F, Jarrahi A, Adineh H, Sohrabivafa M, Goodarzi E. GLOBAL INCIDENCE AND MORTALITY OF SKIN CANCER BY HISTOLOGICAL SUBTYPE AND ITS RELATIONSHIP WITH THE HUMAN DEVELOPMENT INDEX (HDI); AN ECOLOGY STUDY IN 2018. World Cancer Res J 2019.

[36] Sneyd MJ, Cox B. A comparison of trends in melanoma mortality in New Zealand and Australia: The two countries with the highest melanoma incidence and mortality in the world. BMC Cancer 2013. https://doi.org/10.1186/1471-2407-13-372.

[37] Stang A, Pukkala E, Sankila R, Söderman B, Hakulinen T. Time trend analysis of the skin melanoma incidence of Finland from 1953 through 2003 including 16,414 cases. Int J Cancer 2006. https://doi.org/10.1002/ijc.21836.

[38] Watson M, Geller AC, Tucker MA, Guy GP, Weinstock MA. Melanoma burden and recent trends among non-Hispanic whites aged 15–49 years, United States. Prev Med (Baltim) 2016. https://doi.org/10.1016/j.ypmed.2016.08.032.

[39] Cho E, Rosner BA, Colditz GA. Risk factors for melanoma by body for whites. Cancer Epidemiol Biomarkers Prev 2005. https://doi.org/10.1158/1055-9965.EPI-04-0632.

[40] Pérez-Gómez B, Aragonés N, Gustavsson P, Lope V, López-Abente G, Pollán M. Do sex and site matter? Different age distribution in melanoma of the trunk among Swedish men and women. Br J Dermatol 2008. https://doi.org/10.1111/j.1365-2133.2007.08429.x.

[41] Parkin DM, Mesher D, Sasieni P. Cancers attributable to solar (ultraviolet) radiation exposure in the UK in 2010. Br J Cancer 2011. https://doi.org/10.1038/bjc.2011.486.

[42] Wu S, Han J, Laden F, Qureshi AA. Long-term ultraviolet flux, other potential risk factors, and skin cancer risk: A cohort Study. Cancer Epidemiol Biomarkers Prev 2014. https://doi.org/10.1158/1055-9965.EPI-13-0821.

[43] Moan J, Grigalavicius M, Baturaite Z, Dahlback A, Juzeniene A. The relationship between UV exposure and incidence of skin cancer. Photodermatol Photoimmunol Photomed 2015. https://doi.org/10.1111/phpp.12139.

[44] Pfahlberg A, Kölmel KF, Gefeller O. Timing of excessive ultraviolet radiation and melanoma: Epidemiology does not support the existence of a critical period of high susceptibility to solar ultraviolet radiation-induced melanoma. Br J Dermatol 2001. https://doi.org/10.1046/j.1365-2133.2001.04070.x.

[45] Lew RA, Cook N, Marvell R, Fitzpatrick TB. Sun Exposure Habits in Patients with Cutaneous Melanoma: A Case Control Study. J Dermatol Surg Oncol 1983. https://doi.org/10.1111/j.1524-4725.1983.tb01051.x.

[46] Wehner MR, Chren MM, Nameth D, Choudhry A, Gaskins M, Nead KT, et al. International prevalence of indoor tanning a systematic review and meta-analysis. JAMA Dermatology 2014. https://doi.org/10.1001/jamadermatol.2013.6896.

[47] Cymerman RM, Shao Y, Wang K, Zhang Y, Murzaku EC, Penn LA, et al. De Novo vs Nevus-Associated Melanomas: Differences in Associations With Prognostic Indicators

and Survival. J Natl Cancer Inst 2016. https://doi.org/10.1093/jnci/djw121.

[48] Bode AM, Dong Z. Mitogen-activated protein kinase activation in UV-induced signal transduction. Sci STKE 2003. https://doi.org/10.1126/scisignal.1672003re2.

[49] Scolyer RA, Long G V., Thompson JF. Evolving concepts in melanoma classification and their relevance to multidisciplinary melanoma patient care. Mol Oncol 2011. https://doi.org/10.1016/j.molonc.2011.03.002.

[50] Davis LE, Shalin SC, Tackett AJ. Current state of melanoma diagnosis and treatment. Cancer Biol Ther 2019;20:1366–79. https://doi.org/10.1080/15384047.2019.1640032.

[51] Rebecca VW, Sondak VK, Smalley KSM. A brief history of melanoma: From mummies to mutations. Melanoma Res 2012. https://doi.org/10.1097/CMR.0b013e328351fa4d.

[52] Elmore JG, Elder DE, Barnhill RL, Knezevich SR, Longton GM, Titus LJ, et al. Concordance and Reproducibility of Melanoma Staging According to the 7th vs 8th Edition of the AJCC Cancer Staging Manual. JAMA Netw Open 2018;1. https://doi.org/10.1001/jamanetworkopen.2018.0083.

[53] Bartlett EK, Karakousis GC. Current staging and prognostic factors in melanoma. Surg Oncol Clin N Am 2015;24:215–27. https://doi.org/10.1016/j.soc.2014.12.001.

[54] Gadeliya Goodson A, Grossman D. Strategies for early melanoma detection: Approaches to the patient with nevi. J Am Acad Dermatol 2009;60:719–35. https://doi.org/10.1016/j.jaad.2008.10.065.

[55] Cormier J, Voss R, Woods T, Cromwell K, Nelson K. Improving outcomes in patients with melanoma: strategies to ensure an early diagnosis. Patient Relat Outcome Meas 2015:229. https://doi.org/10.2147/prom.s69351.

[56] Guy GP, Ekwueme DU, Tangka FK, Richardson LC. Melanoma treatment costs: A systematic review of the literature, 1990-2011. Am J Prev Med 2012;43:537–45. https://doi.org/10.1016/j.amepre.2012.07.031.

[57] Naik PP. Cutaneous Malignant Melanoma: A Review of Early Diagnosis and Management. World J Oncol 2021;12:7–19. https://doi.org/10.14740/wjon1349.

[58] Van Laar R, Lincoln M, Van Laar B. Development and validation of a plasmabased melanoma biomarker suitable for clinical use. Br J Cancer 2018. https://doi.org/10.1038/bjc.2017.477.

[59] Elmore JG, Barnhill RL, Elder DE, Longton GM, Pepe MS, Reisch LM, et al. Pathologists' diagnosis of invasive melanoma and melanocytic proliferations: Observer accuracy and reproducibility study. BMJ 2017. https://doi.org/10.1136/bmj.j2813.

[60] Rey-Barroso L, Peña-Gutiérrez S, Yáñez C, Burgos-Fernández FJ, Vilaseca M, Royo S. Optical technologies for the improvement of skin cancer diagnosis: A review. Sensors (Switzerland) 2021;21:1–31. https://doi.org/10.3390/s21010252.

[61] Dell'Olio F, Su J, Huser T, Sottile V, Cortés-Hernández LE, Alix-Panabières C. Liquid Biopsies: Photonic Technologies for Liquid Biopsies: Recent Advances and Open Research Challenges (Laser Photonics Rev. 15(1)/2021). Laser Photon Rev 2021.

https://doi.org/10.1002/lpor.202170012.

[62] Meacham CE, Morrison SJ. Tumour heterogeneity and cancer cell plasticity. Nature 2013. https://doi.org/10.1038/nature12624.

[63] Marjanovic ND, Weinberg RA, Chaffer CL. Cell plasticity and heterogeneity in cancer. Clin Chem 2013. https://doi.org/10.1373/clinchem.2012.184655.

[64] Visvader JE. Cells of origin in cancer. Nature 2011;469:314–22. https://doi.org/10.1038/nature09781.

[65] Shackleton M, Quintana E, Fearon ER, Morrison SJ. Heterogeneity in Cancer: Cancer Stem Cells versus Clonal Evolution. Cell 2009. https://doi.org/10.1016/j.cell.2009.08.017.

[66] Prasetyanti PR, Medema JP. Intra-tumor heterogeneity from a cancer stem cell perspective. Mol Cancer 2017. https://doi.org/10.1186/s12943-017-0600-4.

[67] Cabrera MC. Cancer stem cell plasticity and tumor hierarchy. World J Stem Cells 2015. https://doi.org/10.4252/wjsc.v7.i1.27.

[68] Durrett R, Foo J, Leder K, Mayberry J, Michor F. Intratumor heterogeneity in evolutionary models of tumor progression. Genetics 2011. https://doi.org/10.1534/genetics.110.125724.

[69] McGranahan N, Swanton C. Clonal Heterogeneity and Tumor Evolution: Past, Present, and the Future. Cell 2017;168:613–28. https://doi.org/10.1016/j.cell.2017.01.018.

[70] O'Brien CA, Kreso A, Dick JE. Cancer Stem Cells in Solid Tumors: An Overview. Semin Radiat Oncol 2009. https://doi.org/10.1016/j.semradonc.2008.11.001.

[71] Dick JE. Looking ahead in cancer stem cell research. Nat Biotechnol 2009. https://doi.org/10.1038/nbt0109-44.

[72] Vermeulen L, de Sousa e Melo F, Richel DJ, Medema JP. The developing cancer stem-cell model: Clinical challenges and opportunities. Lancet Oncol 2012;13. https://doi.org/10.1016/S1470-2045(11)70257-1.

[73] Vermeulen L, De Sousa E Melo F, Van Der Heijden M, Cameron K, De Jong JH, Borovski T, et al. Wnt activity defines colon cancer stem cells and is regulated by the microenvironment. Nat Cell Biol 2010. https://doi.org/10.1038/ncb2048.

[74] Scheel C, Eaton EN, Li SHJ, Chaffer CL, Reinhardt F, Kah KJ, et al. Paracrine and autocrine signals induce and maintain mesenchymal and stem cell states in the breast. Cell 2011. https://doi.org/10.1016/j.cell.2011.04.029.

[75] Mani SA, Guo W, Liao MJ, Eaton EN, Ayyanan A, Zhou AY, et al. The Epithelial-Mesenchymal Transition Generates Cells with Properties of Stem Cells. Cell 2008. https://doi.org/10.1016/j.cell.2008.03.027.

[76] Chaffer CL, Brueckmann I, Scheel C, Kaestli AJ, Wiggins PA, Rodrigues LO, et al. Normal and neoplastic nonstem cells can spontaneously convert to a stem-like state. Proc Natl Acad Sci U S A 2011. https://doi.org/10.1073/pnas.1102454108.

[77] Bocci F, Jolly MK, George JT, Levine H, Onuchic JN. A mechanism-based computational

model to capture the interconnections among epithelial-mesenchymal transition, cancer stem cells and Notch-Jagged signaling. Oncotarget 2018. https://doi.org/10.18632/oncotarget.25692.

[78] Gupta PB, Pastushenko I, Skibinski A, Blanpain C, Kuperwasser C. Phenotypic Plasticity: Driver of Cancer Initiation, Progression, and Therapy Resistance. Cell Stem Cell 2019;24:65–78. https://doi.org/10.1016/j.stem.2018.11.011.

[79] Lotti F, Jarrar AM, Pai RK, Hitomi M, Lathia J, Mace A, et al. Chemotherapy activates cancer-associated fibroblasts to maintain colorectal cancer-initiating cells by IL-17A. J Exp Med 2013. https://doi.org/10.1084/jem.20131195.

[80] Shelton M, Anene CA, Nsengimana J, Roberts W, Newton-Bishop J, Boyne JR. The role of CAF derived exosomal microRNAs in the tumour microenvironment of melanoma. Biochim Biophys Acta - Rev Cancer 2021;1875:188456. https://doi.org/10.1016/j.bbcan.2020.188456.

[81] Zheng Y, Cai Z, Wang S, Zhang X, Qian J, Hong S, et al. Macrophages are an abundant component of myeloma microenvironment and protect myeloma cells from chemotherapy drug-induced apoptosis. Blood 2009. https://doi.org/10.1182/blood-2009-05-220285.

[82] Amit M, Gil Z. Macrophages increase the resistance of pancreatic adenocarcinoma cells to gemcitabine by upregulating cytidine deaminase. Oncoimmunology 2013. https://doi.org/10.4161/onci.27231.

[83] Najafi M, Mortezaee K, Ahadi R. Cancer stem cell (a)symmetry & plasticity: Tumorigenesis and therapy relevance. Life Sci 2019;231. https://doi.org/10.1016/j.lfs.2019.05.076.

[84] Hernández-Camarero P, Jiménez G, López-Ruiz E, Barungi S, Marchal JA, Perán M. Revisiting the dynamic cancer stem cell model: Importance of tumour edges. Crit Rev Oncol Hematol 2018;131:35–45. https://doi.org/10.1016/j.critrevonc.2018.08.004.

[85] Sutherland KD, Visvader JE. Cellular Mechanisms Underlying Intertumoral Heterogeneity. Trends in Cancer 2015. https://doi.org/10.1016/j.trecan.2015.07.003.

[86] Thankamony AP, Saxena K, Murali R, Jolly MK, Nair R. Cancer Stem Cell Plasticity – A Deadly Deal. Front Mol Biosci 2020;7. https://doi.org/10.3389/fmolb.2020.00079.

[87] Reya T, Morrison SJ, Clarke MF, Weissman IL. Stem cells, cancer, and cancer stem cells. Nature 2001. https://doi.org/10.1038/35102167.

[88] Al-Hajj M, Clarke MF. Self-renewal and solid tumor stem cells. Oncogene 2004. https://doi.org/10.1038/sj.onc.1207947.

[89] Batlle E, Clevers H. Cancer stem cells revisited. Nat Med 2017. https://doi.org/10.1038/nm.4409.

[90] Bonnet D, Dick JE. Human acute myeloid leukemia is organized as a hierarchy that originates from a primitive hematopoietic cell. Nat Med 1997. https://doi.org/10.1038/nm0797-730.

[91] Al-Hajj M, Wicha MS, Benito-Hernandez A, Morrison SJ, Clarke MF. Prospective

identification of tumorigenic breast cancer cells. Proc Natl Acad Sci U S A 2003. https://doi.org/10.1073/pnas.0530291100.

[92] Allegra A, Alonci A, Penna G, Innao V, Gerace D, Rotondo F, et al. The Cancer Stem Cell Hypothesis: A Guide to Potential Molecular Targets. Cancer Invest 2014;32:470–95. https://doi.org/10.3109/07357907.2014.958231.

[93] Islam F, Gopalan V, Smith RA, Lam AK-Y. Translational potential of cancer stem cells: A review of the detection of cancer stem cells and their roles in cancer recurrence and cancer treatment. Exp Cell Res 2015;335:135–47. https://doi.org/10.1016/J.YEXCR.2015.04.018.

[94] Marzagalli M, Fontana F, Raimondi M, Limonta P. Cancer Stem Cells—Key Players in Tumor Relapse. Cancers (Basel) 2021;13:376. https://doi.org/10.3390/cancers13030376.

[95] Verga Falzacappa M V., Ronchini C, Reavie LB, Pelicci PG. Regulation of self-renewal in normal and cancer stem cells. FEBS J 2012. https://doi.org/10.1111/j.1742-4658.2012.08727.x.

[96] Takahashi R u., Miyazaki H, Ochiya T. The role of microRNAs in the regulation of cancer stem cells. Front Genet 2013. https://doi.org/10.3389/fgene.2013.00295.

[97] Roy S, Majumdar APN. Signaling in colon cancer stem cells. J Mol Signal 2012. https://doi.org/10.1186/1750-2187-7-11.

[98] Singh SK, Hawkins C, Clarke ID, Squire JA, Bayani J, Hide T, et al. Identification of human brain tumour initiating cells. Nature 2004. https://doi.org/10.1038/nature03128.

[99] Ogden AT, Waziri AE, Lochhead RA, Fusco D, Lopez K, Ellis JA, et al. Identification of A2B5+CD133- tumor-initiating cells in adult human gliomas. Neurosurgery 2008. https://doi.org/10.1227/01.neu.0000316019.28421.95.

[100] Son MJ, Woolard K, Nam DH, Lee J, Fine HA. SSEA-1 Is an Enrichment Marker for Tumor-Initiating Cells in Human Glioblastoma. Cell Stem Cell 2009. https://doi.org/10.1016/j.stem.2009.03.003.

[101] Dirkse A, Golebiewska A, Buder T, Nazarov P V., Muller A, Poovathingal S, et al. Stem cell-associated heterogeneity in Glioblastoma results from intrinsic tumor plasticity shaped by the microenvironment. Nat Commun 2019. https://doi.org/10.1038/s41467-019-09853-z.

[102] Roesch A, Fukunaga-Kalabis M, Schmidt EC, Zabierowski SE, Brafford PA, Vultur A, et al. A Temporarily Distinct Subpopulation of Slow-Cycling Melanoma Cells Is Required for Continuous Tumor Growth. Cell 2010. https://doi.org/10.1016/j.cell.2010.04.020.

[103] Quintana E, Shackleton M, Foster HR, Fullen DR, Sabel MS, Johnson TM, et al. Phenotypic heterogeneity among tumorigenic melanoma cells from patients that is reversible and not hierarchically organized. Cancer Cell 2010. https://doi.org/10.1016/j.ccr.2010.10.012.

[104] Liu S, Cong Y, Wang D, Sun Y, Deng L, Liu Y, et al. Breast cancer stem cells transition between epithelial and mesenchymal states reflective of their normal counterparts. Stem Cell Reports 2014. https://doi.org/10.1016/j.stemcr.2013.11.009.

[105] Iliopoulos D, Hirsch HA, Wang G, Struhl K. Inducible formation of breast cancer stem cells and their dynamic equilibrium with non-stem cancer cells via IL6 secretion. Proc Natl Acad Sci U S A 2011. https://doi.org/10.1073/pnas.1018898108.

[106] Kobayashi S, Yamada-Okabe H, Suzuki M, Natori O, Kato A, Matsubara K, et al. LGR5-positive colon cancer stem cells interconvert with drug-resistant LGR5-negative cells and are capable of tumor reconstitution. Stem Cells 2012. https://doi.org/10.1002/stem.1257.

[107] Fumagalli A, Oost KC, Kester L, Morgner J, Bornes L, Bruens L, et al. Plasticity of Lgr5-Negative Cancer Cells Drives Metastasis in Colorectal Cancer. Cell Stem Cell 2020. https://doi.org/10.1016/j.stem.2020.02.008.

[108] Biddle A, Gammon L, Liang X, Costea DE, Mackenzie IC. Phenotypic Plasticity Determines Cancer Stem Cell Therapeutic Resistance in Oral Squamous Cell Carcinoma. EBioMedicine 2016. https://doi.org/10.1016/j.ebiom.2016.01.007.

[109] Doherty MR, Smigiel JM, Junk DJ, Jackson MW. Cancer stem cell plasticity drives therapeutic resistance. Cancers (Basel) 2016. https://doi.org/10.3390/cancers8010008.

[110] Poli V, Fagnocchi L, Zippo A. Tumorigenic cell reprogramming and cancer plasticity: Interplay between signaling, microenvironment, and epigenetics. Stem Cells Int 2018. https://doi.org/10.1155/2018/4598195.

[111] Dongre A, Weinberg RA. New insights into the mechanisms of epithelial–mesenchymal transition and implications for cancer. Nat Rev Mol Cell Biol 2019. https://doi.org/10.1038/s41580-018-0080-4.

[112] Rubtsova SN, Zhitnyak IY, Gloushankova NA. Phenotypic Plasticity of Cancer Cells Based on Remodeling of the Actin Cytoskeleton and Adhesive Structures. Int J Mol Sci 2021;22:1821. https://doi.org/10.3390/ijms22041821.

[113] Roche J. The epithelial-to-mesenchymal transition in cancer. Cancers (Basel) 2018. https://doi.org/10.3390/cancers10020052.

[114] Nieto MA, Huang RYYJ, Jackson RAA, Thiery JPP. EMT: 2016. Cell 2016. https://doi.org/10.1016/j.cell.2016.06.028.

[115] Beerling E, Seinstra D, de Wit E, Kester L, van der Velden D, Maynard C, et al. Plasticity between Epithelial and Mesenchymal States Unlinks EMT from Metastasis-Enhancing Stem Cell Capacity. Cell Rep 2016. https://doi.org/10.1016/j.celrep.2016.02.034.

[116] Pattabiraman DR, Bierie B, Kober KI, Thiru P, Krall JA, Zill C, et al. Activation of PKA leads to mesenchymal-to-epithelial transition and loss of tumor-initiating ability. Science (80-) 2016. https://doi.org/10.1126/science.aad3680.

[117] Chen W, Dong J, Haiech J, Kilhoffer MC, Zeniou M. Cancer stem cell quiescence and plasticity as major challenges in cancer therapy. Stem Cells Int 2016. https://doi.org/10.1155/2016/1740936.

[118] Begicevic RR, Falasca M. ABC transporters in cancer stem cells: Beyond chemoresistance. Int J Mol Sci 2017. https://doi.org/10.3390/ijms18112362.

[119] Goodell MA, Brose K, Paradis G, Conner AS, Mulligan RC. Isolation and functional

properties of murine hematopoietic stem cells that are replicating in vivo. J Exp Med 1996. https://doi.org/10.1084/jem.183.4.1797.

[120] Goodell MA, Rosenzweig M, Kim H, Marks DF, Demaria M, Paradis G, et al. Dye efflux studies suggest that hematopoietic stem cells expressing low or undetectable levels of CD34 antigen exist in multiple species. Nat Med 1997. https://doi.org/10.1038/nm1297-1337.

[121] Wu C, Alman BA. Side population cells in human cancers. Cancer Lett 2008. https://doi.org/10.1016/j.canlet.2008.03.048.

[122] Raha D, Wilson TR, Peng J, Peterson D, Yue P, Evangelista M, et al. The cancer stem cell marker aldehyde dehydrogenase is required to maintain a drug-tolerant tumor cell subpopulation. Cancer Res 2014;74:3579–90. https://doi.org/10.1158/0008-5427.

[123] Cojoc M, Mäbert K, Muders MH, Dubrovska A. A role for cancer stem cells in therapy resistance: Cellular and molecular mechanisms. Semin Cancer Biol 2015. https://doi.org/10.1016/j.semcancer.2014.06.004.

[124] Prieto-Vila M, Takahashi RU, Usuba W, Kohama I, Ochiya T. Drug resistance driven by cancer stem cells and their niche. Int J Mol Sci 2017. https://doi.org/10.3390/ijms18122574.

[125] Peitzsch C, Kurth I, Kunz-Schughart L, Baumann M, Dubrovska A. Discovery of the cancer stem cell related determinants of radioresistance. Radiother Oncol 2013. https://doi.org/10.1016/j.radonc.2013.06.003.

[126] Yun CW, Lee SH. The roles of autophagy in cancer. Int J Mol Sci 2018. https://doi.org/10.3390/ijms19113466.

[127] Das B, Tsuchida R, Malkin D, Koren G, Baruchel S, Yeger H. Hypoxia Enhances Tumor Stemness by Increasing the Invasive and Tumorigenic Side Population Fraction. Stem Cells 2008. https://doi.org/10.1634/stemcells.2007-0724.

[128] Majmundar AJ, Wong WJ, Simon MC. Hypoxia-Inducible Factors and the Response to Hypoxic Stress. Mol Cell 2010. https://doi.org/10.1016/j.molcel.2010.09.022.

[129] Almog N. Molecular mechanisms underlying tumor dormancy. Cancer Lett 2010. https://doi.org/10.1016/j.canlet.2010.03.004.

[130] Li X shan, Xu Q, Fu X yang, Luo W sheng. ALDH1A1 overexpression is associated with the progression and prognosis in gastric cancer. BMC Cancer 2014. https://doi.org/10.1186/1471-2407-14-705.

[131] Clark DW, Palle K. Aldehyde dehydrogenases in cancer stem cells: Potential as therapeutic targets. Ann Transl Med 2016. https://doi.org/10.21037/atm.2016.11.82.

[132] Phi LTH, Sari IN, Yang YG, Lee SH, Jun N, Kim KS, et al. Cancer stem cells (CSCs) in drug resistance and their therapeutic implications in cancer treatment. Stem Cells Int 2018. https://doi.org/10.1155/2018/5416923.

[133] Rausch V, Liu L, Apel A, Rettig T, Gladkich J, Labsch S, et al. Autophagy mediates survival of pancreatic tumour-initiating cells in a hypoxic microenvironment. J Pathol

2012. https://doi.org/10.1002/path.3994.

[134] Bao B, Ali S, Ahmad A, Azmi AS, Li Y, Banerjee S, et al. Hypoxia-Induced Aggressiveness of Pancreatic Cancer Cells Is Due to Increased Expression of VEGF, IL-6 and miR-21, Which Can Be Attenuated by CDF Treatment. PLoS One 2012. https://doi.org/10.1371/journal.pone.0050165.

[135] Yamashina T, Baghdadi M, Yoneda A, Kinoshita I, Suzu S, Dosaka-Akita H, et al. Cancer stem-like cells derived from chemoresistant tumors have a unique capacity to prime tumorigenic myeloid cells. Cancer Res 2014. https://doi.org/10.1158/0008-5472.CAN-13-2169.

[136] McDonald OG, Wu H, Timp W, Doi A, Feinberg AP. Genome-scale epigenetic reprogramming during epithelial-to-mesenchymal transition. Nat Struct Mol Biol 2011. https://doi.org/10.1038/nsmb.2084.

[137] Ferretti R, Bhutkar A, McNamara MC, Lees JA. BMI1 induces an invasive signature in melanoma that promotes metastasis and chemoresistance. Genes Dev 2016. https://doi.org/10.1101/gad.267757.115.

[138] Kim SH, Joshi K, Ezhilarasan R, Myers TR, Siu J, Gu C, et al. EZH2 protects Glioma stem cells from radiation-induced cell death in a MELK/FOXM1-dependent manner. Stem Cell Reports 2015. https://doi.org/10.1016/j.stemcr.2014.12.006.

[139] Zhang B, Strauss AC, Chu S, Li M, Ho Y, Shiang KD, et al. Effective Targeting of Quiescent Chronic Myelogenous Leukemia Stem Cells by Histone Deacetylase Inhibitors in Combination with Imatinib Mesylate. Cancer Cell 2010. https://doi.org/10.1016/j.ccr.2010.03.011.

[140] Zabierowski SE, Herlyn M. Melanoma stem cells: The dark seed of melanoma. J Clin Oncol 2008. https://doi.org/10.1200/JCO.2007.15.5465.

[141] Visvader JE, Lindeman GJ. Cancer stem cells in solid tumours: Accumulating evidence and unresolved questions. Nat Rev Cancer 2008. https://doi.org/10.1038/nrc2499.

[142] Lapidot T, Sirard C, Vormoor J, Murdoch B, Hoang T, Caceres-Cortes J, et al. A cell initiating human acute myeloid leukaemia after transplantation into SCID mice. Nature 1994. https://doi.org/10.1038/367645a0.

[143] Hurt EM, Kawasaki BT, Klarmann GJ, Thomas SB, Farrar WL. CD44+CD24- prostate cells are early cancer progenitor/stem cells that provide a model for patients with poor prognosis. Br J Cancer 2008. https://doi.org/10.1038/sj.bjc.6604242.

[144] Huang EH, Hynes MJ, Zhang T, Ginestier C, Dontu G, Appelman H, et al. Aldehyde dehydrogenase 1 is a marker for normal and malignant human colonic stem cells (SC) and tracks SC overpopulation during colon tumorigenesis. Cancer Res 2009. https://doi.org/10.1158/0008-5472.CAN-08-4418.

[145] Ginestier C, Hur MH, Charafe-Jauffret E, Monville F, Dutcher J, Brown M, et al. ALDH1 Is a Marker of Normal and Malignant Human Mammary Stem Cells and a Predictor of Poor Clinical Outcome. Cell Stem Cell 2007. https://doi.org/10.1016/j.stem.2007.08.014.

[146] Feng J, Qi Q, Khanna A, Todd NW, Deepak J, Lingxiao X, et al. Aldehyde dehydrogenase 1 is a tumor stem cell-Associated marker in lung cancer. Mol Cancer Res 2009. https://doi.org/10.1158/1541-7786.MCR-08-0393.

[147] Moserle L, Ghisi M, Amadori A, Indraccolo S. Side population and cancer stem cells: Therapeutic implications. Cancer Lett 2010. https://doi.org/10.1016/j.canlet.2009.05.020.

[148] Tirino V, Desiderio V, Paino F, De Rosa A, Papaccio F, La Noce M, et al. Cancer stem cells in solid tumors: An overview and new approaches for their isolation and characterization. FASEB J 2013;27:13–24. https://doi.org/10.1096/fj.12-218222.

[149] Roy Choudhury A, Gupta S, Chaturvedi PK, Kumar N, Pandey D. Mechanobiology of Cancer Stem Cells and Their Niche. Cancer Microenviron 2019. https://doi.org/10.1007/s12307-019-00222-4.

[150] Zhang W, Kai K, Choi DS, Iwamoto T, Nguyen YH, Wong H, et al. Microfluidics separation reveals the stem-cell-like deformability of tumor-initiating cells. Proc Natl Acad Sci U S A 2012. https://doi.org/10.1073/pnas.1209893109.

[151] Zhang Y, Wu M, Han X, Wang P, Qin L. High-Throughput, Label-Free Isolation of Cancer Stem Cells on the Basis of Cell Adhesion Capacity. Angew Chemie - Int Ed 2015. https://doi.org/10.1002/anie.201505294.

[152] Etzrodt M, Endele M, Schroeder T. Quantitative single-cell approaches to stem cell research. Cell Stem Cell 2014. https://doi.org/10.1016/j.stem.2014.10.015.

[153] Skylaki S, Hilsenbeck O, Schroeder T. Challenges in long-term imaging and quantification of single-cell dynamics. Nat Biotechnol 2016. https://doi.org/10.1038/nbt.3713.

[154] Hou Y, Guo H, Cao C, Li X, Hu B, Zhu P, et al. Single-cell triple omics sequencing reveals genetic, epigenetic, and transcriptomic heterogeneity in hepatocellular carcinomas. Cell Res 2016. https://doi.org/10.1038/cr.2016.23.

[155] Suhail Y, Cain MP, Vanaja K, Kurywchak PA, Levchenko A, Kalluri R, et al. Systems Biology of Cancer Metastasis. Cell Syst 2019. https://doi.org/10.1016/j.cels.2019.07.003.

[156] Brinckerhoff CE. Cancer Stem Cells (CSCs) in melanoma: There's smoke, but is there fire? J Cell Physiol 2017. https://doi.org/10.1002/jcp.25796.

[157] Kumar D, Gorain M, Kundu G, Kundu GC. Therapeutic implications of cellular and molecular biology of cancer stem cells in melanoma. Mol Cancer 2017. https://doi.org/10.1186/s12943-016-0578-3.

[158] La Porta C. Cancer stem cells: Lessons from melanoma. Stem Cell Rev Reports 2009. https://doi.org/10.1007/s12015-008-9048-7.

[159] Lang D, Mascarenhas JB, Shea CR. Melanocytes, melanocyte stem cells, and melanoma stem cells. Clin Dermatol 2013. https://doi.org/10.1016/j.clindermatol.2012.08.014.

[160] Grasso C, Anaka M, Hofmann O, Sompallae R, Broadley K, Hide W, et al. Iterative sorting reveals CD133+ and CD133- melanoma cells as phenotypically distinct populations. BMC Cancer 2016. https://doi.org/10.1186/s12885-016-2759-2.

[161] Guanziroli E, Venegoni L, Fanoni D, Cavicchini S, Coggi A, Ferrero S, et al. Immunohistochemical expression and prognostic role of CD10, CD271 and Nestin in primary and recurrent cutaneous melanoma. Immunohistochem Expr Progn Role CD10, CD271 Nestin Prim Recurr Cutan Melanoma 2018. https://doi.org/10.23736/S0392-0488.18.06145-X.

[162] Nielsen PS, Riber-Hansen R, Steiniche T. Immunohistochemical CD271 expression correlates with melanoma progress in a case-control study. Pathology 2018. https://doi.org/10.1016/j.pathol.2017.12.340.

[163] Jang JW, Song Y, Kim SH, Kim J, Seo HR. Potential mechanisms of CD133 in cancer stem cells. Life Sci 2017. https://doi.org/10.1016/j.lfs.2017.07.008.

[164] Sharma BK, Manglik V, Elias EG. Immuno-expression of human melanoma stem cell markers in tissues at different stages of the disease. J Surg Res 2010. https://doi.org/10.1016/j.jss.2010.03.043.

[165] Wang S, Tang L, Lin J, Shen Z, Yao Y, Wang W, et al. ABCB5 promotes melanoma metastasis through enhancing NF-κB p65 protein stability. Biochem Biophys Res Commun 2017. https://doi.org/10.1016/j.bbrc.2017.08.052.

[166] Monzani E, Facchetti F, Galmozzi E, Corsini E, Benetti A, Cavazzin C, et al. Melanoma contains CD133 and ABCG2 positive cells with enhanced tumourigenic potential. Eur J Cancer 2007. https://doi.org/10.1016/j.ejca.2007.01.017.

[167] Luo Y, Nguyen N, Fujita M. Isolation of human melanoma stem cells UNIT 3.8 using ALDH as a marker. Curr Protoc Stem Cell Biol 2013. https://doi.org/10.1002/9780470151808.sc0308s26.

[168] Biomarker Working Group F-N. FDA-NIH Biomarker Working Group. BEST (Biomarkers, EndpointS, and other Tools). Silver Sprig (MD) 2016.

[169] Califf RM. Biomarker definitions and their applications. Exp Biol Med 2018. https://doi.org/10.1177/1535370217750088.

[170] Belter B, Haase-Kohn C, Pietzsch J. Biomarkers in Malignant Melanoma: Recent Trends and Critical Perspective. Cutan. Melanoma Etiol. Ther., 2017, p. 39–56. https://doi.org/10.15586/codon.cutaneousmelanoma.2017.ch3.

[171] Davis LE, Shalin SC, Tackett AJ. Current state of melanoma diagnosis and treatment. Cancer Biol Ther 2019. https://doi.org/10.1080/15384047.2019.1640032.

[172] Pantel K, Alix-Panabières C. Real-time liquid biopsy in cancer patients: Fact or fiction? Cancer Res 2013;73:6384–8. https://doi.org/10.1158/0008-5472.CAN-13-2030.

[173] Vereecken P, Cornelis F, Van Baren N, Vandersleyen V, Baurain JF. A synopsis of serum biomarkers in cutaneous melanoma patients. Dermatol Res Pract 2012. https://doi.org/10.1155/2012/260643.

[174] Pinzani P, D'Argenio V, Del Re M, Pellegrini C, Cucchiara F, Salvianti F, et al. Updates on liquid biopsy: Current trends and future perspectives for clinical application in solid tumors. Clin Chem Lab Med 2021. https://doi.org/10.1515/cclm-2020-1685.

[175] Martins I, Ribeiro IP, Jorge J, Gonçalves AC, Sarmento-Ribeiro AB, Melo JB, et al. Liquid Biopsies: Applications for Cancer Diagnosis and Monitoring. Genes (Basel) 2021;12:349. https://doi.org/10.3390/genes12030349.

[176] Patelli G, Vaghi C, Tosi F, Mauri G, Amatu A, Massihnia D, et al. Liquid Biopsy for Prognosis and Treatment in Metastatic Colorectal Cancer: Circulating Tumor Cells vs Circulating Tumor DNA. Target Oncol 2021. https://doi.org/10.1007/s11523-021-00795-5.

[177] Couraud S, Vaca-Paniagua F, Villar S, Oliver J, Schuster T, Blanché H, et al. Noninvasive diagnosis of actionable mutations by deep sequencing of circulating free DNA in lung cancer from never-smokers: a proof-of-concept study from BioCAST/IFCT-1002. Clin Cancer Res 2014;20:4613–24. https://doi.org/10.1158/1078-0432.CCR-13-3063.

[178] Mian S, Ugurel S, Parkinson E, Schlenzka I, Dryden I, Lancashire L, et al. Serum proteomic fingerprinting discriminates between clinical stages and predicts disease progression in melanoma patients. J Clin Oncol 2005;23:5088–93. https://doi.org/10.1200/JCO.2005.03.164.

[179] Drabovich AP, Pavlou MP, Batruch I, Diamandis EP. Proteomic and mass spectrometry technologies for biomarker discovery. Proteomic Metabolomic Approaches to Biomark. Discov., 2019, p. 17–37. https://doi.org/10.1016/B978-0-12-818607-7.00002-5.

[180] Matharoo-Ball B, Ratcliffe L, Lancashire L, Ugurel S, Miles AK, Weston DJ, et al. Diagnostic biomarkers differentiating metastatic melanoma patients from healthy controls identified by an integrated MALDI-TOF mass spectrometry/bioinformatic approach. Proteomics - Clin Appl 2007;1:605–20. https://doi.org/10.1002/prca.200700022.

[181] Lim SY, Lee JH, Welsh SJ, Ahn SB, Breen E, Khan A, et al. Evaluation of two high-throughput proteomic technologies for plasma biomarker discovery in immunotherapy-treated melanoma patients. Biomark Res 2017;5. https://doi.org/10.1186/s40364-017-0112-9.

[182] Calapre L, Warburton L, Millward M, Ziman M, Gray ES. Circulating tumour DNA (ctDNA) as a liquid biopsy for melanoma. Cancer Lett 2017;404:62–9. https://doi.org/10.1016/j.canlet.2017.06.030.

[183] Gray ES, Rizos H, Reid AL, Boyd SC, Pereira MR, Lo J, et al. Circulating tumor DNA to monitor treatment response and detect acquired resistance in patients with metastatic melanoma. Oncotarget 2015;6:42008–18. https://doi.org/10.18632/oncotarget.5788.

[184] Wouters J, Vizoso M, Martinez-Cardus A, Carmona FJ, Govaere O, Laguna T, et al. Comprehensive DNA methylation study identifies novel progression-related and prognostic markers for cutaneous melanoma. BMC Med 2017;15. https://doi.org/10.1186/s12916-017-0851-3.

[185] Aftab MN, Dinger ME, Perera RJ. The role of microRNAs and long non-coding RNAs in the pathology, diagnosis, and management of melanoma. Arch Biochem Biophys 2014;563:60–70. https://doi.org/10.1016/j.abb.2014.07.022.

[186] Fattore L, Costantini S, Malpicci D, Ruggiero CF, Ascierto PA, Croce CM, et al. MicroRNAs in melanoma development and resistance to target therapy. Oncotarget

2017;8:22262–78. https://doi.org/10.18632/oncotarget.14763.

[187] Isola AL, Eddy K, Chen S. Biology, therapy and implications of tumor exosomes in the progression of melanoma. Cancers (Basel) 2016;8:110. https://doi.org/10.3390/cancers8120110.

[188] Pfeffer S, Grossmann K, Cassidy P, Yang C, Fan M, Kopelovich L, et al. Detection of Exosomal miRNAs in the Plasma of Melanoma Patients. J Clin Med 2015;4:2012–27. https://doi.org/10.3390/jcm4121957.

[189] Hida T, Yoneta A, Wakamatsu K, Yanagisawa K, Ishii-Osai Y, Kan Y, et al. Circulating melanoma cells as a potential biomarker to detect metastasis and evaluate prognosis. Australas J Dermatol 2016;57:145–9. https://doi.org/10.1111/ajd.12455.

[190] Martens A, Wistuba-Hamprecht K, Foppen MG, Yuan J, Postow MA, Wong P, et al. Baseline peripheral blood biomarkers associated with clinical outcome of advanced melanoma patients treated with ipilimumab. Clin Cancer Res 2016;22:2908–18. https://doi.org/10.1158/1078-0432.CCR-15-2412.

[191] Balch CM, Gershenwald JE, Soong SJ, Thompson JF, Atkins MB, Byrd DR, et al. Final version of 2009 AJCC melanoma staging and classification. J Clin Oncol 2009. https://doi.org/10.1200/JCO.2009.23.4799.

[192] Agarwala SS, Keilholz U, Gilles E, Bedikian AY, Wu J, Kay R, et al. LDH correlation with survival in advanced melanoma from two large, randomised trials (Oblimersen GM301 and EORTC 18951). Eur J Cancer 2009. https://doi.org/10.1016/j.ejca.2009.04.016.

[193] Long G V., Grob JJ, Nathan P, Ribas A, Robert C, Schadendorf D, et al. Factors predictive of response, disease progression, and overall survival after dabrafenib and trametinib combination treatment: a pooled analysis of individual patient data from randomised trials. Lancet Oncol 2016. https://doi.org/10.1016/S1470-2045(16)30578-2.

[194] Diem S, Kasenda B, Martin-Liberal J, Lee A, Chauhan D, Gore M, et al. Prognostic score for patients with advanced melanoma treated with ipilimumab. Eur J Cancer 2015. https://doi.org/10.1016/j.ejca.2015.09.007.

[195] Tetta C, Ghigo E, Silengo L, Deregibus MC, Camussi G. Extracellular vesicles as an emerging mechanism of cell-to-cell communication. Endocrine 2013;44:11–9. https://doi.org/10.1007/s12020-012-9839-0.

[196] Kalluri R, LeBleu VS. The biology, function, and biomedical applications of exosomes. Science (80-) 2020;367. https://doi.org/10.1126/science.aau6977.

[197] Kowal J, Tkach M, Théry C. Biogenesis and secretion of exosomes. Curr Opin Cell Biol 2014;29:116–25. https://doi.org/10.1016/j.ceb.2014.05.004.

[198] Thery C, Witwer K, Aikawa E, Jose Alcaraz M, Anderson J, Andriantsitohaina R, et al. Minimal information for studies of extracellular vesicles 2018 (MISEV2018). J Extracell Vesicles 2018;7:1535750:1–47.

[199] Colombo M, Raposo G, Théry C. Biogenesis, Secretion, and Intercellular Interactions of

Exosomes and Other Extracellular Vesicles. Annu Rev Cell Dev Biol 2014;30:255–89. https://doi.org/10.1146/annurev-cellbio-101512-122326.

[200] van Niel G, D'Angelo G, Raposo G. Shedding light on the cell biology of extracellular vesicles. Nat Rev Mol Cell Biol 2018. https://doi.org/10.1038/nrm.2017.125.

[201] Mathivanan S, Fahner CJ, Reid GE, Simpson RJ. ExoCarta 2012: Database of exosomal proteins, RNA and lipids. Nucleic Acids Res 2012;40. https://doi.org/10.1093/nar/gkr828.

[202] Hood JL. Natural melanoma-derived extracellular vesicles. Semin Cancer Biol 2019;59:251–65. https://doi.org/10.1016/j.semcancer.2019.06.020.

[203] Vaiselbuh SR. Exosomes in Cancer Research. Cancer Res Front 2015;1:11–24. https://doi.org/10.17980/2015.11.

[204] Hernández-Barranco A, Nogués L, Peinado H. Could Extracellular Vesicles Contribute to Generation or Awakening of "Sleepy" Metastatic Niches? Front Cell Dev Biol 2021;9. https://doi.org/10.3389/fcell.2021.625221.

[205] Peinado H, Lavotshkin S, Lyden D. The secreted factors responsible for pre-metastatic niche formation: Old sayings and new thoughts. Semin Cancer Biol 2011;21:139–46. https://doi.org/10.1016/j.semcancer.2011.01.002.

[206] Wendler F, Favicchio R, Simon T, Alifrangis C, Stebbing J, Giamas G. Extracellular vesicles swarm the cancer microenvironment: From tumor-stroma communication to drug intervention. Oncogene 2017;36:877–84. https://doi.org/10.1038/onc.2016.253.

[207] Lindoso RS, Collino F, Vieyra A. Extracellular vesicles as regulators of tumor fate: Crosstalk among cancer stem cells, tumor cells and mesenchymal stem cells. Stem Cell Investig 2017;4. https://doi.org/10.21037/sci.2017.08.08.

[208] Hood JL, San Roman S, Wickline SA. Exosomes released by melanoma cells prepare sentinel lymph nodes for tumor metastasis. Cancer Res 2011;71:3792–801. https://doi.org/10.1158/0008-5472.CAN-10-4455.

[209] Peinado H, Alečković M, Lavotshkin S, Matei I, Costa-Silva B, Moreno-Bueno G, et al. Melanoma exosomes educate bone marrow progenitor cells toward a pro-metastatic phenotype through MET. Nat Med 2012;18:883–91. https://doi.org/10.1038/nm.2753.

[210] Xiao D, Barry S, Kmetz D, Egger M, Pan J, Rai SN, et al. Melanoma cell-derived exosomes promote epithelial-mesenchymal transition in primary melanocytes through paracrine/autocrine signaling in the tumor microenvironment. Cancer Lett 2016;376:318–27. https://doi.org/10.1016/j.canlet.2016.03.050.

[211] Plebanek MP, Angeloni NL, Vinokour E, Li J, Henkin A, Martinez-Marin D, et al. Pre-metastatic cancer exosomes induce immune surveillance by patrolling monocytes at the metastatic niche. Nat Commun 2017. https://doi.org/10.1038/s41467-017-01433-3.

[212] Peinado H. Melanoma exosomes educate bone marrow progenitor cells. Nat Med 2013;18:883–91.

[213] Felicetti F, De Feo A, Coscia C, Puglisi R, Pedini F, Pasquini L, et al. Exosome-mediated transfer of miR-222 is sufficient to increase tumor malignancy in melanoma. J Transl Med

2016;14. https://doi.org/10.1186/s12967-016-0811-2.

[214] Boukouris S, Mathivanan S. Exosomes in bodily fluids are a highly stable resource of disease biomarkers. Proteomics - Clin Appl 2015;9:358–67. https://doi.org/10.1002/prca.201400114.

[215] Alegre E, Zubiri L, Perez-Gracia JL, González-Cao M, Soria L, Martín-Algarra S, et al. Circulating melanoma exosomes as diagnostic and prognosis biomarkers. Clin Chim Acta 2016;454:28–32. https://doi.org/10.1016/j.cca.2015.12.031.

[216] Hoshino A, Costa-Silva B, Shen TL, Rodrigues G, Hashimoto A, Tesic Mark M, et al. Tumour exosome integrins determine organotropic metastasis. Nature 2015;527:329–35. https://doi.org/10.1038/nature15756.

[217] Altadill T, Campoy I, Lanau L, Gill K, Rigau M, Gil-Moreno A, et al. Enabling metabolomics based biomarker discovery studies using molecular phenotyping of exosome-like vesicles. PLoS One 2016;11. https://doi.org/10.1371/journal.pone.0151339.

[218] Bonhoure A, Henry L, Morille M, Aissaoui N, Bellot G, Stoebner PE, et al. Exosomal melanotransferrin as a potential biomarker for metastatic melanoma. BioRxiv 2020. https://doi.org/10.1101/2020.11.09.373852.

[219] He X, Park S, Chen Y, Lee H. Extracellular Vesicle-Associated miRNAs as a Biomarker for Lung Cancer in Liquid Biopsy. Front Mol Biosci 2021;8. https://doi.org/10.3389/fmolb.2021.630718.

[220] Beger RD, Dunn W, Schmidt MA, Gross SS, Kirwan JA, Cascante M, et al. Metabolomics enables precision medicine: "A White Paper, Community Perspective." Metabolomics 2016. https://doi.org/10.1007/s11306-016-1094-6.

[221] Xia J, Broadhurst DI, Wilson M, Wishart DS. Translational biomarker discovery in clinical metabolomics: An introductory tutorial. Metabolomics 2013;9:280–99. https://doi.org/10.1007/s11306-012-0482-9.

[222] Schrimpe-Rutledge AC, Codreanu SG, Sherrod SD, McLean JA. Untargeted Metabolomics Strategies—Challenges and Emerging Directions. J Am Soc Mass Spectrom 2016. https://doi.org/10.1007/s13361-016-1469-y.

[223] Menyhárt O, Győrffy B. Multi-omics approaches in cancer research with applications in tumor subtyping, prognosis, and diagnosis. Comput Struct Biotechnol J 2021;19:949–60. https://doi.org/10.1016/j.csbj.2021.01.009.

[224] Cajka T, Fiehn O. Toward Merging Untargeted and Targeted Methods in Mass Spectrometry-Based Metabolomics and Lipidomics. Anal Chem 2016;88:524–45. https://doi.org/10.1021/acs.analchem.5b04491.

[225] Klassen A, Faccio AT, Canuto GAB, da Cruz PLR, Ribeiro HC, Tavares MFM, et al. Metabolomics: Definitions and significance in systems biology. Adv. Exp. Med. Biol., 2017. https://doi.org/10.1007/978-3-319-47656-8_1.

[226] Pitt JJ. Principles and applications of liquid chromatography-mass spectrometry in clinical biochemistry. Clin Biochem Rev 2009.

[227] Liang L, Sun F, Wang H, Hu Z. Metabolomics, metabolic flux analysis and cancer pharmacology. Pharmacol Ther 2021;224:107827. https://doi.org/10.1016/j.pharmthera.2021.107827.

[228] Ren Z, Rajani C, Jia W. The Distinctive Serum Metabolomes of Gastric, Esophageal and Colorectal Cancers. Cancers (Basel) 2021;13:720. https://doi.org/10.3390/cancers13040720.

[229] Donnelly D, Aung PP, Jour G. The "-OMICS" facet of melanoma: Heterogeneity of genomic, proteomic and metabolomic biomarkers. Semin Cancer Biol 2019;59:165–74. https://doi.org/10.1016/j.semcancer.2019.06.014.

[230] Abaffy T, Möller MG, Riemer DD, Milikowski C, DeFazio RA. Comparative analysis of volatile metabolomics signals from melanoma and benign skin: A pilot study. Metabolomics 2013;9:998–1008. https://doi.org/10.1007/s11306-013-0523-z.

[231] Santana-Filho AP De, Jacomasso T, Riter DS, Barison A, Iacomini M, Winnischofer SMB, et al. NMR metabolic fingerprints of murine melanocyte and melanoma cell lines: Application to biomarker discovery. Sci Rep 2017;7. https://doi.org/10.1038/srep42324.

[232] Bayci AWL, Baker DA, Somerset AE, Turkoglu O, Hothem Z, Callahan RE, et al. Metabolomic identification of diagnostic serum-based biomarkers for advanced stage melanoma. Metabolomics 2018;14. https://doi.org/10.1007/s11306-018-1398-9.

[233] Kosmopoulou M, Giannopoulou AF, Iliou A, Benaki D, Panagiotakis A, Velentzas AD, et al. Human melanoma-cell metabolic profiling: Identification of novel biomarkers indicating metastasis. Int J Mol Sci 2020. https://doi.org/10.3390/ijms21072436.

[234] Taylor NJ, Gaynanova I, Eschrich SA, Welsh EA, Garrett TJ, Beecher C, et al. Metabolomics of primary cutaneous melanoma and matched adjacent extratumoral microenvironment. PLoS One 2020. https://doi.org/10.1371/journal.pone.0240849.

[235] Jiménez G, Hackenberg M, Catalina P, Boulaiz H, Griñán-Lisón C, García MÁ, et al. Mesenchymal stem cell's secretome promotes selective enrichment of cancer stem-like cells with specific cytogenetic profile. Cancer Lett 2018;429:78–88. https://doi.org/10.1016/j.canlet.2018.04.042.

[236] Morata-Tarifa C, Jiménez G, García MA, Entrena JM, Griñán-Lisón C, Aguilera M, et al. Low adherent cancer cell subpopulations are enriched in tumorigenic and metastatic epithelial-to-mesenchymal transition-induced cancer stem-like cells. Sci Rep 2016;6. https://doi.org/10.1038/srep18772.

[237] Shimoda M, Ota M, Okada Y. Isolation of cancer stem cells by side population method. Methods Mol. Biol., vol. 1692, 2018, p. 49–59. https://doi.org/10.1007/978-1-4939-7401-6_5.

[238] Costa-Silva B, Aiello NM, Ocean AJ, Singh S, Zhang H, Thakur BK, et al. Pancreatic cancer exosomes initiate pre-metastatic niche formation in the liver. Nat Cell Biol 2015;17:816–26. https://doi.org/10.1038/ncb3169.

[239] García-Fontana B, Morales-Santana S, Díaz Navarro C, Rozas-Moreno P, Genilloud O, Vicente Pérez F, et al. Metabolomic profile related to cardiovascular disease in patients

with type 2 diabetes mellitus: A pilot study. Talanta 2016;148:135–43. https://doi.org/10.1016/j.talanta.2015.10.070.

[240] Xia J, Wishart DS. Web-based inference of biological patterns, functions and pathways from metabolomic data using MetaboAnalyst. Nat Protoc 2011;6:743–60. https://doi.org/10.1038/nprot.2011.319.

[241] Godzien J, Ciborowski M, Angulo S, Barbas C. From numbers to a biological sense: How the strategy chosen for metabolomics data treatment may affect final results. A practical example based on urine fingerprints obtained by LC-MS. Electrophoresis 2013;34:2812–26. https://doi.org/10.1002/elps.201300053.

[242] Obuchowski NA, Lieber ML, Wians FH. ROC curves in Clinical Chemistry: Uses, misuses, and possible solutions. Clin Chem 2004;50:1118–25. https://doi.org/10.1373/clinchem.2004.031823.

[243] Schatton T, Murphy GF, Frank NY, Yamaura K, Waaga-Gasser AM, Gasser M, et al. Identification of cells initiating human melanomas. Nature 2008;451:345–9. https://doi.org/10.1038/nature06489.

[244] Civenni G, Walter A, Kobert N, Mihic-Probst D, Zipser M, Belloni B, et al. Human CD271-positive melanoma stem cells associated with metastasis establish tumor heterogeneity and long-term growth. Cancer Res 2011;71:3098–109. https://doi.org/10.1158/0008-5472.CAN-10-3997.

[245] Lim SY, Lee JH, Diefenbach RJ, Kefford RF, Rizos H. Liquid biomarkers in melanoma: Detection and discovery. Mol Cancer 2018;17. https://doi.org/10.1186/s12943-018-0757-5.

[246] Melo SA, Luecke LB, Kahlert C, Fernandez AF, Gammon ST, Kaye J, et al. Glypican-1 identifies cancer exosomes and detects early pancreatic cancer. Nature 2015;523:177–82. https://doi.org/10.1038/nature14581.

[247] Lener T, Gimona M, Aigner L, Börger V, Buzas E, Camussi G, et al. Applying extracellular vesicles based therapeutics in clinical trials - An ISEV position paper. J Extracell Vesicles 2015;4. https://doi.org/10.3402/jev.v4.30087.

[248] Dunn WB, Broadhurst DI, Atherton HJ, Goodacre R, Griffin JL. Systems level studies of mammalian metabolomes: the roles of mass spectrometry and nuclear magnetic resonance spectroscopy. Chem Soc Rev 2011;40:387–426. https://doi.org/10.1039/B906712B.

[249] Kind T, Fiehn O. Seven Golden Rules for heuristic filtering of molecular formulas obtained by accurate mass spectrometry. BMC Bioinformatics 2007. https://doi.org/10.1186/1471-2105-8-105.

[250] Xi B, Gu H, Baniasadi H, Raftery D. Statistical analysis and modeling of mass spectrometry-based metabolomics data. Methods Mol Biol 2014;1198:333–53. https://doi.org/10.1007/978-1-4939-1258-2_22.

[251] Keller S, Ridinger J, Rupp AK, Janssen JWG, Altevogt P. Body fluid derived exosomes as a novel template for clinical diagnostics. J Transl Med 2011;9. https://doi.org/10.1186/1479-5876-9-86.

[252] Al-Nedawi K, Meehan B, Rak J. Microvesicles: Messengers and mediators of tumor progression. Cell Cycle 2009;8:2014–8. https://doi.org/10.4161/cc.8.13.8988.

[253] Piccin A, Murphy WG, Smith OP. Circulating microparticles: pathophysiology and clinical implications. Blood Rev 2007;21:157–71. https://doi.org/10.1016/j.blre.2006.09.001.

[254] Doyle L, Wang M. Overview of Extracellular Vesicles, Their Origin, Composition, Purpose, and Methods for Exosome Isolation and Analysis. Cells 2019;8:727. https://doi.org/10.3390/cells8070727.

[255] Haraszti RA, Didiot MC, Sapp E, Leszyk J, Shaffer SA, Rockwell HE, et al. High-resolution proteomic and lipidomic analysis of exosomes and microvesicles from different cell sources. J Extracell Vesicles 2016;5. https://doi.org/10.3402/jev.v5.32570.

[256] Skotland T, Ekroos K, Kauhanen D, Simolin H, Seierstad T, Berge V, et al. Molecular lipid species in urinary exosomes as potential prostate cancer biomarkers. Eur J Cancer 2017;70:122–32. https://doi.org/10.1016/j.ejca.2016.10.011.

[257] Ridger VC, Boulanger CM, Angelillo-Scherrer A, Badimon L, Blanc-Brude O, Bochaton-Piallat ML, et al. Microvesicles in vascular homeostasis and diseases position paper of the european society of cardiology (ESC) working group on atherosclerosis and vascular biology. Thromb Haemost 2017;117:1296–316. https://doi.org/10.1160/TH16-12-0943.

[258] Iero M, Valenti R, Huber V, Filipazzi P, Parmiani G, Fais S, et al. Tumour-released exosomes and their implications in cancer immunity. Cell Death Differ 2008;15:80–8. https://doi.org/10.1038/sj.cdd.4402237.

[259] Subra C, Grand D, Laulagnier K, Stella A, Lambeau G, Paillasse M, et al. Exosomes account for vesicle-mediated transcellular transport of activatable phospholipases and prostaglandins. J Lipid Res 2010;51:2105–20. https://doi.org/10.1194/jlr.M003657.

[260] Record M, Silvente-Poirot S, Poirot M, Wakelam MJO. Extracellular vesicles: Lipids as key components of their biogenesis and functions. J Lipid Res 2018;59:1316–24. https://doi.org/10.1194/jlr.E086173.

[261] Felicetti F, Parolini I, Bottero L, Fecchi K, Errico MC, Raggi C, et al. Caveolin-1 tumor-promoting role in human melanoma. Int J Cancer 2009;125:1514–22. https://doi.org/10.1002/ijc.24451.

[262] Xiao D, Ohlendorf J, Chen Y, Taylor DD, Rai SN, Waigel S, et al. Identifying mRNA, MicroRNA and Protein Profiles of Melanoma Exosomes. PLoS One 2012;7. https://doi.org/10.1371/journal.pone.0046874.

[263] Alamodi AA, Eshaq AM, Hassan S-Y, Al Hmada Y, El Jamal SM, Fothan AM, et al. Cancer stem cell as therapeutic target for melanoma treatment. Histol Histopathol 2016:11791. https://doi.org/10.14670/HH-11-791.

[264] Boiko AD, Razorenova O V., Van De Rijn M, Swetter SM, Johnson DL, Ly DP, et al. Human melanoma-initiating cells express neural crest nerve growth factor receptor CD271. Nature 2010;466:133–7. https://doi.org/10.1038/nature09161.

[265] Maan M, Peters JM, Dutta M, Patterson AD. Lipid metabolism and lipophagy in cancer.

Biochem Biophys Res Commun 2018;504:582–9. https://doi.org/10.1016/j.bbrc.2018.02.097.

[266] Beloribi-Djefaflia S, Vasseur S, Guillaumond F. Lipid metabolic reprogramming in cancer cells. Oncogenesis 2016;5:e189. https://doi.org/10.1038/oncsis.2015.49.

[267] Zhao Z, Xiao Y, Elson P, Tan H, Plummer SJ, Berk M, et al. Plasma lysophosphatidylcholine levels: Potential biomarkers for colorectal cancer. J Clin Oncol 2007;25:2696–701. https://doi.org/10.1200/JCO.2006.08.5571.

[268] Süllentrop F, Moka D, Neubauer S, Haupt G, Engelmann U, Hahn J, et al. 31P NMR spectroscopy of blood plasma: Determination and quantification of phospholipid classes in patients with renal cell carcinoma. NMR Biomed 2002;15:60–8. https://doi.org/10.1002/nbm.758.

[269] Kühn T, Floegel A, Sookthai D, Johnson T, Rolle-Kampczyk U, Otto W, et al. Higher plasma levels of lysophosphatidylcholine 18:0 are related to a lower risk of common cancers in a prospective metabolomics study. BMC Med 2016;14. https://doi.org/10.1186/s12916-016-0552-3.

[270] Zhou X, Mao J, Ai J, Deng Y, Roth MR, Pound C, et al. Identification of Plasma Lipid Biomarkers for Prostate Cancer by Lipidomics and Bioinformatics. PLoS One 2012;7. https://doi.org/10.1371/journal.pone.0048889.

[271] Sánchez-Martínez R, Cruz-Gil S, de Cedrón MG, Álvarez-Fernández M, Vargas T, Molina S, et al. A link between lipid metabolism and epithelial-mesenchymal transition provides a target for colon cancer therapy. Oncotarget 2015;6:38719–36. https://doi.org/10.18632/oncotarget.5340.

[272] Raynor A, Jantscheff P, Ross T, Schlesinger M, Wilde M, Haasis S, et al. Saturated and mono-unsaturated lysophosphatidylcholine metabolism in tumour cells: A potential therapeutic target for preventing metastases. Lipids Health Dis 2015;14. https://doi.org/10.1186/s12944-015-0070-x.

[273] Dong H, Xiao J, Zhu R, Liu B, Dong M, Luo D, et al. Serum sphingosine 1-phosphate in hepatocellular carcinoma patients is related to HBV infection. J BUON 2018.

[274] Melone MAB, Valentino A, Margarucci S, Galderisi U, Giordano A, Peluso G. The carnitine system and cancer metabolic plasticity review-article. Cell Death Dis 2018. https://doi.org/10.1038/s41419-018-0313-7.

[275] Jee SH, Kim M, Kim M, Yoo HJ, Kim H, Jung KJ, et al. Metabolomics profiles of hepatocellular carcinoma in a Korean prospective cohort: The Korean cancer prevention study-II. Cancer Prev Res 2018. https://doi.org/10.1158/1940-6207.CAPR-17-0249.

[276] Tian Y, Wang Z, Liu X, Duan J, Feng G, Yin Y, et al. Prediction of chemotherapeutic efficacy in non–small cell lung cancer by serum metabolomic profiling. Clin Cancer Res 2018. https://doi.org/10.1158/1078-0432.CCR-17-2855.

[277] Bandu R, Mok HJ, Kim KP. Phospholipids as cancer biomarkers: Mass spectrometry-based analysis. Mass Spectrom Rev 2018. https://doi.org/10.1002/mas.21510.

[278] Yang L, Cui X, Zhang N, Li M, Bai Y, Han X, et al. Comprehensive lipid profiling of plasma in patients with benign breast tumor and breast cancer reveals novel biomarkers. Anal Bioanal Chem 2015. https://doi.org/10.1007/s00216-015-8484-x.

[279] Waki M, Ide Y, Ishizaki I, Nagata Y, Masaki N, Sugiyama E, et al. Single-cell time-of-flight secondary ion mass spectrometry reveals that human breast cancer stem cells have significantly lower content of palmitoleic acid compared to their counterpart non-stem cancer cells. Biochimie 2014. https://doi.org/10.1016/j.biochi.2014.10.003.

[280] Tan B, Qiu Y, Zou X, Chen T, Xie G, Cheng Y, et al. Metabonomics identifies serum metabolite markers of colorectal cancer. J Proteome Res 2013. https://doi.org/10.1021/pr400337b.

[281] Wang B, Chen D, Chen Y, Hu Z, Cao M, Xie Q, et al. Metabonomic profiles discriminate hepatocellular carcinoma from liver cirrhosis by ultraperformance liquid chromatography-mass spectrometry. J Proteome Res 2012. https://doi.org/10.1021/pr2009252.

[282] Ono M, Handa K, Sonnino S, Withers DA, Nagai H, Hakomori SI. GM3 ganglioside inhibits CD9-facilitated haptotactic cell motility: Coexpression of GM3 and CD9 is essential in the downregulation of tumor cell motility and malignancy. Biochemistry 2001. https://doi.org/10.1021/bi0101998.

[283] Svedman FC, Pillas D, Taylor A, Kaur M, Linder R, Hansson J. Stage-specific survival and recurrence in patients with cutaneous malignant melanoma in Europe – A systematic review of the literature. Clin Epidemiol 2016. https://doi.org/10.2147/CLEP.S99021.

[284] Asiago VM, Alvarado LZ, Shanaiah N, Gowda GAN, Owusu-Sarfo K, Ballas RA, et al. Early detection of recurrent breast cancer using metabolite profiling. Cancer Res 2010. https://doi.org/10.1158/0008-5472.CAN-10-1319.

[285] Hu JD, Tang HQ, Zhang Q, Fan J, Hong J, Gu JZ, et al. Prediction of gastric cancer metastasis through urinary metabolomic investigation using GC/MS. World J Gastroenterol 2011. https://doi.org/10.3748/wjg.v17.i6.727.

[286] Hori S, Nishiumi S, Kobayashi K, Shinohara M, Hatakeyama Y, Kotani Y, et al. A metabolomic approach to lung cancer. Lung Cancer 2011. https://doi.org/10.1016/j.lungcan.2011.02.008.

[287] Zhang A, Sun H, Yan G, Wang P, Han Y, Wang X. Metabolomics in diagnosis and biomarker discovery of colorectal cancer. Cancer Lett 2014. https://doi.org/10.1016/j.canlet.2013.11.011.

[288] Holmes E, Wilson ID, Nicholson JK. Metabolic Phenotyping in Health and Disease. Cell 2008. https://doi.org/10.1016/j.cell.2008.08.026.

[289] Tulipani S, Llorach R, Urpi-Sarda M, Andres-Lacueva C. Comparative analysis of sample preparation methods to handle the complexity of the blood fluid metabolome: When less is more. Anal Chem 2013. https://doi.org/10.1021/ac302919t.

[290] Christie WW, Han X. Lipid Analysis: Isolation, Separation, Identification and Lipidomic Analysis: Fourth Edition. 2010. https://doi.org/10.1533/9780857097866.

[291] Cancer Research UK. Melanoma tests. Cancer Res UK 2014.

http://www.cancerresearchuk.org/about-cancer/type/melanoma/diagnosis/melanoma-tests.

[292] Eisenstein A, Gonzalez EC, Raghunathan R, Xu X, Wu M, McLean EO, et al. Emerging Biomarkers in Cutaneous Melanoma. Mol Diagnosis Ther 2018;22:203–18. https://doi.org/10.1007/s40291-018-0318-z.

[293] Mumford SL, Towler BP, Pashler AL, Gilleard O, Martin Y, Newbury SF. Circulating microRNA biomarkers in melanoma: Tools and challenges in personalised medicine. Biomolecules 2018;8. https://doi.org/10.3390/biom8020021.

[294] Frolkis A, Knox C, Lim E, Jewison T, Law V, Hau DD, et al. SMPDB: The small molecule pathway database. Nucleic Acids Res 2009. https://doi.org/10.1093/nar/gkp1002.

[295] Hazen SL. Oxidized phospholipids as endogenous pattern recognition ligands in innate immunity. J Biol Chem 2008. https://doi.org/10.1074/jbc.R700054200.

[296] Ashraf MZ, Kar NS, Podrez EA. Oxidized phospholipids: Biomarker for cardiovascular diseases. Int J Biochem Cell Biol 2009. https://doi.org/10.1016/j.biocel.2008.11.002.

[297] Tsuzura S, Ikeda Y, Suehiro T, Ota K, Osaki F, Arii K, et al. Correlation of plasma oxidized low-density lipoprotein levels to vascular complications and human serum paraoxonase in patients with type 2 diabetes. Metabolism 2004. https://doi.org/10.1016/j.metabol.2003.10.009.

[298] Hammad LA, Wu G, Saleh MM, Klouckova I, Dobrolecki LE, Hickey RJ, et al. Elevated levels of hydroxylated phosphocholine lipids in the blood serum of breast cancer patients. Rapid Commun Mass Spectrom 2009. https://doi.org/10.1002/rcm.3947.

[299] Kamphorst JJ, Cross JR, Fan J, De Stanchina E, Mathew R, White EP, et al. Hypoxic and Ras-transformed cells support growth by scavenging unsaturated fatty acids from lysophospholipids. Proc Natl Acad Sci U S A 2013. https://doi.org/10.1073/pnas.1307237110.

ANNEXES

SUPPLEMENTARY INFORMATION CHAPTER 1

SUPPLEMENTARY INFORMATION CHAPTER 1

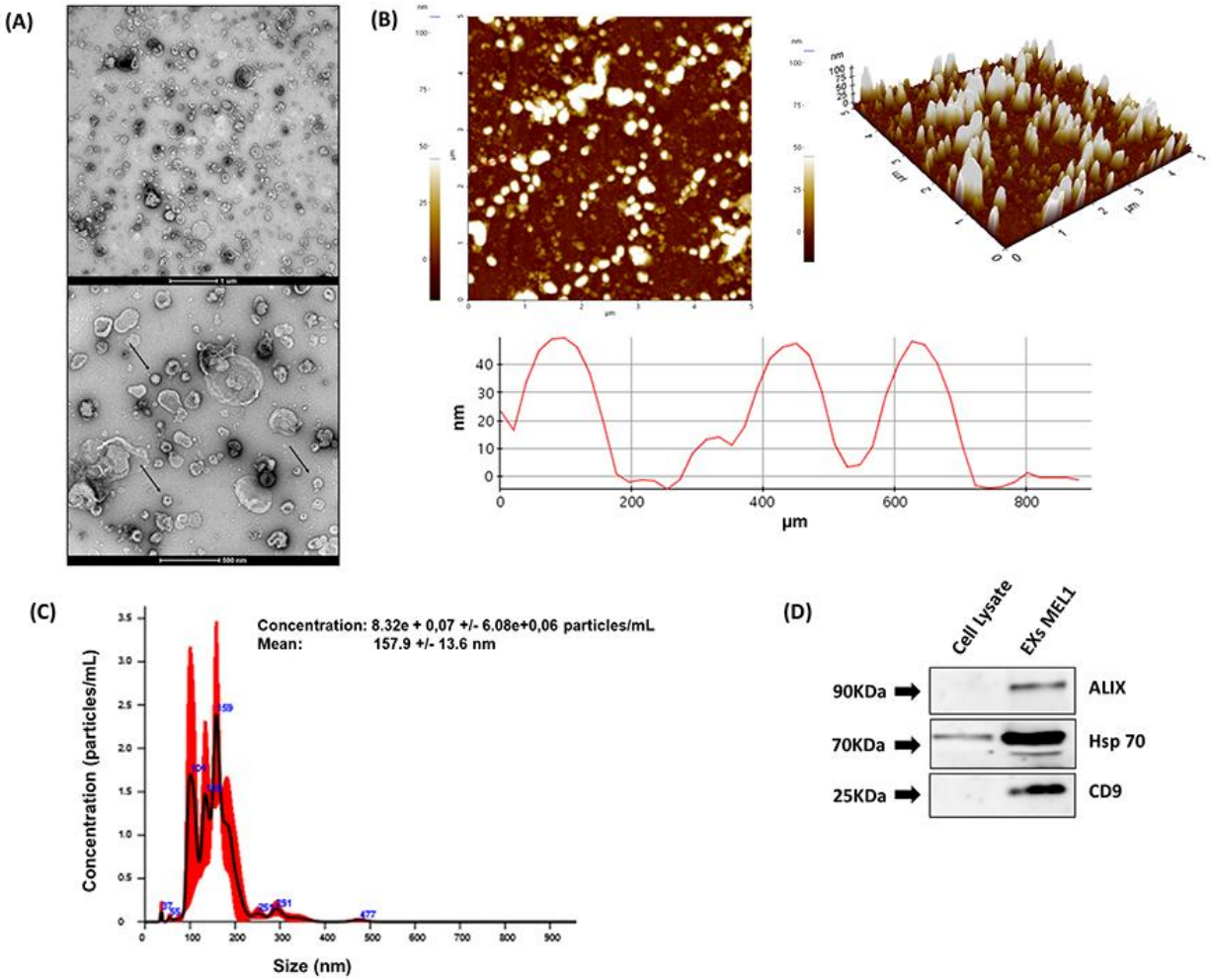

Figure S1. Characterization of exosomes derived from Mel1 differentiated tumor cells. **(A)** Transmission electron microscopy images of isolated exosomes with a saucer-like shape limited by a lipid bilayer. EVs isolated from Mel1 culture supernatants had diameters ranging from ~50–240 nm. Black arrow heads point to exosomes; **(B)** Topography of exosomes derived from Mel1 adherent cells observed under atomic force microscopy (AFM). Exosomes on a mica surface revealed heterogeneity in size and shape as well as forming aggregates in both 2-dimensional 2D (left) images and 3D profiles (right). Acquisition areas were 5 x 5 μm^2; **(C)** The size distribution of exosomes isolated from Mel1 adherent cells was analyzed by NTA; **(D)** Western blot analysis of CD9, Alix and the Hsp70 exosomal surface markers.

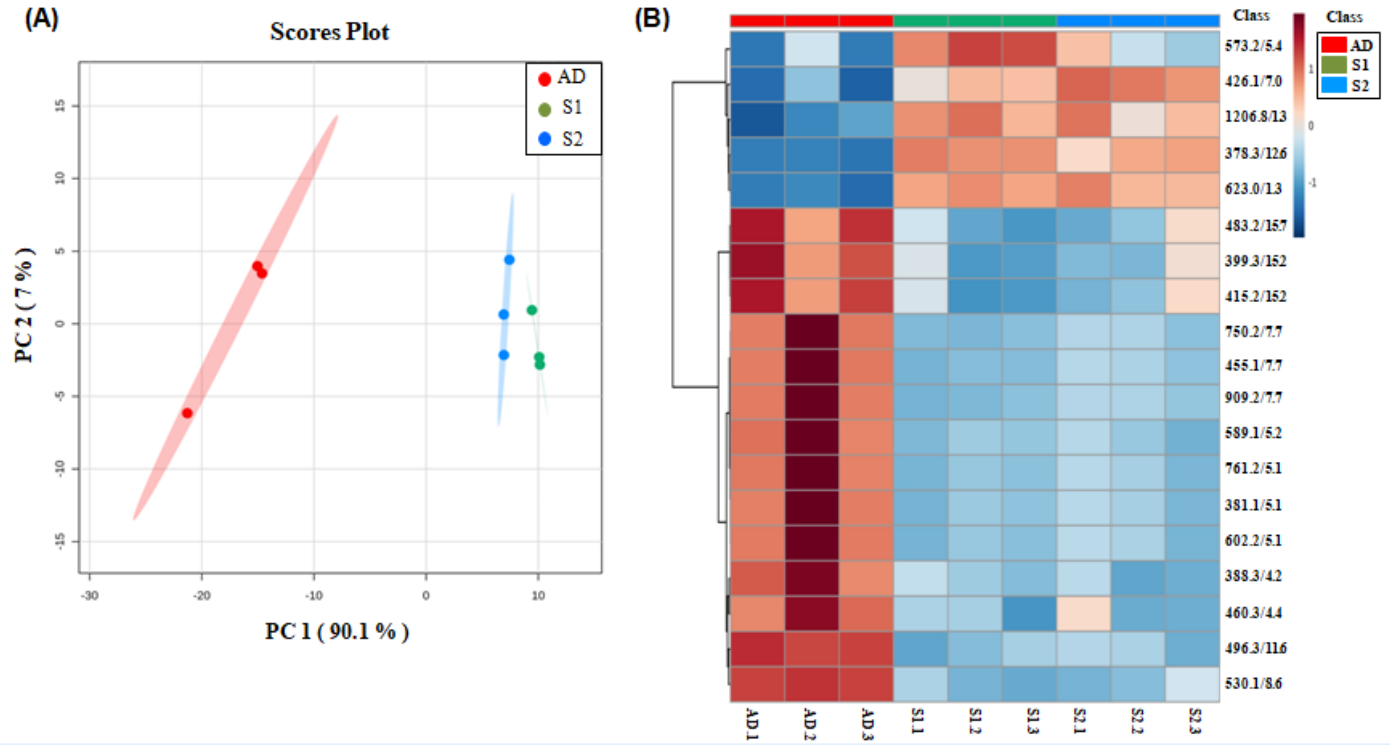

Figure S2. **Metabolomic analysis of exosomes derived from Mel1 patient-derived cell line. (A)** PCA scores plots based on HPLC/MS data of exosome samples derived from adherent cells (red), primary spheres (green) and secondary spheres (blue). **(B)** Heatmap showing the significantly different metabolites when comparing exosomes derived from adherent cells (red), primary spheres (green) and secondary spheres (blue). Each row on the heatmap represents a unique metabolite with a characteristic mass-to-charge ratio and retention time while each column represents one exosome sample. The colour code (blue to red) represents the normalized intensity with which each metabolite is detected.